ATMOSPHERIC AND VORTEX DESCRIPTION
FOR IDAHO FALLS B-757
RUN 9 on September 25, 1990
REVISION NO. 1

APRIL 1994

Prepared for:
DOT/RSPA/John A.Volpe National Tranportation Systems Center
DTS-53
Kendall Square
Cambridge, MA 02142-1093

Prepared by:
System Resources Corporation
128 Wheeler Road
Burlington, MA 01803

VOLPE CENTER

VORTEX WAKE

TABLE OF CONTENTS

ATMOSPHERIC AND VORTEX DESCRIPTION FOR IDF B-757 RUN 9

REVISION 1, APRIL 1994

1. INTRODUCTION

This revised report has new material regarding: The automated calculation of time height cross-sections, turbulence data, and the use of relative aircraft coordinates for wind components.

The DOT/RSPA/John A. Volpe National Transportation Systems Center (Volpe Center) has been developing data processing software for the meteorological tower and tethersonde data observed during the special wake vortex experiment conducted at Idaho Falls in 1990. In addition, the data have been analyzed by Volpe Center meteorological support personnel for the purpose of preparing "canonical cases" for study by wake vortex modelers. The following material is the first such case developed for a particularly strong and persistent vortex pair from Run 9, a B-757 flyby at 0818 Local Standard Time (LST) on 25 September, 1990. Data are provided in three forms: Raw data, data smoothed in time and height, and best fit polynomials.

Except at the turbulent scale, the bulk characteristics of a local airmass change slowly relative to the lifecycle of a vortex pair from a single aircraft; therefore, the dataset from this case taken over the space of a few minutes by the instrumented tower and a tethersonde less than 2000 feet away should be reasonably representative of Run 9 on Sept 25, 1990. In future experiments, we must further test and prove this hypothesis; however, in the present case, it seems like a reasonable working assumption without evidence to the contrary.

We grouped the tower and the tethersonde data into a unified height vs time coordinate system for the morning hours of 9/25/90, and then extrapolated the values to a uniform grid in height-time space. The technique is known as a Barnes analysis which uses an exponential weighting function to smooth and grid the data and is further explained in the next section.

The smoothed Run 9 data were also fit to fourth order polynomials which provided an analytical description of the profiles of wind, temperature, and derived parameters. This also removed more of the irregularities while preserving the larger scale vertical structure. Thus the users of this dataset can choose from several optional forms of the data.

Note, we have presented the processed wind data in terms of wind components relative to the aircraft: u_a, (positive when a headwind, negative when a tailwind), and v_a, (positive when parallel to the starboard (right) wing, negative when parallel to the port wing), rather than in units of direction and speed. Only the original, raw wind components are shown in earth coordinates.

2. TECHNICAL DISCUSSION

2.1 RAW DATA

Tables 2-1 and 2-2 provide the original unsmoothed temperature (C) and wind component (m/sec) vertical profiles from the meteorological tower and the tethersonde respectively, along with the derived parameters: lapse rate, Brunt-Vaisalla frequency (B-V), and Richardson Number (Ri). These are also the data that are provided in a Volpe Center data processing and display system (see Attachment C), except that the current version of that package uses direction and speed for the wind. The tower data are from three-minute averages at the heights shown; whereas, the tethersonde data from 0816 LST (the closest available in time) are from 10 second averages at each observation level. Therefore, the tower data vary less with height and time than do the tethersonde data which have a larger noise component due, in part, to the bobbing of the balloon during its flight.

TABLE 2-1. UNSMOOTHED TOWER DATA FROM IDF B-757 RUN #9

Height (ft)	Temp (C)	u (m/sec)	v (m/sec)	Lapse (C/100ft)	B-V Freq (sec-1)	Rich Num
6.25	8.4	-1.01	-1.62	XXXX	XXXX	XXXX
12.5	8.4	-1.27	-1.81	0.00	0.018	0.012
25	8.3	-1.24	-2.14	-0.80	IMAG.	-0.077
50	8.2	-1.42	-2.45	-0.40	IMAG.	-0.052
100	8.4	-2.10	-3.12	0.40	0.028	0.204
150	9.0	-3.20	-4.10	1.20	0.041	0.183
200	9.6	-3.28	-4.68	1.20	0.041	1.144

TABLE 2-2. UNSMOOTHED TETHERSONDE DATA FROM IDF B-757 RUN #9

Height (ft)	Temp (C)	u (m/sec)	v (m/sec)	Lapse (C/100ft)	B-V Freq (sec-1)	Rich Num
112	8.3	-0.59	-3.03	XXXX	XXXX	XXXX
224	8.8	-2.22	-6.10	0.45	0.029	0.082
297	9.5	-1.70	-5.56	1.00	0.038	1.222
409	11.6	-1.51	-7.78	1.89	0.050	0.573
449	11.9	-1.23	-5.79	0.73	0.034	0.045
549	12.4	-0.90	-5.12	0.56	0.031	1.282
624	12.6	-2.04	-5.94	0.23	0.024	0.208

Note: The derived parameters (last three columns of each table) are centered on the layer bounded by the height of that row and the height of the row immediately preceding. The term "IMAG" is for imaginary B-V frequencies (unstable lapse rate cases).

2.2 SMOOTHED DATA IN HEIGHT AND TIME

The tethersonde data were noisy, were not synchronized with the flyby times, were not taken simultaneously at all levels, and were taken at a location about 1800 feet from the instrumented tower. Therefore, it was determined that these data could only be grouped with the tower data if they were assumed to be co-located with the tower and then extrapolated to a

regular grid of points in height-time space. This was accomplished by creating automated height vs.time cross-sections of temperature and wind components (converted to knots in aircraft coordinates) from the tower and tethersonde data. The data were extrapolated to a uniform vertical grid system by a technique known as a Barnes analysis which uses an exponential weighting function to average and grid the raw data. The weighting function acts as a low-pass filter which removes Fourier components with wavelengths equal to or less than twice a pre-specified characteristic length or period. By repeated use of the filter, wavelengths greater than or equal to three times the characteristic value can be restored to over 75-percent of their original value (see Attachment A). Thus, it is possible to create height vs. time cross-sections of the meteorological data and derived parameters that have been purged of undesireable artifacts of what appear to be significant observational noise associated with the tethersonde technique employed (Clawson, Kirk L., NOAA/ERL, personal communication). The impact on the better quality tower data will be minimal. Table 2-3 shows the filtered data for Run 9 picked off of the cross-sections.

TABLE 2-3. SMOOTHED TOWER AND SONDE DATA FROM B-757 RUN #9						
Height (ft)	Temp (C)	Ua (knots)	Va (knots)	Pot Temp	B-V Freq	Rich Num
					(sec-1)	
6.25	8.55	-0.39	-4.19	288.0	IMAG	-0.13
12.5	8.48	-0.42	-4.50	288.0	IMAG	-0.12
25	8.38	-0.38	-4.98	287.9	0.016	0.09
50	8.37	-0.34	-5.78	287.9	0.026	0.35
100	8.51	-0.38	-7.06	288.2	0.031	0.31
150	8.77	-0.38	-8.71	288.6	0.031	0.32
200	9.05	-0.02	-10.28	289.0	0.031	0.36
300	9.84	2.69	-12.24	290.1	0.050	0.63
400	11.61	4.67	-13.40	292.2	0.035	0.9
500	12.33	3.42	-11.15	293.2	0.029	1.27
600	12.64	2.41	-11.10	293.9	0.017	0.8

Figures 2-1 through 2-6 show the cross-sections of temperature (T), u_a and v_a, Potential Temperature (PT), Brunt-Vaisalla frequency (B-V), and Richardson Number (Ri) after three Barnes passes. From the PT, B-V, and Ri sections, it is easy to see the transition from very stable conditions prior to Run 9 to the development of an unstable layer near the surface as solar heating effects begin to dominate later in the morning. It is interesting that this transition begins in earnest just after Run 9. We might assume that in this region, the atmosphere would be turbulent. However, Run 9 at 0818L was still dominated by strong static stability through a deep layer above about 25 feet and was probably smooth.

FIG 2-1. TEMPERATURE (C) AFTER 3 BARNES PASSES

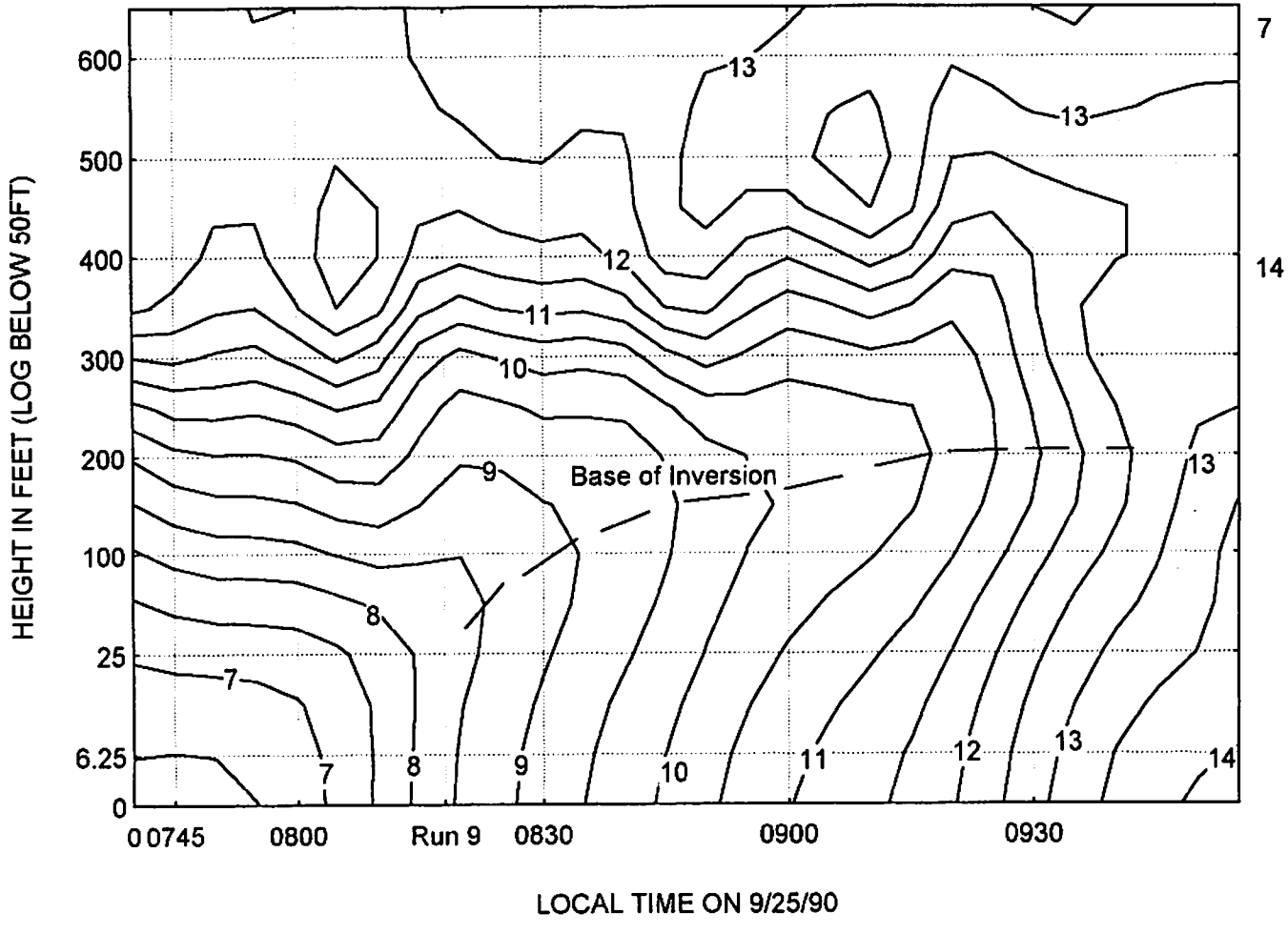

FIG 2-2. U-COMPONENT (KNOTS) RELATIVE TO A/C (AFTER 3 PASSES)

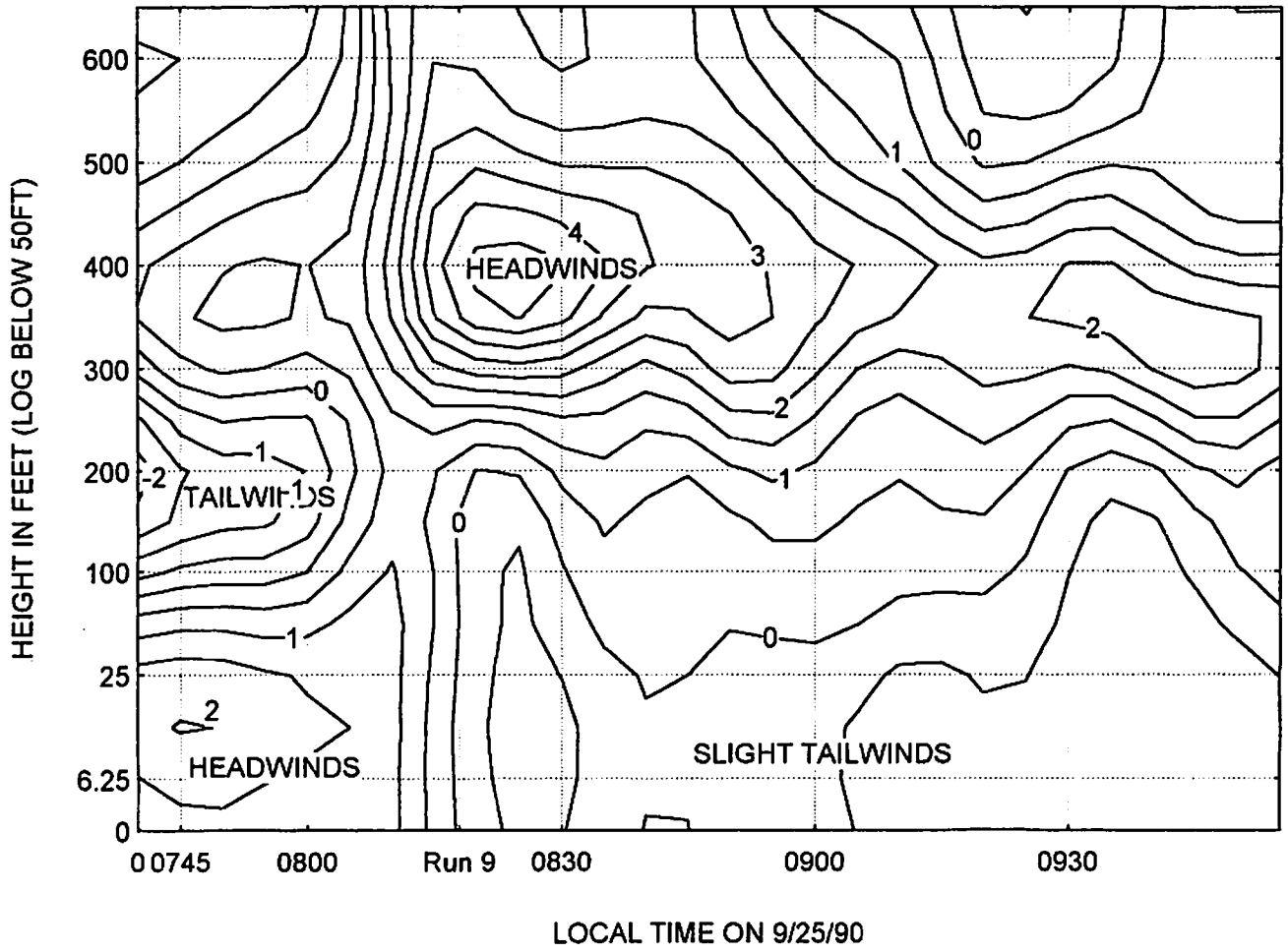

FIG 2-3. V-COMPONENT (KNOTS) RELATIVE TO A/C (AFTER 3 PASSES)

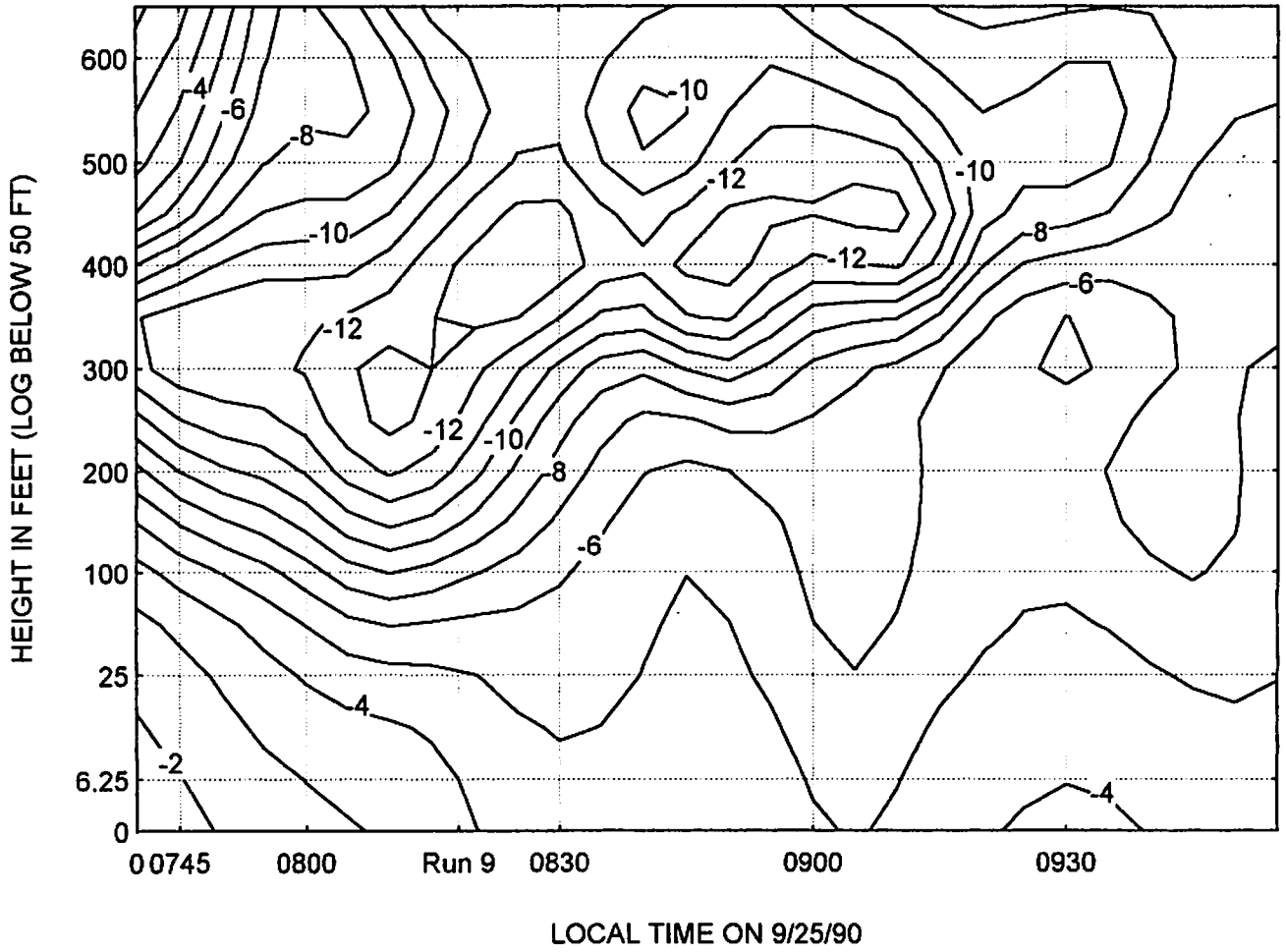

FIG 2-4. POTENTIAL TEMPERATURE (K) AFTER 3 PASSES

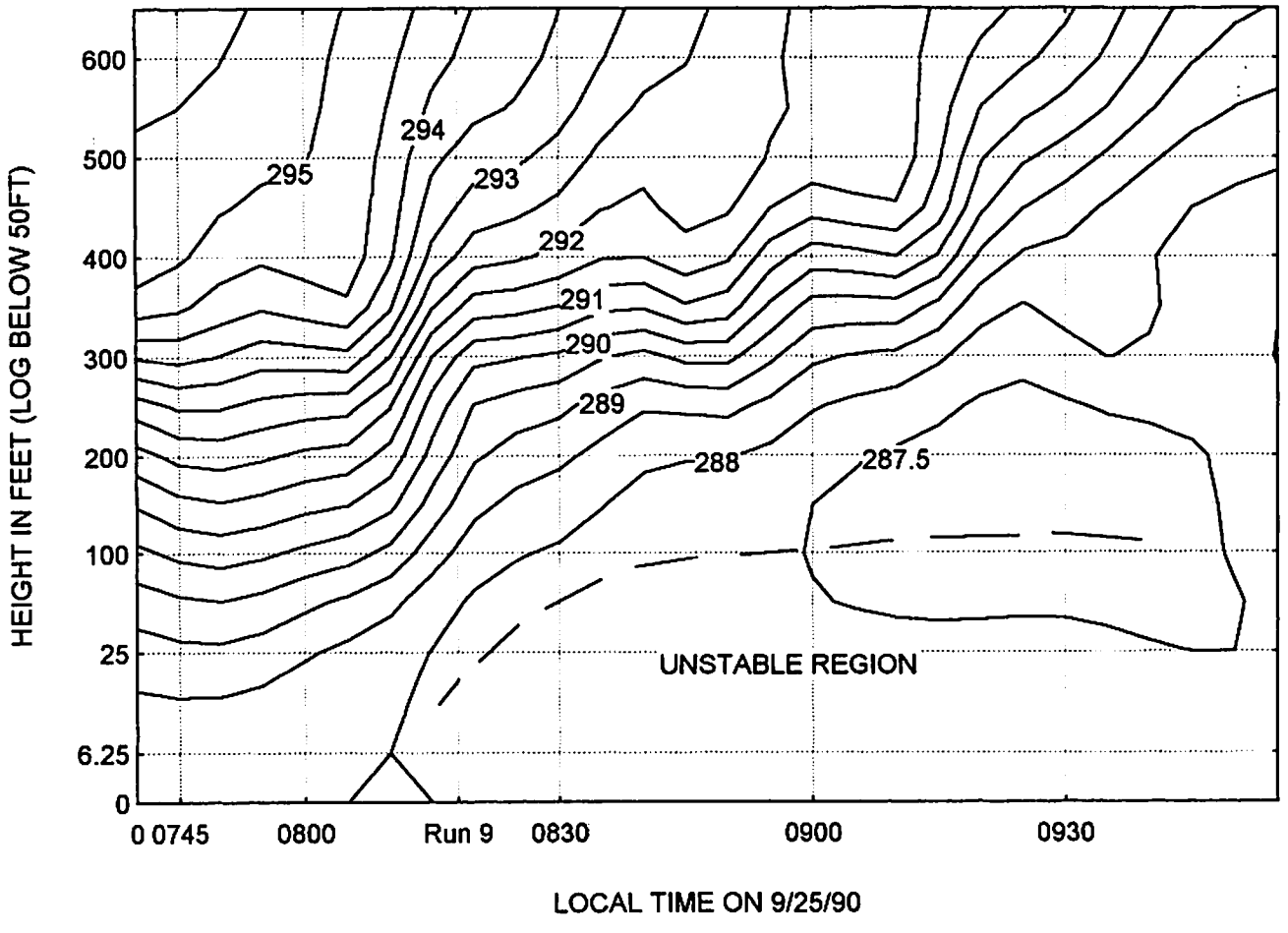

FIG 2-5. BRUNT-VAISALLA FREQUENCY (1/SEC) AFTER 3 PASSES

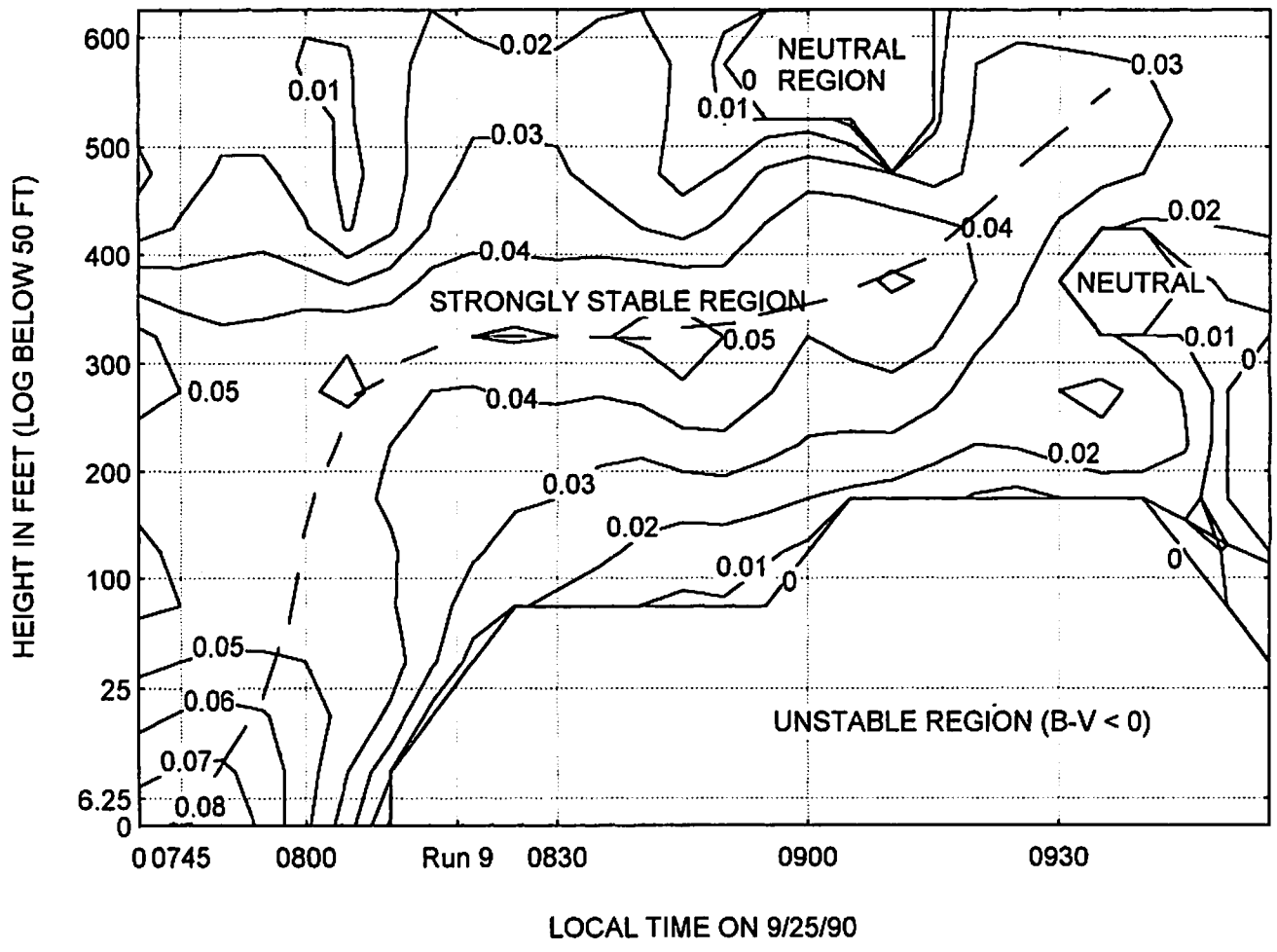

FIG 2-6. RICHARDSON NUMBER AFTER 3 PASSES

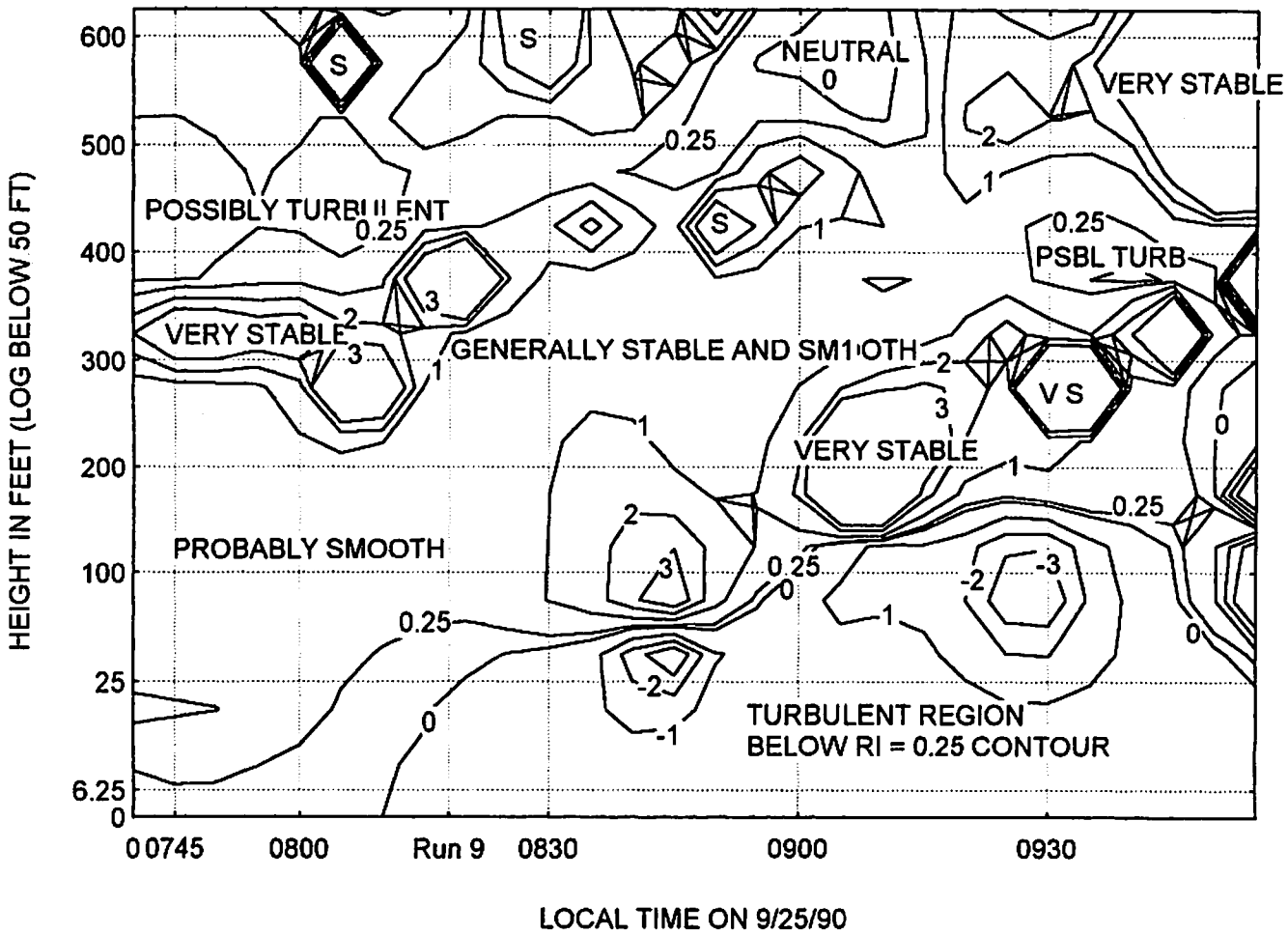

The average sampling period at the tower was 6.75 minutes, and was12 minutes from the tethersonde. The average vertical sampling distance was about 90 feet from the sonde and a little less than 50 feet from the tower (due to the log spacing below 50 ft). Based on the notion that it takes at least four time or height intervals to specify the smallest representative Fourier component, and the fact that the Barnes filter will preserve wavelengths three or more times the characteristic length or period (Attachment A), we eventually decided to preserve waves with periods of 30 minutes or greater, and vertical lengths of 300 ft. or more. The height-time grid intervals should be roughly as dense as the average distance between supporting data points. This becomes a trade-off between smooth presentation and computational efficiency, and we chose 5 minute and 50 foot intervals. This was also convenient for the Barnes filter which could then use a characteristic length of two grid units in either coordinate which met our filter criteria.

2.3 FITTING CURVES TO THE SMOOTHED DATA

The smoothed profiles for Run 9 were picked off of the cross-section and were fitted with polynomials of various orders, and 4th order functions seemed to do a reasonable job for both temperature and wind components. Figures 2-7 and 2-8 show the smoothed curves for temperature and u and v along with the polynomial fits and their equations.

2.4 DERIVED PARAMETERS FROM THE FITTED DATA

Since we now have analytical versions of the profiles in the form of polynomials, it is possible to solve analytically for the derived parameters: lapse rate, B-V, and Ri. This was done and the results are shown in Attachment B as two figures and a table which are the output from a MATHCAD program. Also shown are the analytical expressions used in the computation. If the reader wishes to work with the equations, be aware that heights are in 100's of feet (e.g., $z = 5$ corresponds to 500 ft), and there are some mixed units because winds are in knots. This required the correction term 3505.89 in the expression for Ri.

3. METEOROLOGICAL DATA SUMMARY

3.1 COMMENTS ON THE TIME TRENDS

Up to about the time of Run 9, the atmosphere was quite stable from the surface to at least 400 feet suggested by the strong temperature inversion in that space-time region (Figures 2-1, -5, and -7). At the time of Run 9, Figure 2-5 showed large values of B-V above 25 feet which would indicate smooth conditions; however, the same region had strong wind shear (e.g., note the v-component gradients in Figure 2-3) which tended to reduce Ri values between 50 and

FIG. 2-7. SMOOTHED AND FITTED TEMPERATURE PROFILE FOR B-757 RUN#9

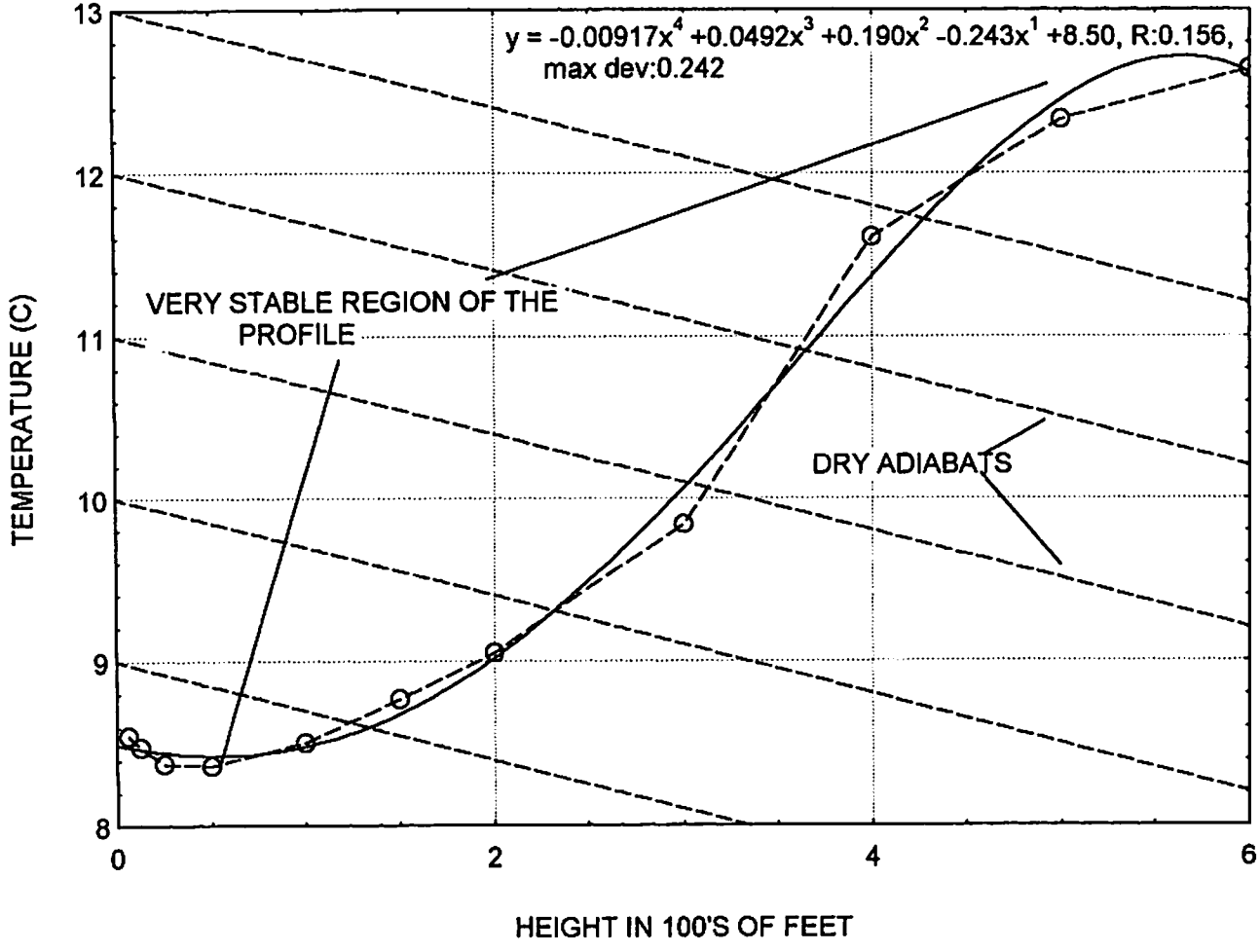

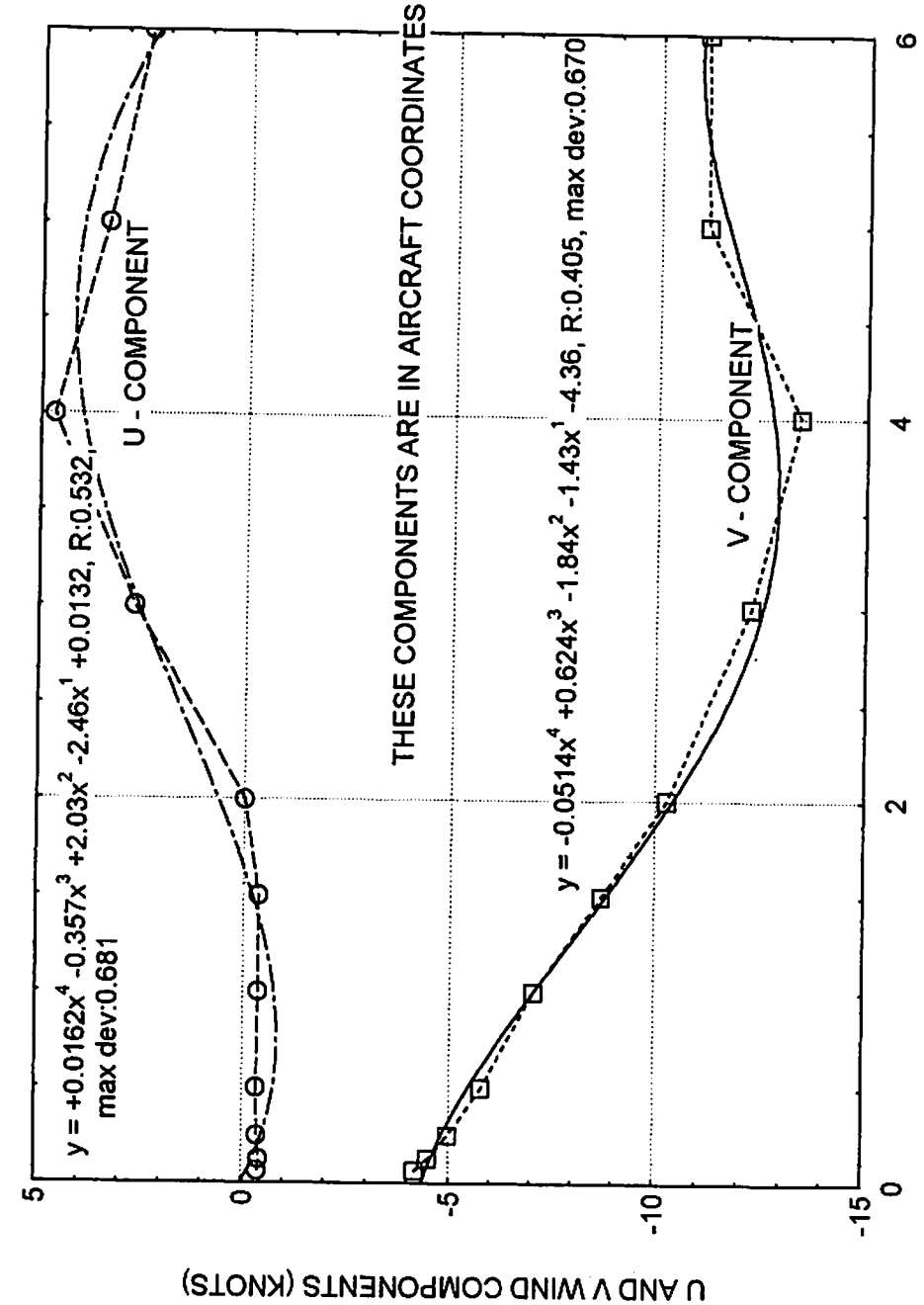

FIG. 2-8. SMOOTHED AND FITTED PROFILES OF U AND V FOR B-757 RUN #9

300 feet to just above the critical value of 0.25 (Figure 2-6). Because Ri (Figure 2-6) was consistently positive above 25 feet, Run 9 probably had smooth conditions. One can also see in Figure 2-2 the switch from a light headwind to a light tailwind component which occurred almost exactly with Run 9.

After Run 9, the stable layer and the strong wind shear layer lifted as much as 200 feet as the surface layer heated and became neutral to unstable with probable turbulent eddies up to about 150 feet by 0900. This also shows up in the potential temperature (PT, Figure 2-4) as a rapid weakening of the vertical PT gradient toward neutral (no gradient) or unstable (decrease of PT with height) as bounded by the dashed line. The wind gradients (Figure 2-3) decreased with time in the stable layer, raising the Ri values dramatically just above the turbulent layer, indicating that the vertical transition might have been very sharp between a smooth layer aloft and turbulence near the ground. In later reports, we will analyze a series of vortex runs that experienced this transition, and will look for possible weather impacts on the vortex lifetimes.

3.2 COMMENTS ON THE METEOROLOGICAL DATASETS

The Run 9 meteorological dataset has been prepared in three forms: Raw data, smoothed height vs. time cross-sections, and best fit polynomials. The users can therefore choose what they believe to be the best dataset for their purpose. No digital form of the best fit data are available; however, the raw and smoothed cross-section data can be obtained on floppy disks from the Volpe Center. Attachment C describes the Center's data base, and data processing and display software system for examining the September 1990 Idaho Falls data taken from the vortex and meteorological sensors.

Section 4 below discusses Run 9 vortex characteristics and some *in situ* turbulence measurements taken from the instrumented tower.

4. WAKE VORTEX INFORMATION

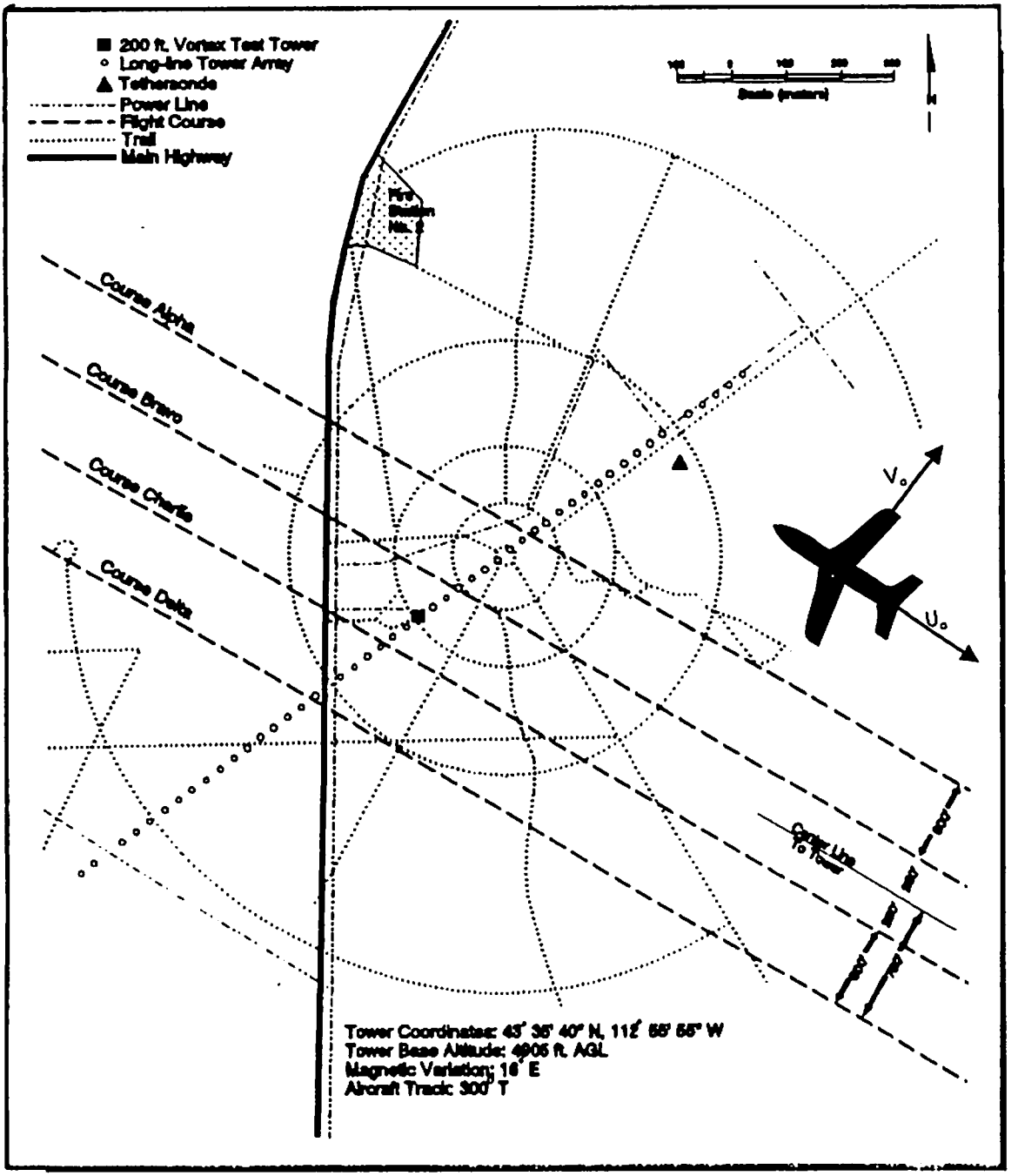

Figure 4-1. NOAA Wake Vortex Test Site and Aircraft Flight Paths

4.1 VORTEX TRAJECTORIES

The aircraft flight path (Course Bravo) is shown in Figure 4-1, which was extracted from the NOAA Wake Vortex Technical Memorandum ERL ARL-199. Figure 4-2 shows the vortex trajectories *perpendicular* to the flight path, including data from the Laser Doppler Velocimeter (LDV) and Monostatic Acoustic Vortex Sensing System (MAVSS). Note that the first downwind vortex rises again after its initial descent.

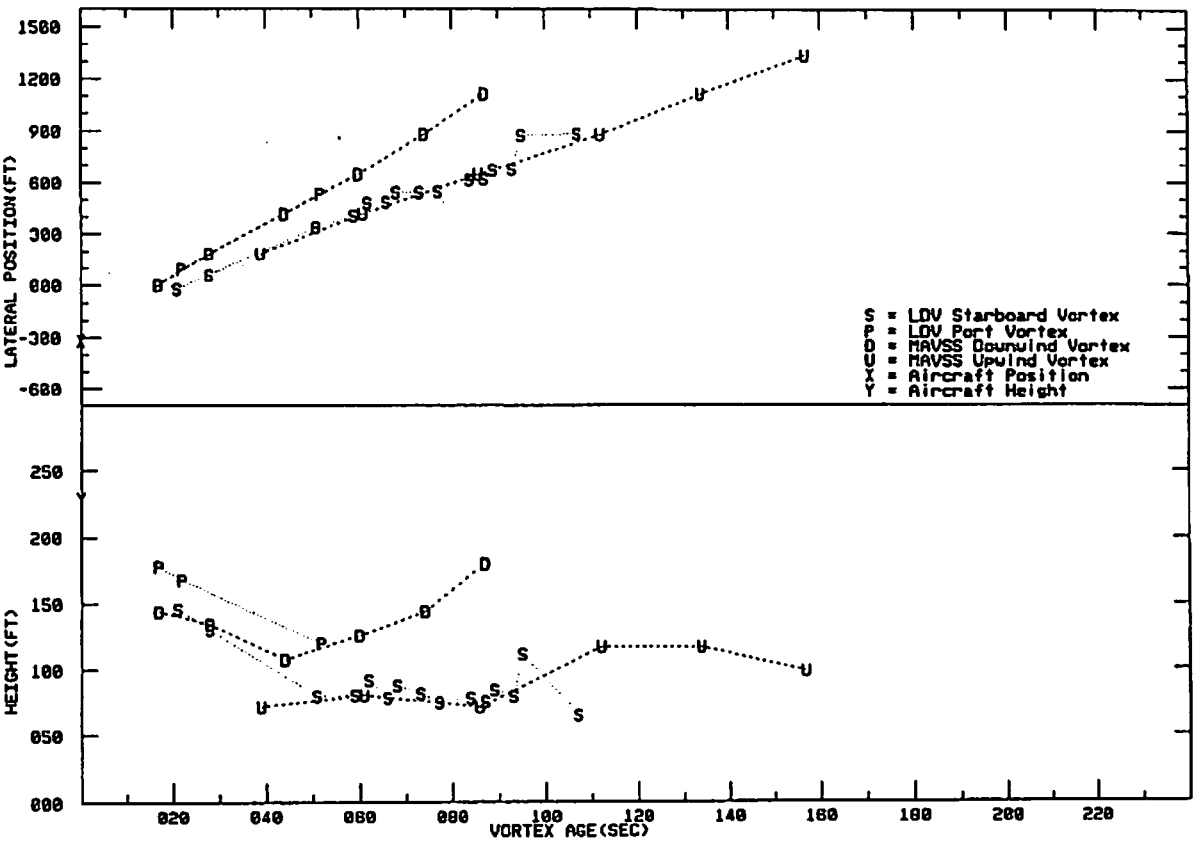

Figure 4-2. LDV and MAVSS Vortex Positions for B-757 Run 9

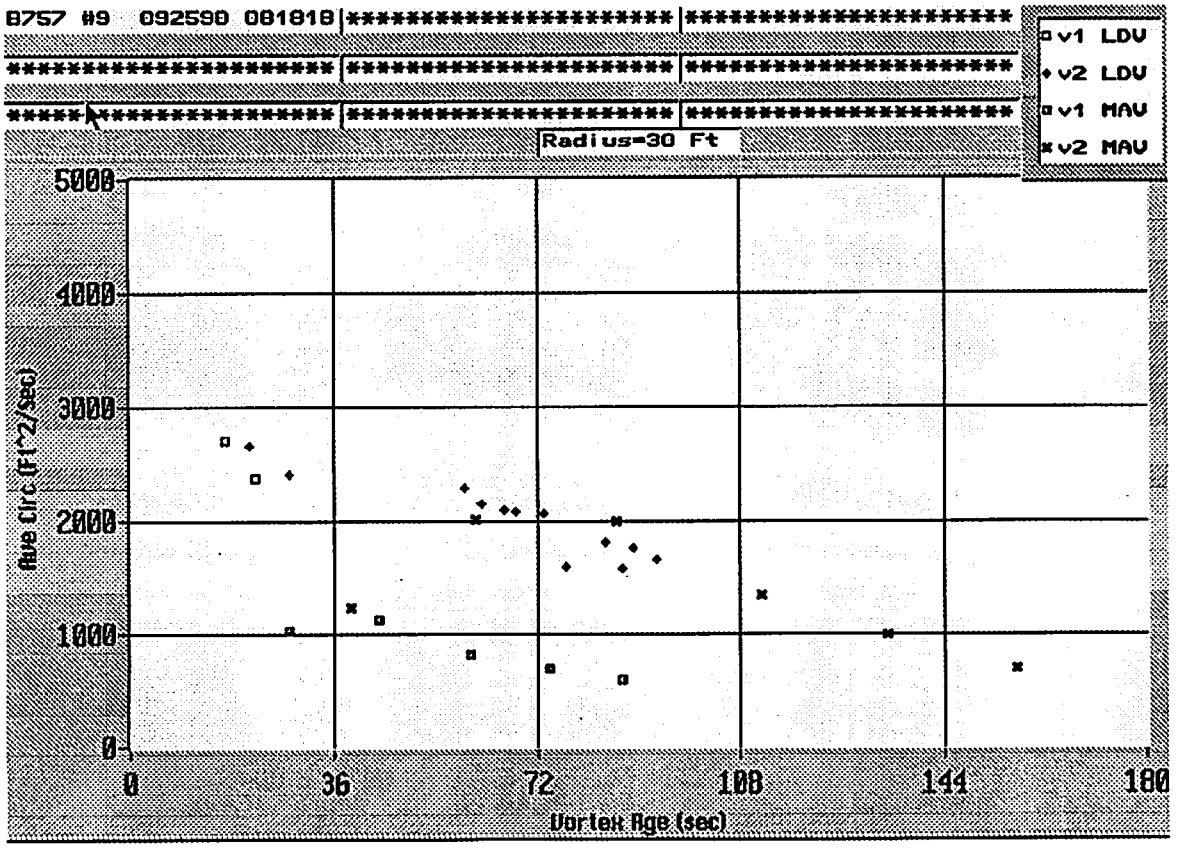

Figure 4-3. 30-Foot Average Circulation, B-757, Run 9

4.2 AVERAGE CIRCULATION

Figure 4-3 shows the 30-foot average circulation calculated from both MAVSS and LDV data. The second (upwind) vortex is much stronger and longer lasting than the first (downwind) vortex. Note that the vorticity of the second vortex has the same sign as the wind shear vorticity and hence cannot decay by mixing with the ambient wind shear vorticity.

Note that Figures 4-2 and 4-3 represent the original 1991 processing algorithms.

4.3 EQUIPMENT LAYOUT

Figure 4-4 shows the overall layout of the vortex measurement instrumentation at the NOAA Idaho Falls test site. Three types of instrumentation were installed:

1) Single-element hot-film anemometers were installed at 2-foot intervals on a 200-foot tower and on 30-foot poles at 100-foot intervals out to 2500 feet from the 200-foot tower. The normal sample rate for the hot-film anemometers was 100 Hz. Eight tower anemometers (100, 110, 120, 130, 140, 150, 160 and 170 feet) were also recorded in parallel at 4000 Hz.

2) Eight MAVSS antennas were installed at approximately 250-foot intervals out to 1700 feet along the line of 30-foot poles. The antennas located next to the poles were displaced by about 30 feet from the pole line to avoid the guy wires for the poles. The first antenna was located about 130 feet from the 200-foot tower along a line parallel to the aircraft flight paths. It was offset from the tower to avoid tower reflections and the noise from the smoke grenades.

   Each MAVSS antenna measures a vertical profile of the vertical wind field up to a height of 235 feet above the ground.

3) The LDV was located to the side of the 300-foot 30-foot pole. Because of the angle of the flight path, its distance from the tower was only 220 feet when measured perpendicular to the aircraft flight path. The LDV measures the absolute value of the line-of-sight velocity and has an effective range of about 100 to 600 feet. It scans one arc per second at each of a number of ranges. An operator selects the arc limits and the ranges to be scanned. The LDV location was selected to cover the same space as the instrumented tower location in order to facilitate comparisons of the two measurement techniques.

Figure 4-5 shows the coverage of the instrumentation in the plane perpendicular to the aircraft flight path, which was fixed toward the northwest (300□ True) by site security considerations. The ambient wind is generally from the northeast or the southwest. The hot-film anemometers were deployed to accommodate either wind direction, but the other vortex sensing systems assumed a northeasterly ambient wind which normally occurs at dawn.

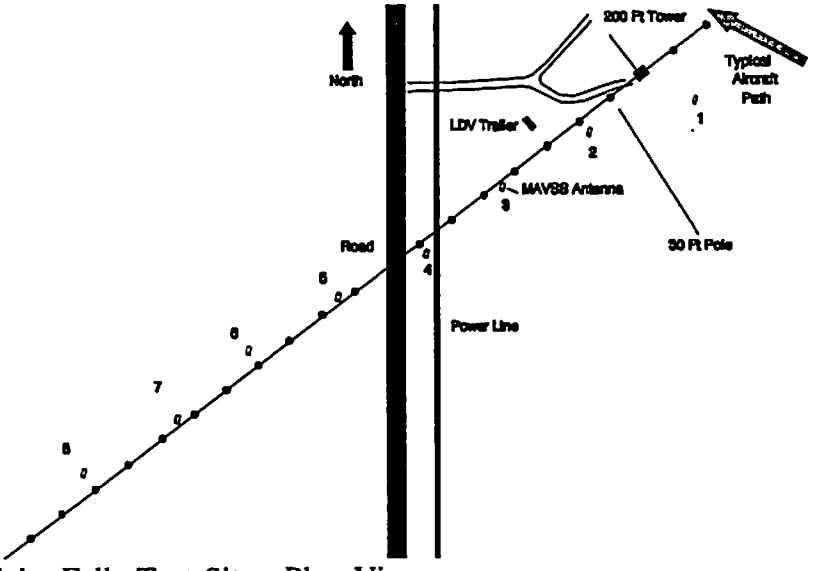

Figure 4-4. Idaho Falls Test Site: Plan View

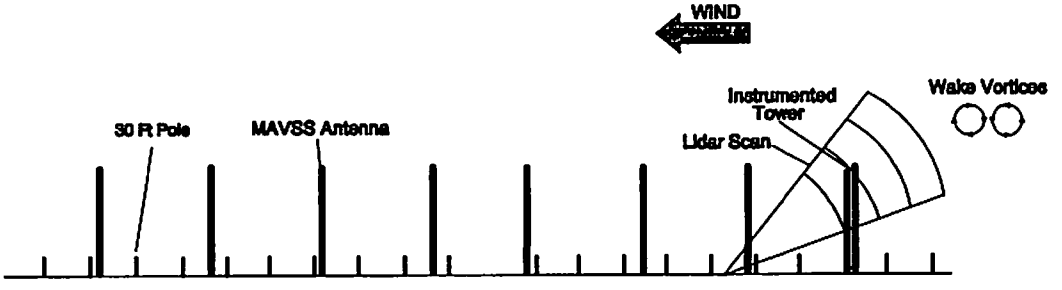

Figure 4-5. Idaho Falls Test Site: View from Flight Direction

The vortex generating aircraft flew upwind of the instrumented tower at an altitude and offset designed to have the wake vortices descent and strike the 200-foot tower out of ground effect (above 100 feet). On a successful run both vortices hit the tower and hence gave vortex measurements at two vortex ages, which depended upon the lateral offset of the flight path and the strength of the ambient crosswind. The lidar could track the vortices from a point slightly before they hit the tower until they got too close to the lidar location for the lidar operator to track their motion. Often (as for B-757 Run 9) the operator was able to reacquire the second vortex after it had passed the lidar location. On the other hand, the MAVSS antennas could detect the vortices until they decayed. Only a few vortices reached the last MAVSS antenna. Thus, only the MAVSS was able to reliably determine the vortex lifetimes.

4.4 VELOCITY PROFILES

The LDV can measure the velocity profile of a vortex when it is within about 600 feet of the LDV. The quality of the velocity profile is degraded as the distance to the vortex increases and/or when the LDV scan range is not exactly the same as the distance to the vortex. Since the lowest signal-to-noise ratio is in the vortex core, degraded velocity profiles have missing velocity data near the vortex core. The LDV normally scans at three or more ranges specified as a multiple of 10 meters. When the vortices were moving slowly, the ranges were set 10 meters apart. In order to track fast moving vortices, 20-meter range spacings were used. The measured vortex range is assigned to the scan range that has the smallest vortex core with the highest velocities. Thus, the best velocity profiles will likely have an accurate vortex range assigned. Since the calculated vortex circulation is proportional to the range, range errors have a direct impact on circulation accuracy.

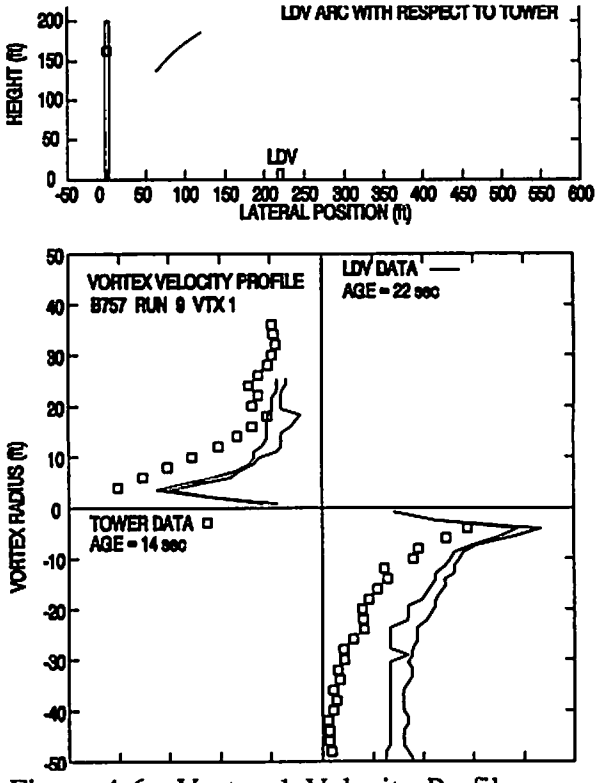

Figure 4-6. Vortex 1 Velocity Profile

Two algorithms are used to obtain the vortex tangential velocity from the spectrum. The original algorithm defines the tangential velocity as the highest spectral bin that is above the noise level. Any spectral broadening will, of course, cause this algorithm to overestimate the tangential velocity. A new algorithm defines the tangential velocity as the highest peak in the spectrum. It looks down in frequency from the first algorithm location until the intensity starts to decrease. This algorithm gives a noisier plot but likely provides an unbiased estimate of tangential velocity. The LDV tangential velocity plots include both algorithms; naturally the second gives a lower velocity.

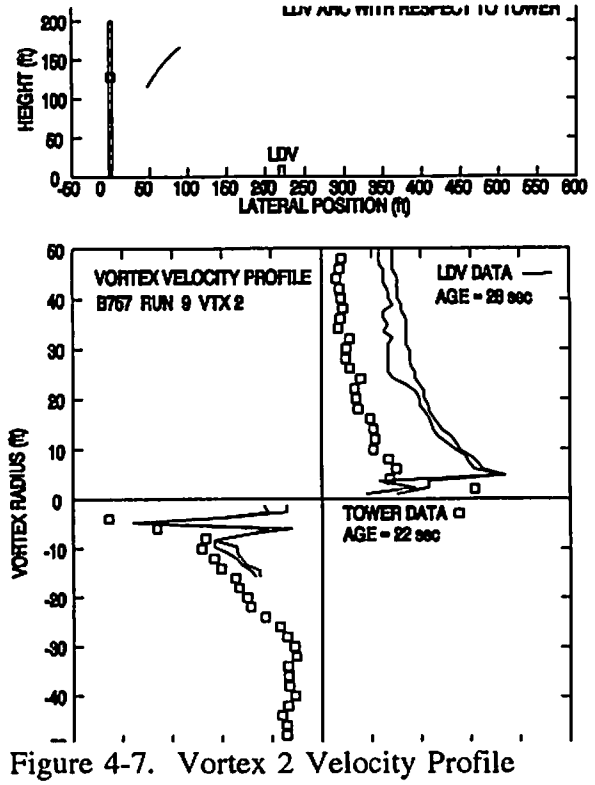

Figure 4-7. Vortex 2 Velocity Profile

Three LDV velocity plots (Figures 4-6 to 4-8) are included: Vortex 1 at age 22 seconds and Vortex 2 at ages 28 and 66 seconds. The two early plots are included to provide velocity

profile comparisons with the instrumented tower measurements (plotted as boxes). The LDV data is taken from slightly later times to get the better quality associated with closer range to the LDV.

The top of each plot shows the spatial location of the LDV arc scan where the LDV velocity measurements were taken. The break in the arc is the location of the vortex core. The height on the tower where the vortex core hit is marked with a box. The bottom of each plot shows the vortex tangential velocity profile. Both LDV velocity algorithms are plotted as lines (the highest peak algorithm giving the lower velocity, of course). The tower measurements are plotted as boxes and have been corrected for the ambient wind before the vortex arrival and hence have an offset from the LDV data. It would be more appropriate to compare the uncorrected tower data with the LDV data; note that the ambient wind is significantly affected by the vortex which brings air down with it from the height of vortex generation. In general, the LDV measurements shows somewhat larger tangential velocities, even from the highest peak algorithm.

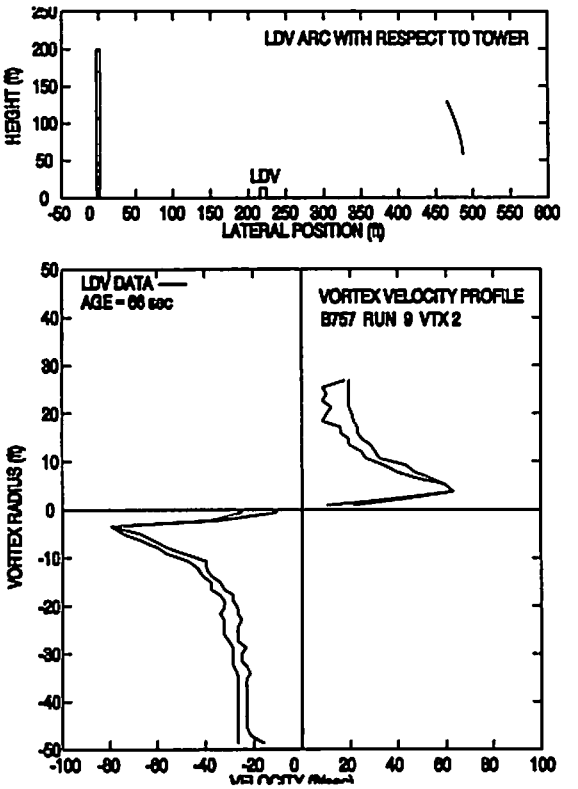

Figure 4-8. Vortex 2 Velocity Profile

4.5 CIRCULATION PROFILES

Plots of circulation as a function of vortex radius (Figures 4-9 to 4-11) were generated from the velocity profiles in Figures 4-6 to 4-8. The LDV circulation using the highest peak algorithm velocities are plotted as two lines, one for each side of the vortex. A velocity offset was added to the LDV data to make the velocity profiles symmetrical (using velocity data for radii between 10 and 20 feet). The tower data from one side of the vortex is plotted as a square and from the other side as a plus. Neither the early LDV or tower circulation profiles are of particularly good quality for this run. The 66-second LDV data for Vortex 2 shows cleaner data.

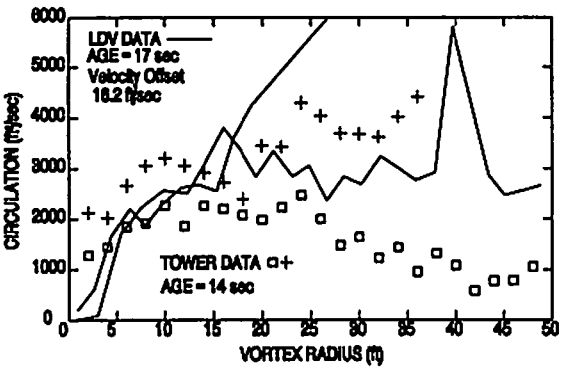

Figure 4-9. Vortex 1 Circulation Profiles

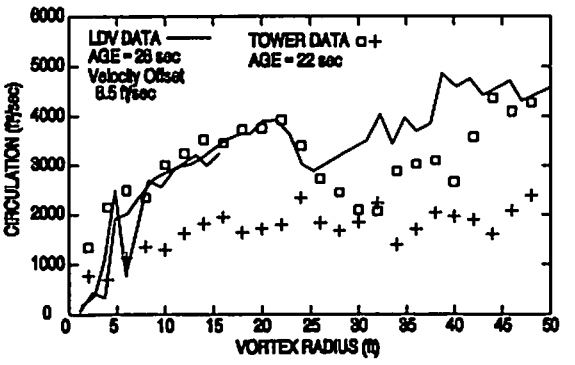

Figure 4-10. Vortex 2 Circulation Profiles

The traditional way of analyzing circulation profiles is to compute the average circulation for different averaging radii (Figure 4-3). A different algorithm was developed to use the LDV data to give a more detailed picture of vortex decay. Two parameters are used to define the circulation profile: total circulation and core radius. In this case, the radii used to estimate the total vortex circulation is limited because the LDV data do not extend out to large radii. The circulation was averaged over two ranges of radii: 15-20 feet (termed 20) and 20-25 feet (termed 25); data must exist from both sides of the vortex. The core radius was then defined as the radius where the measured circulation is half the total circulation; again both sides of the vortex were averaged. Two plots from this analysis are included for B-757 Run 9. Figure 4-12 shows the circulation for the two vortices (V1 and V2) for the two ranges of radii (20, 25). Figure 4-13 shows the core radius; note that the 66-second point shows a particularly small radius, which results from its very high quality data. The actual core radius for the B-757 landing vortex (determined from instrumented tower data) is much smaller still.

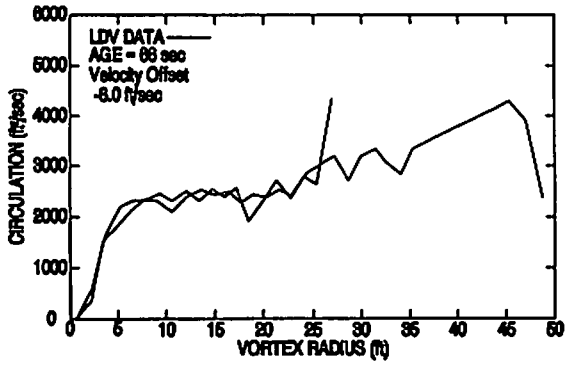

Figure 4-11. Vortex 2 Circulation Profiles

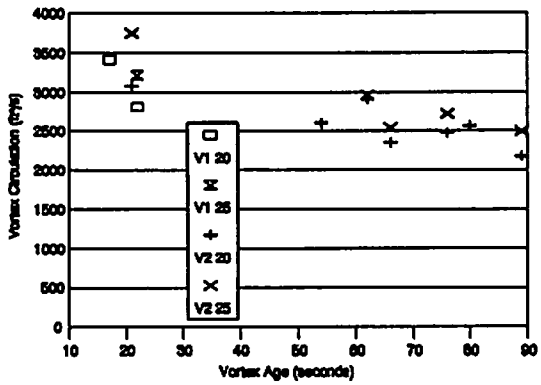

Figure 4-12. Vortex Circulation vs Age

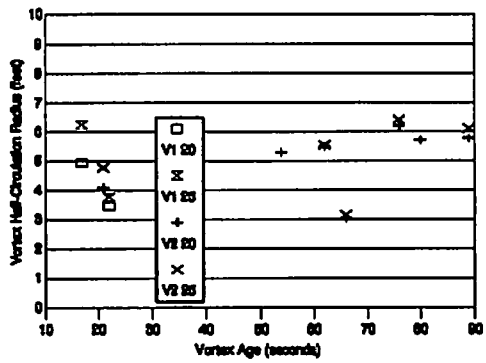

Figure 4-13. Core Radius vs Age

5. METEOROLOGICAL DATA FROM VORTEX SENSORS

The Idaho Falls vortex sensors can be used to measure meteorological parameters. Of particular interest is turbulence which was not measured directly by any meteorological sensors.

1) Attachment D shows the vertical winds from the MAVSS. They may be used to detect the vertical turbulence and the gravity waves generated by the impact of the aircraft wake on the stratified atmosphere.

2) Attachment E shows preliminary turbulence data from the tower hot-film anemometers.

3) Attachment F shows crosswind profiles from the LDV.

ATTACHMENT A

BARNES FILTER RESPONSE

This program, Barnes2, approximates the Barnes filter response as a function of a non-dimensional wavelength n which is the ratio of wavelength to e-folding distance (assumed to be one unit in the calculations). The Barnes search radius is Rmax = 3, and KL is the length of a one-dimensional grid over which the calculations are performed. KK1 and KKL are the limits on the range variable k that limits the processing within Rmax points at either end to avoid boundary problems. L1 and L2 are the range limits over which the simulated Barnes analysis is done at each gridpoint. SUMWT = the constant integral of the Barnes weights used at each gridpoint. The variable yhat is the weighted amplitude of the sine function with a given wavelength ratio n calculated for each gridpoint k. The variable ybar is the mean of the absolute values of yhat for each wavelength n. The value of ybar for a pure sine wave with a unit amplitude would be $2/\pi$ = 0.6366; therefore, the fractional response to the Barnes process may be defined as the variable Resp which is the ratio of ybar to $2/\pi$. In successive Barnes passes, we compute the errors between the Barnes analysis and the original sine function, apply the operator to the errors, and add the analyzed errors at grids to the prior "guess". In the analytical simulation, this effect (after some simple math) can be modeled by the binomial expressions using the variable Resp as given by the terms R2, R3, and R4. The figure shows the response as a function of n for passes 1 through 4. The important conclusions are that: 1) The Barnes analysis essentially eliminates wavelengths less than or equal to twice the e-folding distance, and 2) By the fourth pass, over 75-percent of the amplitudes of wavelength three and above are restored.

$n := 1, 2 .. 12 \qquad Rmax := 3 \qquad KL := 83$

$KK1 := Rmax + 1 \qquad KKL := KL - Rmax \qquad KK2 := KK1 + 1$

$k := KK1, KK2 .. KKL$

$L1(k) := k - Rmax$

$L2(k) := k + Rmax$

$$SUMWT := \int_{-Rmax}^{Rmax} e^{-L^2}\, dL \qquad KK1 = 4 \qquad KKL = 80$$

$SUMWT = 1.772$

$$yhat_{n,k} := \frac{\int_{L1(k)}^{L2(k)} e^{-\left[(L-k)^2\right]} \cdot \sin\left(2 \cdot \pi \cdot \frac{L}{n}\right) dL}{SUMWT}$$

$$ybar_n := \frac{\sum_{k=KK1}^{KKL} |yhat_{n,k}|}{(KKL - KK1) + 1}$$

$$Resp_n := ybar_n \cdot \frac{\pi}{2}$$

$$R2_n := 1 - (1 - Resp_n)^2 \qquad R3_n := 1 - (1 - Resp_n)^3 \qquad R4_n := 1 - (1 - Resp_n)^4$$

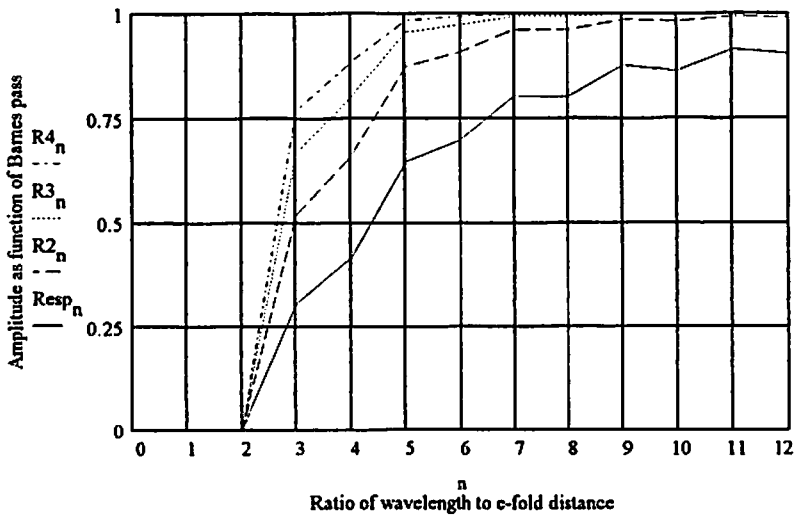

ATTACHMENT B

ANALYTICAL METEOROLOGICAL PROFILES

ATTACHMENT B

THIS PROGRAM, B757NO9, COMPUTES THE ANALYTICAL PROFILES OF TEMP LAPSE RATE, BRUNT-VAISALLA FREQUENCY, AND RICHARDSON NUMBER FROM FOURTH ORDER POLYNOMIAL CURVES OF U, V, AND T BASED ON BARNES-SMOOTHED PROFILES CALCULATED FROM HEIGHT VS. TIME PLOTS FOR B-757 RUN 9.

HEIGHT IN 100'S OF FEET $z := 0, 0.25 .. 6$

TEMPERATURE IN ^0C $T(z) := -.00917 \cdot z^4 + .0492 \cdot z^3 + .190 \cdot z^2 - .243 \cdot z + 8.5$

WIND COMPONENTS IN KNOTS

$u(z) := .0162 \cdot z^4 - .357 \cdot z^3 + 2.03 \cdot z^2 - 2.46 \cdot z + .0132$

$v(z) := -.0514 \cdot z^4 + .624 \cdot z^3 - 1.84 \cdot z^2 - 1.43 \cdot z - 4.36$

TEMP LAPSE RATE IN $^0C/100FT$ $dTdz(z) := -3.668 \cdot 10^{-2} \cdot z^3 + .1476 \cdot z^2 + .38 \cdot z - .243$

VERTICAL WIND SHEAR IN UNITS OF KNOTS/100FT

$dudz(z) := 6.48 \cdot 10^{-2} \cdot z^3 - 1.071 \cdot z^2 + 4.06 \cdot z - 2.46$

$dvdz(z) := -.2056 \cdot z^3 + 1.872 \cdot z^2 - 3.68 \cdot z - 1.43$

BRUNT-VAISALLA FREQ. = $BV(z) := \left[\left(\frac{0.32}{273.16 + T(z)} \right) \cdot (dTdz(z) + .299) \right]^{0.5}$

RICHARDSON NO. = $RI(z) := \left(\frac{BV(z)^2}{dudz(z)^2 + dvdz(z)^2} \right) \cdot 3505.89$

RICHARDSON NUMBER FOR B757 RUN #9

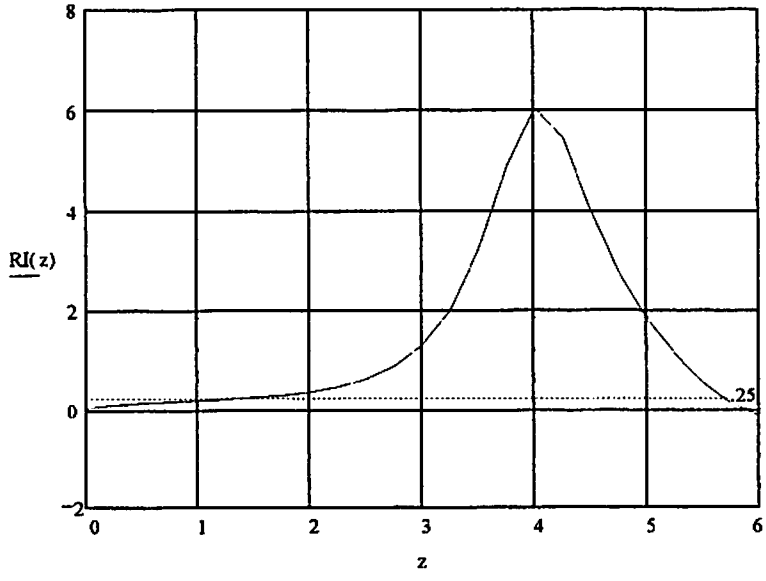

RICHARDSON NUMBER (DIMENSIONLESS). THE CRITICAL VALUE 0.25 IS INDICATED BY A DASHED LINE

HEIGHT IN 100'S OF FEET

BRUNT-VAISALLA FREQUENCY FOR B757 RUN #9

BRUNT-VAISALLA FREQUENCY (SEC^{-1})

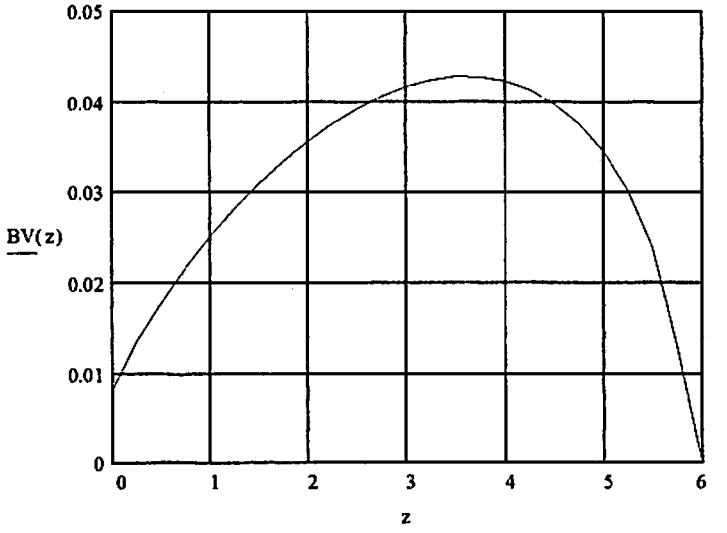

HEIGHT IN 100'S OF FEET

THE FOLLOWING TABLE GIVES TEMPERATURE, U AND V WIND COMPONENTS, LAPSE RATE IN 0C/100FT, BRUNT-VAISALLA FREQUENCY IN SEC-1, AND RICHARDSON NUMBER AS A FUNCTION OF HEIGHT IN FEET FOR THE B757 RUN #9 CASE.

z·100	T(z)	u(z)	v(z)	dTdz(z)	BV(z)	RI(z)	z·100
0	8.5	0.013	- 4.36	- 0.243	0.008	0.028	0
25	8.452	- 0.48	- 4.823	- 0.139	0.013	0.087	25
50	8.432	- 0.753	- 5.46	- 0.021	0.018	0.131	50
75	8.442	- 0.835	- 6.221	0.11	0.022	0.157	75
100	8.487	- 0.758	- 7.057	0.248	0.025	0.178	100
125	8.567	- 0.548	- 7.929	0.391	0.028	0.204	125
150	8.683	- 0.232	- 8.799	0.535	0.031	0.24	150
175	8.834	0.164	- 9.635	0.677	0.033	0.289	175
200	9.021	0.616	- 10.41	0.814	0.036	0.361	200
225	9.241	1.104	- 11.102	0.941	0.037	0.465	225
250	9.491	1.605	- 11.693	1.056	0.039	0.624	250
275	9.767	2.102	- 12.17	1.155	0.041	0.874	275
300	10.067	2.576	- 12.525	1.235	0.042	1.285	300
325	10.383	3.012	- 12.756	1.292	0.042	1.987	325
350	10.71	3.395	- 12.864	1.322	0.043	3.17	350
375	11.042	3.713	- 12.856	1.323	0.043	4.848	375
400	11.369	3.952	- 12.742	1.291	0.042	6.027	400
425	11.684	4.105	- 12.54	1.222	0.041	5.438	425
450	11.977	4.162	- 12.27	1.113	0.04	3.971	450
475	12.237	4.117	- 11.958	0.961	0.038	2.712	475
500	12.454	3.963	- 11.635	0.762	0.034	1.804	500
525	12.614	3.698	- 11.336	0.513	0.03	1.114	525
550	12.706	3.319	- 11.101	0.209	0.024	0.552	550
575	12.714	2.825	- 10.976	- 0.151	0.013	0.118	575
600	12.625	2.216	- 11.01	- 0.572	0.017i	- 0.146	600

ATTACHMENT C

A NOTE ON THE VOLPE CENTER METEOROLOGICAL DATA AND DISPLAY SYSTEM FOR IDAHO FALLS 1990

Version 2 as of December 1993

THE VOLPE CENTER METEOROLOGICAL DATA AND DISPLAY SYSTEM FOR IDAHO FALLS 1990

1. INTRODUCTION

The purpose of this memo is to describe the meteorological data and derived parameters taken during the 1990 wake vortex experiments which are available in a Volpe Center data display package of software for the PC. The meteorological data are from the Idaho Falls (IDF) instrumented tower and tethersonde. The software also displays vortex lateral displacement, height and strength data vs. time for each of the aircraft runs; these will also be briefly discussed. This paper focuses on the substance of the meteorological data and is not intended to be a user's manual for the software.

Figures 1 and 2 are images of two of the screens available from the Volpe Center display program. Each major element of these screens is described below.

2. SCREEN 1: VORTEX AND MET TOWER DATA

Figure 1 shows Screen 1 with vortex plots from B-757 Run 9 displayed along with corresponding vertical atmospheric profile data from the tower. Up to nine separate runs can be simultaneously displayed on this screen. The legend in the upper-right identifies the symbols used to distinguish the vortices (V1 is downwind and V2 is upwind) and the types of sensors used (lidar (LDV) or acoustic (MAV)).

2.1 LATERAL VORTEX DISPLACEMENT

The upper-left window shows plots of lateral displacement (ft) vs. time (sec) of the vortex pair. When the paths are "upward", as in this figure, the vortices drift towards the tower and across the array of acoustic sounders; this is the desired configuration for a successful run, and data will generally be complete in the other two top windows. Note that the time axes are adjustable with a maximum range of 240 seconds.

2.2 VORTEX HEIGHT

The upper-center window shows traces of vortex height (ft) vs. time (sec).

2.3 VORTEX STRENGTH

The upper-right window in Fig. 1 displays vortex strength, defined as average circulation (ft^2/sec) over a selected radius, vs time (sec). In the figure, the legend shows that a radius of 30

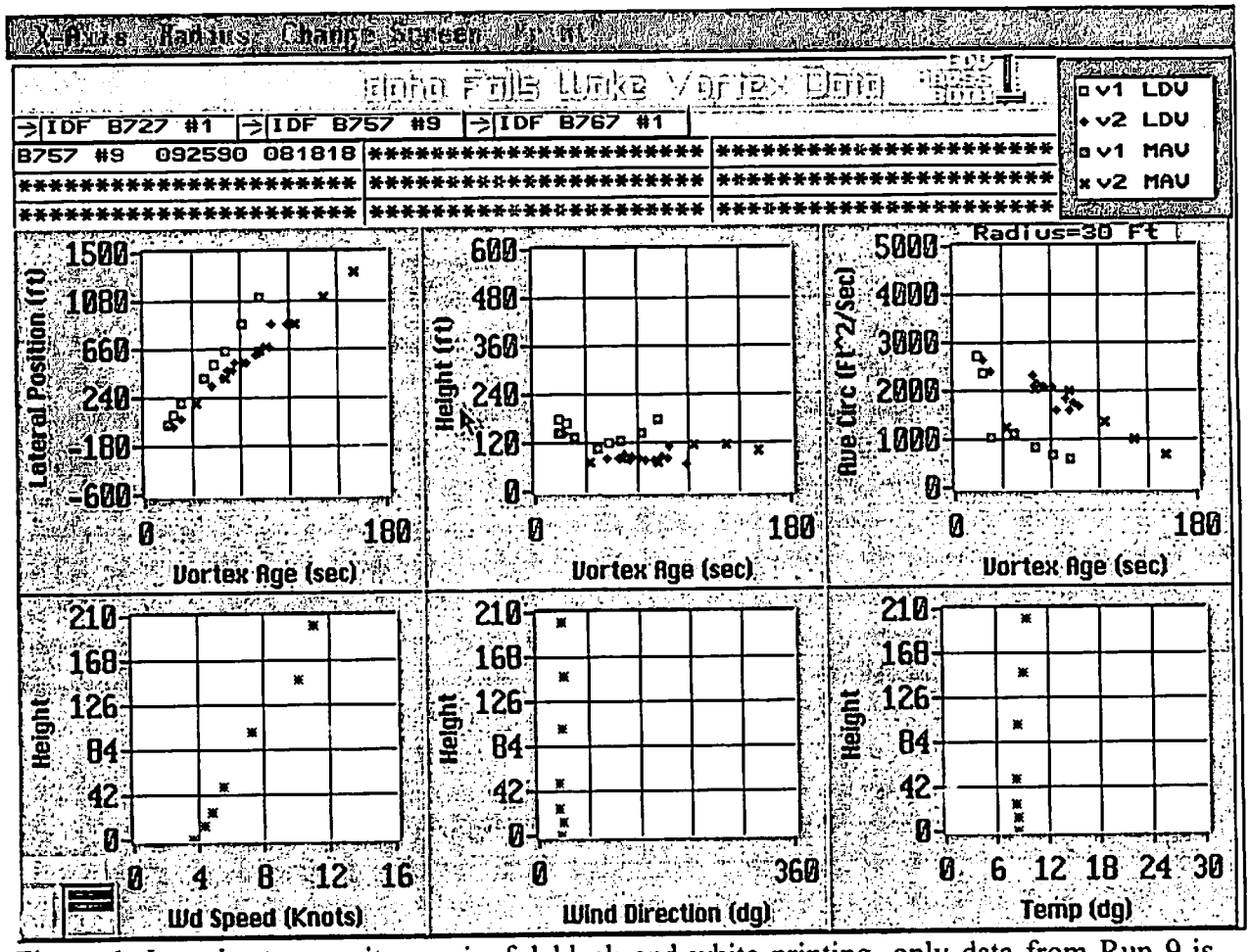

Figure 1. In order to permit meaningful black and white printing, only data from Run 9 is included.

feet was selected for this display.

2.4 WIND SPEED PROFILE

The lower-right window displays the windspeed (three minute average in knots) vs. height (ft) from seven levels on the instrumented tower (6.25, 12.5, 25, 50, 100, 150, and 200 ft).

2.5 WIND DIRECTION PROFILE

The lower-center window displays the wind direction (deg. true) vs. height (ft) at the seven instrumented levels.

As a quality check, one can compare the wind speed normal to the flight path (derived from the speed and direction profiles) at the level of the vortex (seen on the height vs. time trace) with the lateral drift rate derived from the slope of the lateral displacement trace. In Figure 1, we can use Run 9 to derive a lateral speed of V1 as approximately 10.5 ft/sec or 6.2 knots. On the height trace, V1 remains at about 80 to 100 ft.; therefore, we check the wind component at this level for consistency. From the wind direction profile, we see that the wind is from the NNE (about 25 to 30 deg.) which is nearly parallel to the acoustic array; therefore, the speed of 6 to 7 knots at 80 to 100 ft. is consistent with the lateral drift rate.

2.6 TEMPERATURE PROFILE

The lower-right window displays temperature (C) vs height (ft) at the defined seven levels from the instrumented tower.

3. SCREEN 2: METEOROLOGICAL DATA

Figure 2 displays wind direction, speed, and temperature data profiles from the tower and tethersonde. This screen is also used to display the derived parameters: Dewpoint temperature, Richardson Number (Ri), Lapse Rate (LR), and Brunt-Vaisalla Frequency (N). Dry adiabats (neutral stability curves) can also be shown as temperature gradient references. Temperature gradients which are steeper than the dry adiabats are unstable, and gradients that are less steep are stable. The tethersonde is a tethered balloon carrying an instrument package which was reeled up and down between altitudes of 100 and 800 ft and paused at several points to record data. These soundings were made frequently during the experimental flyby runs, but are not synchronized with them. Therefore, one must choose a tethered sounding representative of a desired flyby on the basis of the date and time, not on the sounding number. Because the soundings are made on the basis of pressure, the values will not be recorded at the same geometric heights from sounding to

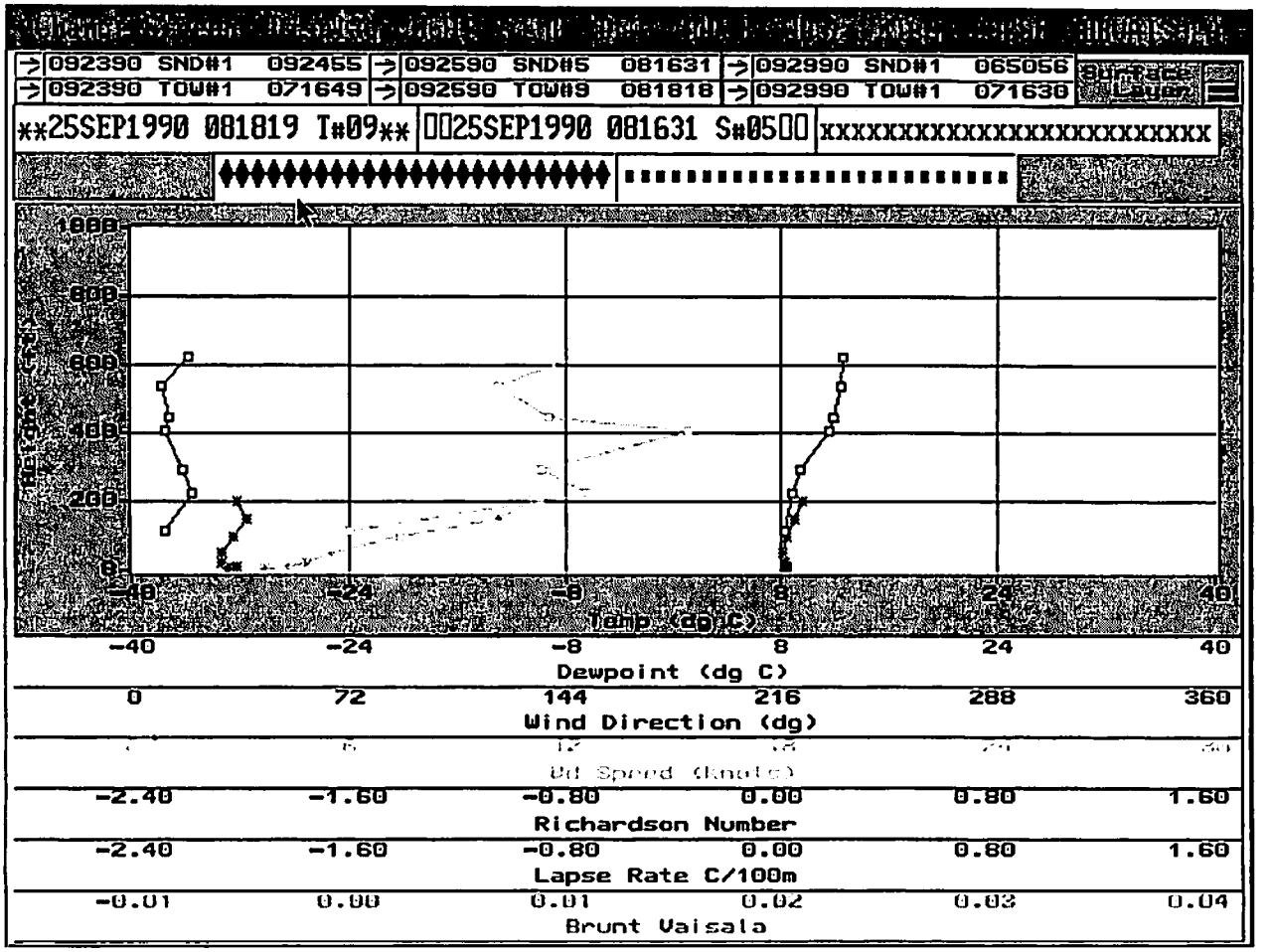

Figure 2. This plot of meteorological data has been simplified to permit the use of black and white printing.

The vertical profiles include only wind direction (left), wind speed (middle) and temperature (right). Both tower and tethersonde data are included. Apart from a displacement of the wind direction, the two sources of data generally agree.

sounding. It is possible to plot up to three soundings simultaneously, and one can turn any of the plotted parameters off and on using the screen controls. The ranges of the height and the plotted parameter scales can be changed using other screen controls.

3.1 MEASURED PARAMETERS

The software displays the following measured tower and tethersonde parameters:

- o Air Temperature plotted in black (C)
- o Wind direction plotted in blue (deg. true)
- o Wind speed plotted in yellow (knots)
- o Wetbulb temperature (not displayed). This is defined as the temperature an air parcel would have if cooled adiabatically to saturation at constant pressure by evaporation of water into it, all latent heat being supplied by the parcel.
- o Dewpoint Temperature from the tethersonde only plotted in purple (C). This is actually calculated from the wetbulb information, and is defined as the temperature to which the air must be cooled at constant pressure and constant water-vapor content in order for saturation to occur.

As a quality check, one can compare the measured parameters from the sounder with those from the tower for nearly coincident date/times. For example, the legend in the upper-left indicates that the tower run is from 0818 and 16 seconds. The sounding is from 0816 and 31 seconds. We see that the wind direction (the far left curve) is about 15 deg at 120ft, and about 20 deg at just over 200ft. These are slightly more northerly than from the tower data (the next curve to the right), but are reasonably consistent considering the instrumentation used and the typical problems encountered in performing field measurements. The tethersonde wind speeds in the overlap range (the next pair of curves to the right) match up quite well with the tower values (6 vs.7 knots at around 100 ft, and a virtual match of 12 knots at 200 ft.), as do the temperatures shown as the last pair of curves.

3.2 DERIVED PARAMETERS

All derived parameters depend on centered finite differences of measured parameters; therefore, they are plotted at the midpoints of the layers bounded by each pair of measurement

levels.

3.2.1 Richardson Number (Ri)

Ri is plotted in white in three selectable scale ranges. Ri is defined as follows:

$$Ri = (g / T_m) (\Delta T / \Delta z + \lambda) / (\Delta \underline{u} / \Delta z)^2 \qquad (1)$$

where: T_m = vertical mean temperature in a layer (K)
g = acceleration of gravity (32 ft/sec^2)
$\Delta T / \Delta z$ = the vertical gradient of temperature (C/ft); the "lapse rate"
Δ indicates a finite vertical difference of the particular parameter,
λ = the negative of the dry adiabatic lapse rate (0.3 deg. C/100ft),
$\Delta \underline{u} / \Delta z$ = vertical vector wind shear (sec^{-1})

Ri is commonly used as a bulk atmospheric parameter to indicate the possible presence of turbulence in a layer and/or to classify an airmass as to its turbulence potential. Observations have shown that a value of Ri = 0.25 is often a critical threshold such that for Ri < 0.25, there can be a relatively sudden onset of turbulence (wind shear dominating atmospheric stability), and for Ri > 0.25, laminar flow will tend to prevail. Very small or negative values of Ri strongly suggest turbulence in a layer, while the opposite is true for positive values larger than 0.25. When the ambient temperature lapse rate is adiabatic (i.e., $\Delta T / \Delta z = -\lambda$), then Ri = 0 and the stability is neutral.

It should be noted in (1) above that the formulation of Ri is derived in a straight forward manner from the common definition found in various references such as the *Glossary of Meteorology* (Huschke, 1959). Using IDF tower data, NOAA also produced a value of what they termed the Richardson Number based, essentially, on the following formula (Clawson, 1990):

$$RN = (g / T_m)(\Delta T / \Delta z) / (\Delta u / \Delta z)^2 \qquad (2)$$

where the terms are defined as in (1) except for the wind shear in the denominator of (2) which uses the vertical difference of the wind speed regardless of direction. Note that the numerator of (2) does not contain the sum of the actual and dry adiabatic lapse rates as in (1). Therefore, from (2), if the lapse rate is isothermal (i.e., $\Delta T / \Delta z = 0$, which is usually considered to be stable), Ri will be positive (the expected result) but RN = 0. Furthermore, when the stability is neutral by conventional reasoning (i.e., $\Delta T / \Delta z = -\lambda$, and Ri = 0), expression (2) shows that RN will be negative. Also in (2), the use of the wind shear term ($\Delta u / \Delta z$) can yield some unfortunate results.

For example, if the wind direction were to reverse from the bottom to the top of the tower with no change in speed, the denominator in (2) would be zero and the magnitude of RN would be infinite; whereas, the denominator in (1) would be non-zero, and the magnitude of Ri would be bounded, which would more properly reflect the impact of wind shear on turbulence potential.

An objective of the current Volpe Center effort is to process the NOAA tower data in a manner similar to what has been accomplished with the tethersonde data. Definition (1) will be used for the Richardson Number, and it is recommended that the values of Richardson Number published by NOAA for the tower (Clawson, 1990) should not be used due to the form of expression (2).

3.2.2 Temperature Lapse Rate

The lapse rate (LR) of temperature alone (plotted in brown) can also be used to classify the turbulence potential of a layer. In particular, the U.S. Nuclear Regulatory Commission has identified the following seven potentially useful lapse rate classes for specifying diffusion conditions in the atmospheric boundary layer:

A. Extremely Unstable:	LR < -1.9 C/100m
B. Moderately Unstable:	-1.9 ≤ LR < -1.7 C/100m
C. Slightly Unstable:	-1.7 ≤ LR < -1.5 C/100m
D. Neutral:	-1.5 ≤ LR < -0.5 C/100m
E. Slightly Stable	-0.5 ≤ LR < 1.5 C/100m
F. Moderately Stable	1.5 ≤ LR < 4.0 C/100m
G. Extremely Stable	LR ≥ 4.0 C/100m

In particular, using these classes, we might assume that turbulence is highly likely for classes A - C, and probable for class D, especially in the presence of heating, moderate wind shear and/or flow over rough terrain.

3.2.3 Brunt-Vaisalla Frequency (N)

The Brunt-Vaisalla frequency (or buoyancy frequency) is the frequency of oscillation of a parcel of air that has been subjected to a vertical perturbation. N is defined as:

$$N = ((g/T_m)(\Delta T / \Delta z + \lambda))^{1/2}$$

In neutral conditions, N = 0, no accelerating force exists, and the displaced parcel will be in

equilibrium with its environment. In stable conditions, $N > 0$, and the parcel oscillates about its original level with a period of $\tau = 2\pi / N$. In unstable conditions N is imaginary and represents an exponentially growing displacement with time. N can be seen in the numerator of Ri, and is used in Greene's analysis (1986) to characterize vortex decay as a function of atmospheric stability.

4. REFERENCES

Clawson, K.L., 1990: NOAA Meteorological Data Summary, Wake Vortex Research Data Package No. NOAA-1, USDOC/NOAA/ERL, 1750 Foote Dr. Idaho Falls, ID 83402.

Greene, G.C., 1986: "An approximate model of vortex decay in the atmosphere", *J. Aircraft*, 23, No. 7.

Huschke, R.E., ed., 1959: Glossary of Meteorology, American Meteorological Society, Boston, MA.

ATTACHMENT D

MAVSS RAW DATA

ATTACHMENT D

MAVSS RAW DATA

The Monostatic Acoustic Vortex Sensing System (MAVSS) records vortex backscatter data from vertically pointing acoustic antennae operating at 2.95 or 3.60 kHz. The pulse width was 20 msec at half amplitude and the pulse repetition period was 458 msec. At Idaho Falls eight MAVSS antennae were installed with 250-foot spacing downwind of the instrumented tower. Antenna 1 was adjacent to the tower; after passing the tower, a vortex reached the higher numbered antennas in turn at later times. Only a few vortices lasted long enough to reach the last antenna (number 8).

A number of halftone display formats were developed to visualize the vortex signals and to detect anomalies in the vortex signals:

1) The first display (file extension .CHn, where n = antenna number) shows the amplitude of the vortex return (blacker for greater return signal) as a function of height (235 feet maximum height) and elapsed time (four minutes total, 535 pulse periods). The aircraft noise appears at the left and the vortex signals appear when the vortex pair reaches the location of each antenna. The vortex scatters much more than the ambient atmosphere at this early morning time (8:18 am, 9/25/90). The upper picture has a factor of five higher gain. The signal has been multiplied by a linear ramp as a function of range to give uniform sensitivity as a function of range. This ramp causes noise, such as the initial aircraft noise, to become darker for higher ranges.

   In the low numbered antennae there is a large return from the vortex core (dark spot) with a lower return from a region around the core. The strong core scattering occurs when the core diameter core is small and the core is oriented perpendicular to the acoustic beam. Noise streaks are also sometimes observed when the core is over the antenna; these are likely associated with the swishing noise heard from small-core wake vortices.

   Apart from these anomalies, the vortex return comes from scattering from density fluctuations imbedded in the vortex flow field. This scattered signal is doppler shifted by the vertical (i.e., line-of-site) component of the flow. There are large fluctuations in the amplitude of the return (much like laser speckle) because of coherent scattering from distributed scatterers.

   [Note that antenna 8 has an abnormally low signal.]

2) The second display (file extension .FTn, where n = antenna number) shows the spectrum for 23 overlapping range gates (32 msec long, each displaced by 16 msec). The spectra for successive range gates after each transmitted pulse are plotted vertically. Within each range gate 22 spectral points are displayed with the transmitted frequency located in the middle. The aircraft noise shows up as a broad spectrum on the left and the zero vertical ambient wind as a narrow peak at the transmitted frequency. The vortices show up as nonzero vertical winds. The region between the two vortices experiences a downdraft (increase in doppler frequency, up in display) and the region outside the vortices

experiences an updraft (decrease in doppler frequency, down in display). Since the acoustic beam is too large to resolve the vortex core velocities, a large frequency spread is noted near the cores.

The dark reflection near the core shows up as an unshifted frequency component because it comes from the vortex core which has little vertical motion and not from the imbedded density fluctuations that move with the vortex flow. This core reflection is observed through antenna 5 (age 106 seconds) for the second vortex. Thus, the small B-757 vortex core lasted for at least 106 seconds.

Spectral processing is essential to determine the vortex location, which is signaled by a reversal in the sign of the doppler shift. The first vortex can be seen out to antenna 6 but not in antenna 7. The second vortex can be seen out to antenna 7 but in not antenna 8.

The MAVSS spectra are processed to generate vertical velocities for each range gate.

3) The MAVSS velocity plots are labeled with a file name with extension .VWn, where n is the antenna number. The velocity algorithm used is good for vertical winds but will reject the large wind gradients near the vortex cores. The raw velocities are noisy because of coherent interference effects.

4) A median filter can be used to reduce the noise of the MAVSS vertical velocities so that the actual ambient vertical wind can be observed.

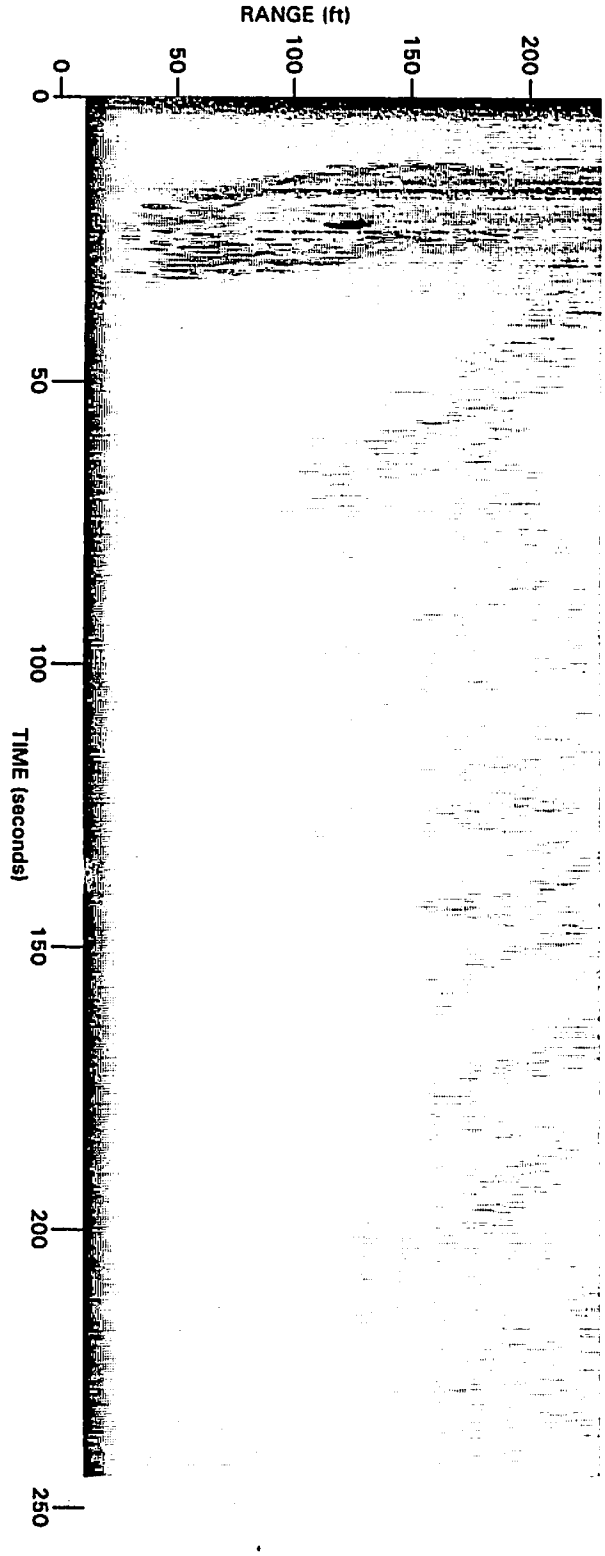

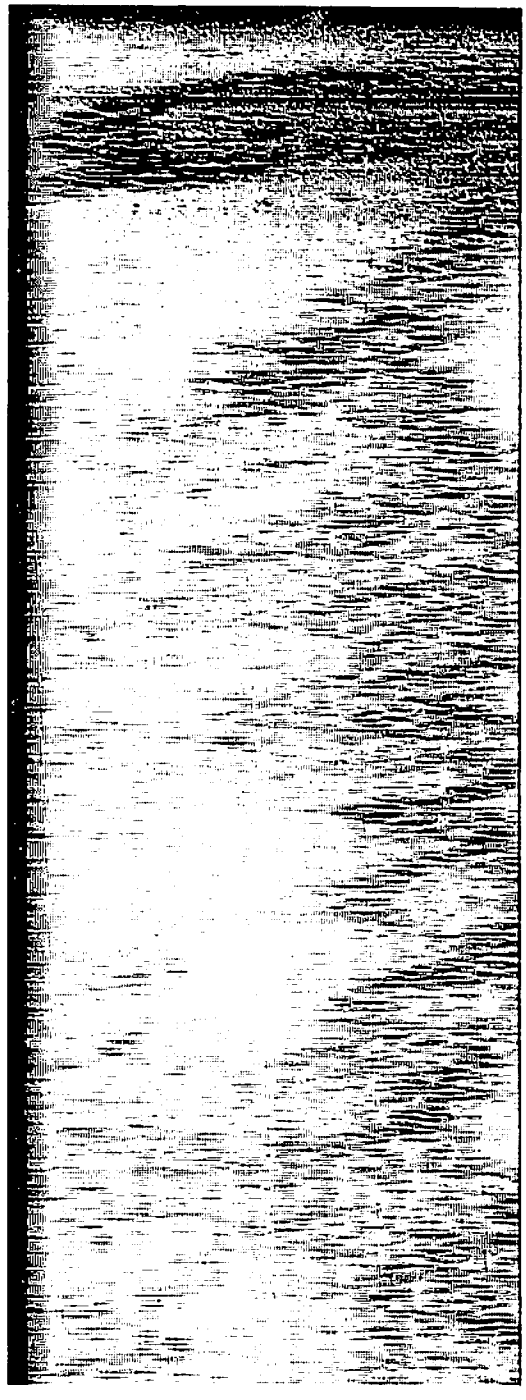

B757RN09.CH1

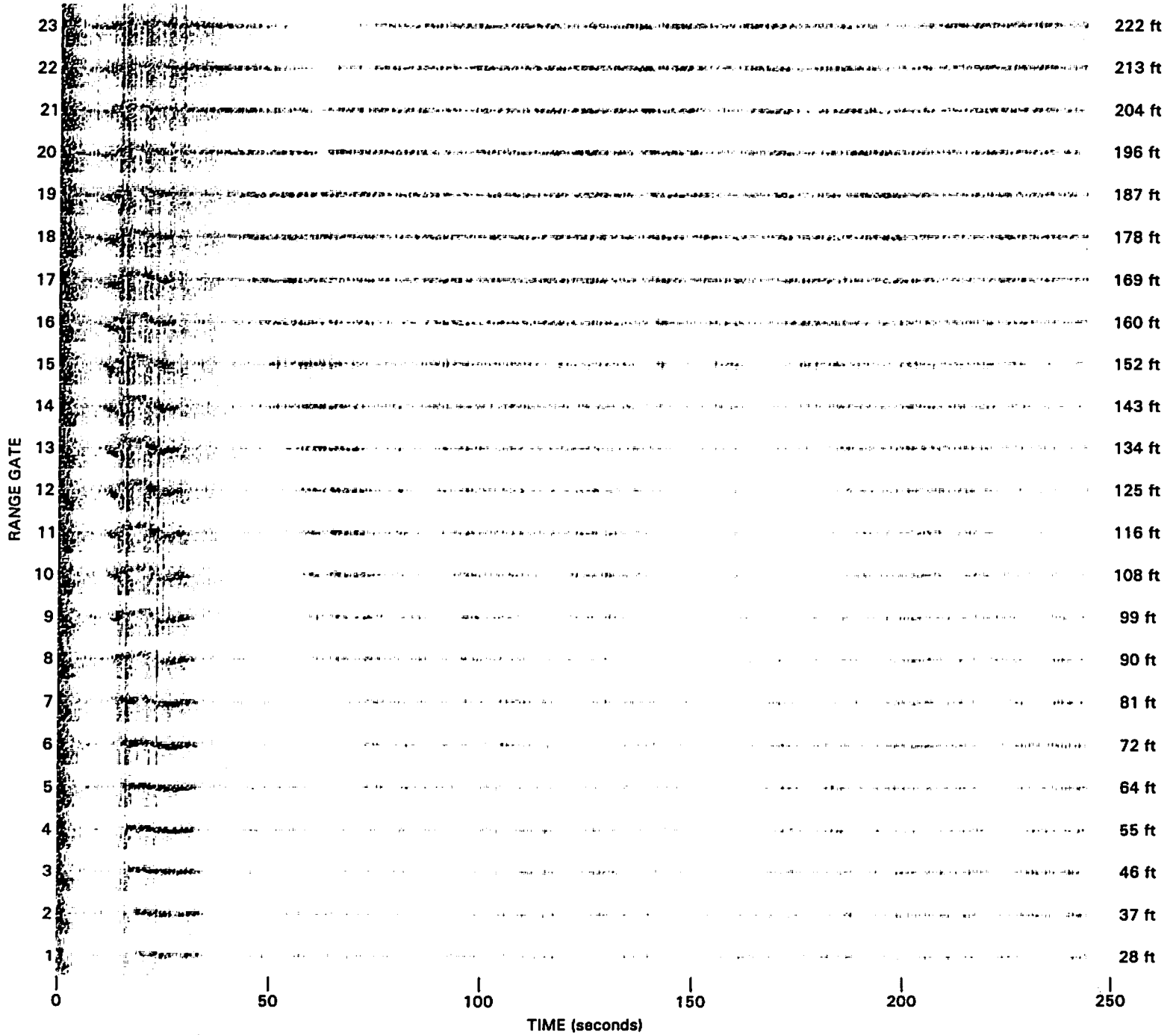

B757RN09.FT1

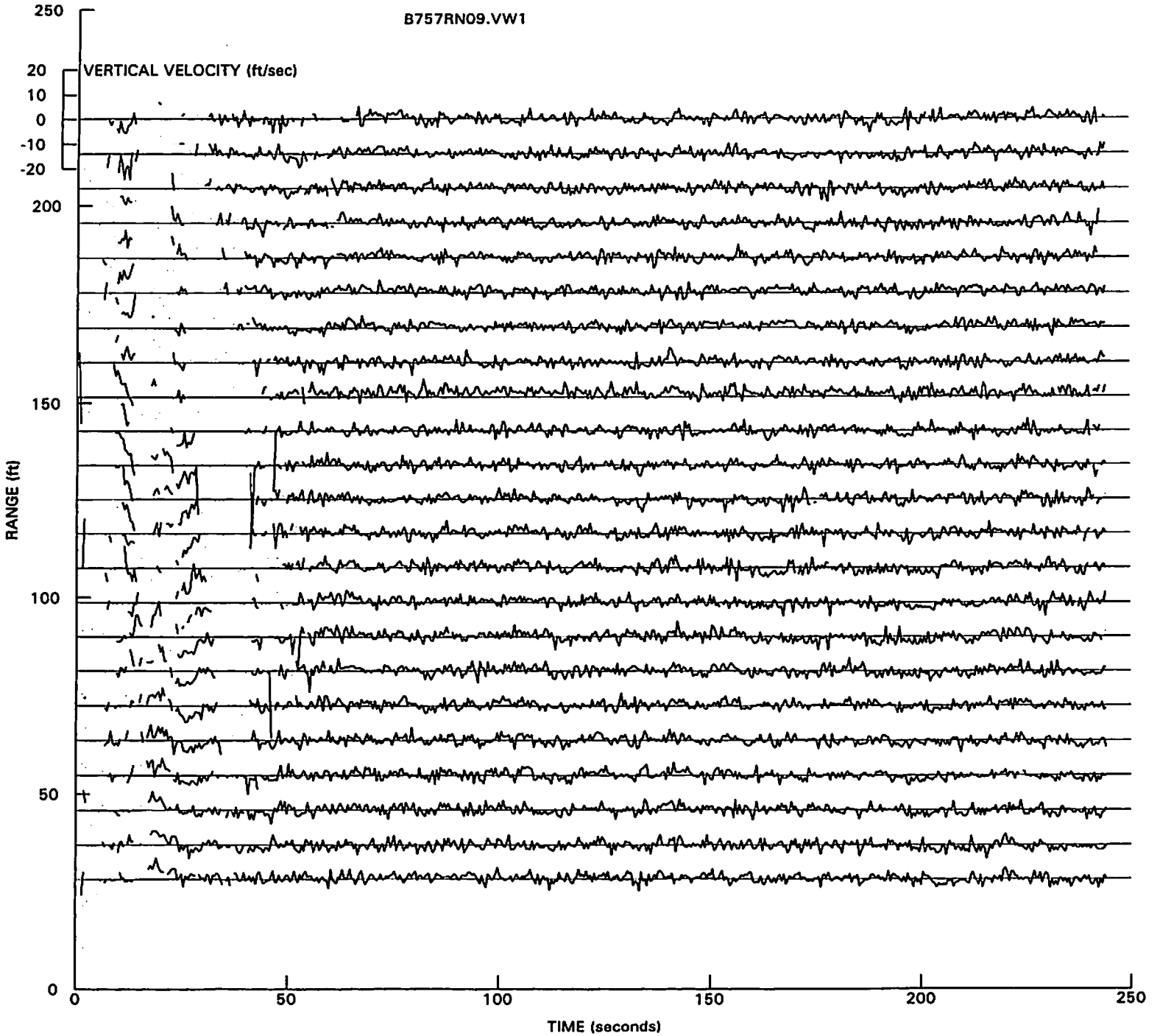
B757RN09.VW1
VERTICAL VELOCITY (ft/sec)
20
10
0
-10
-20
250
200
150
100
50
0
RANGE (ft)
0
50
100
150
200
250
TIME (seconds)

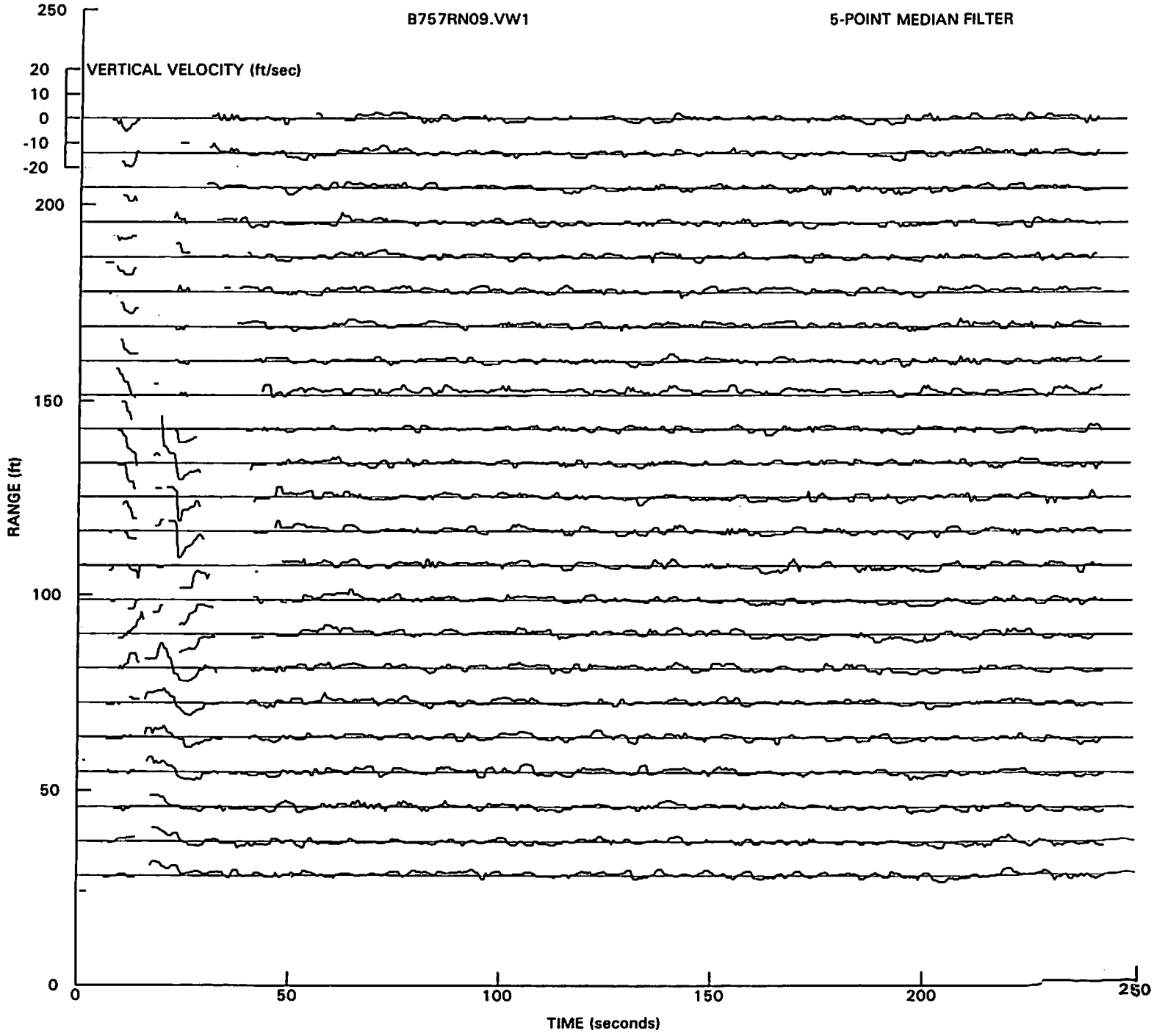
B757RN09.VW1
5-POINT MEDIAN FILTER
VERTICAL VELOCITY (ft/sec)
250
20
10
0
-10
-20
200
150
100
50
0
RANGE (ft)
0
50
100
150
200
250
TIME (seconds)

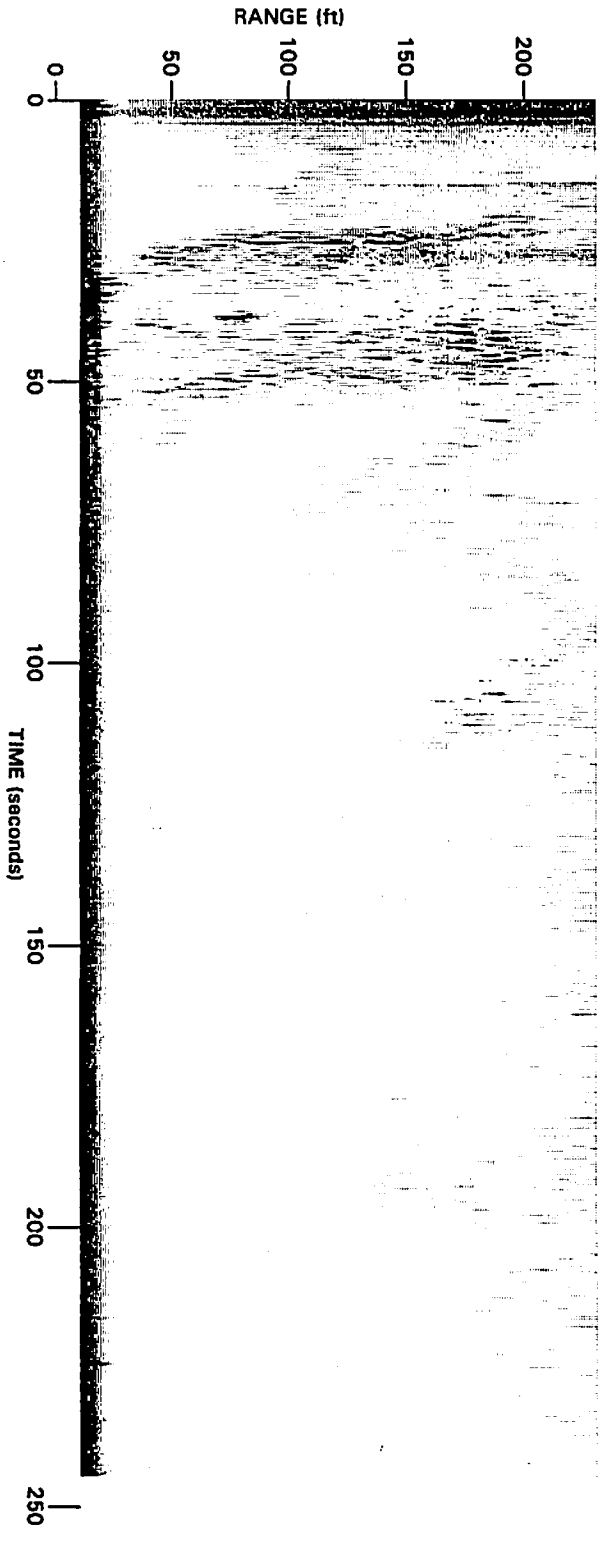

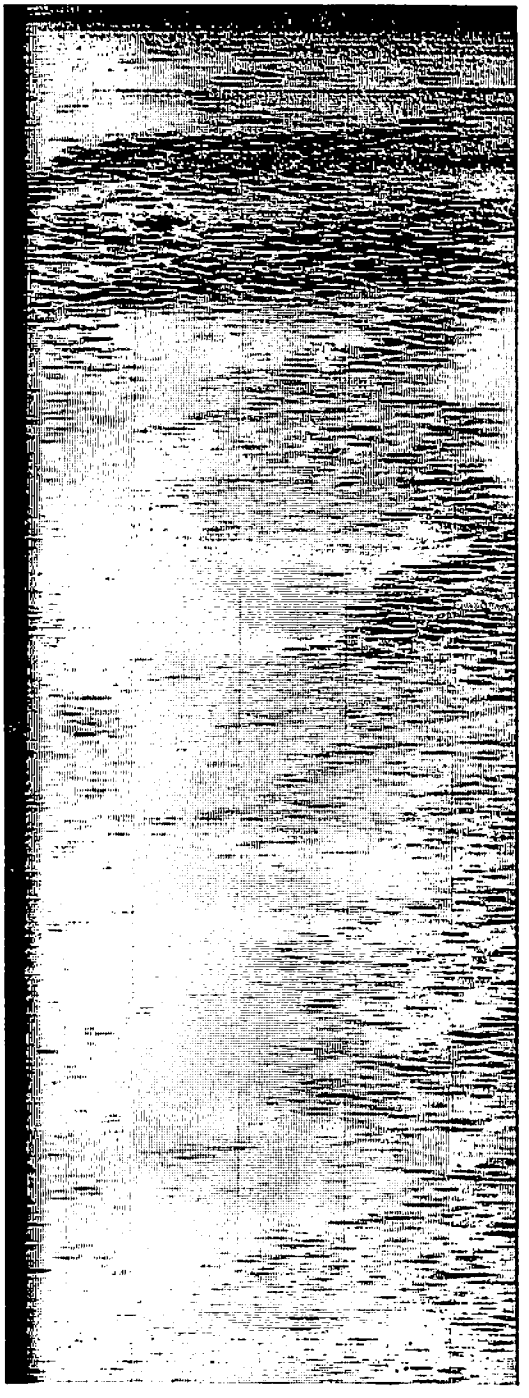

757RN09.CH2

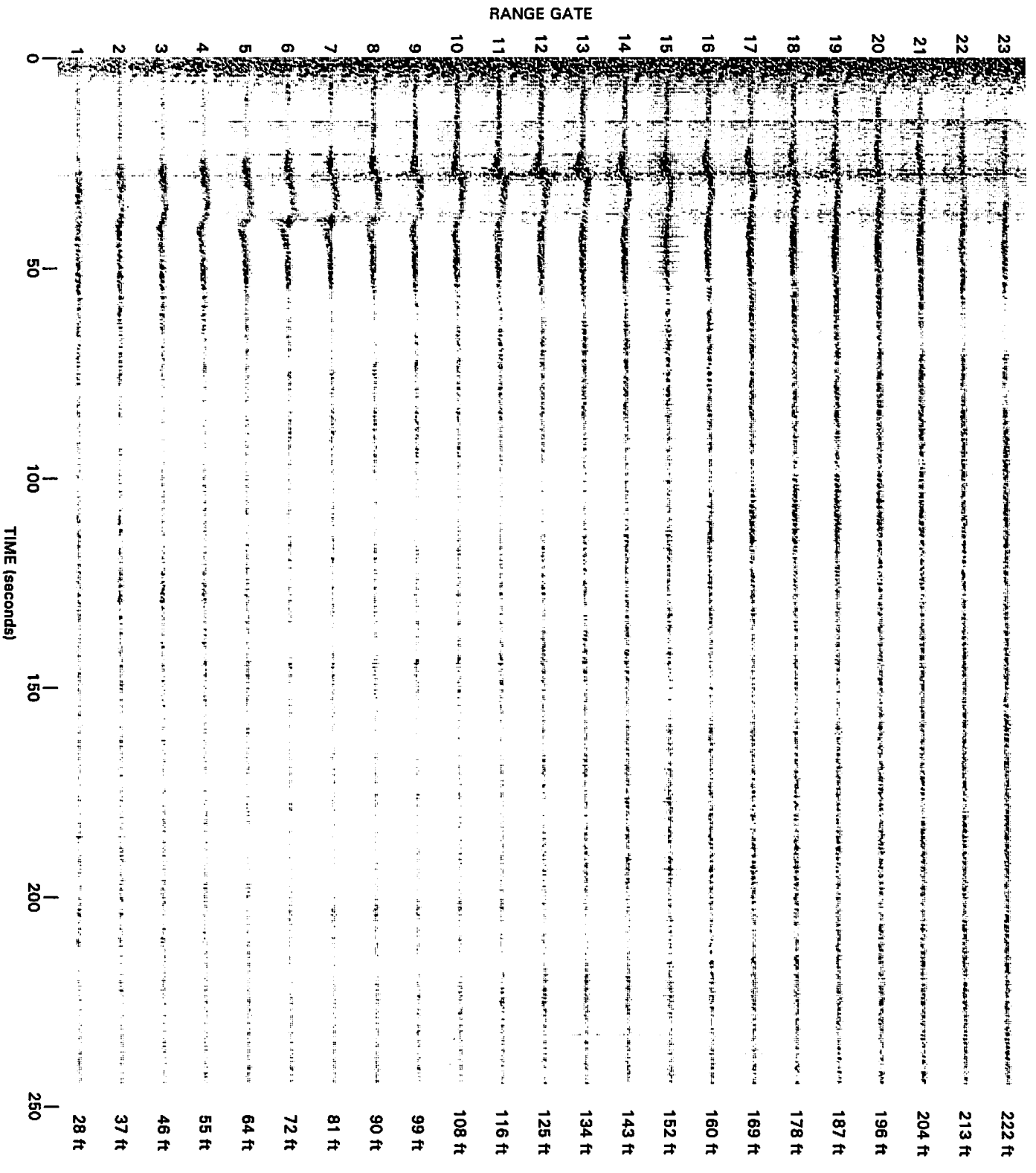

B757RN09.FT2

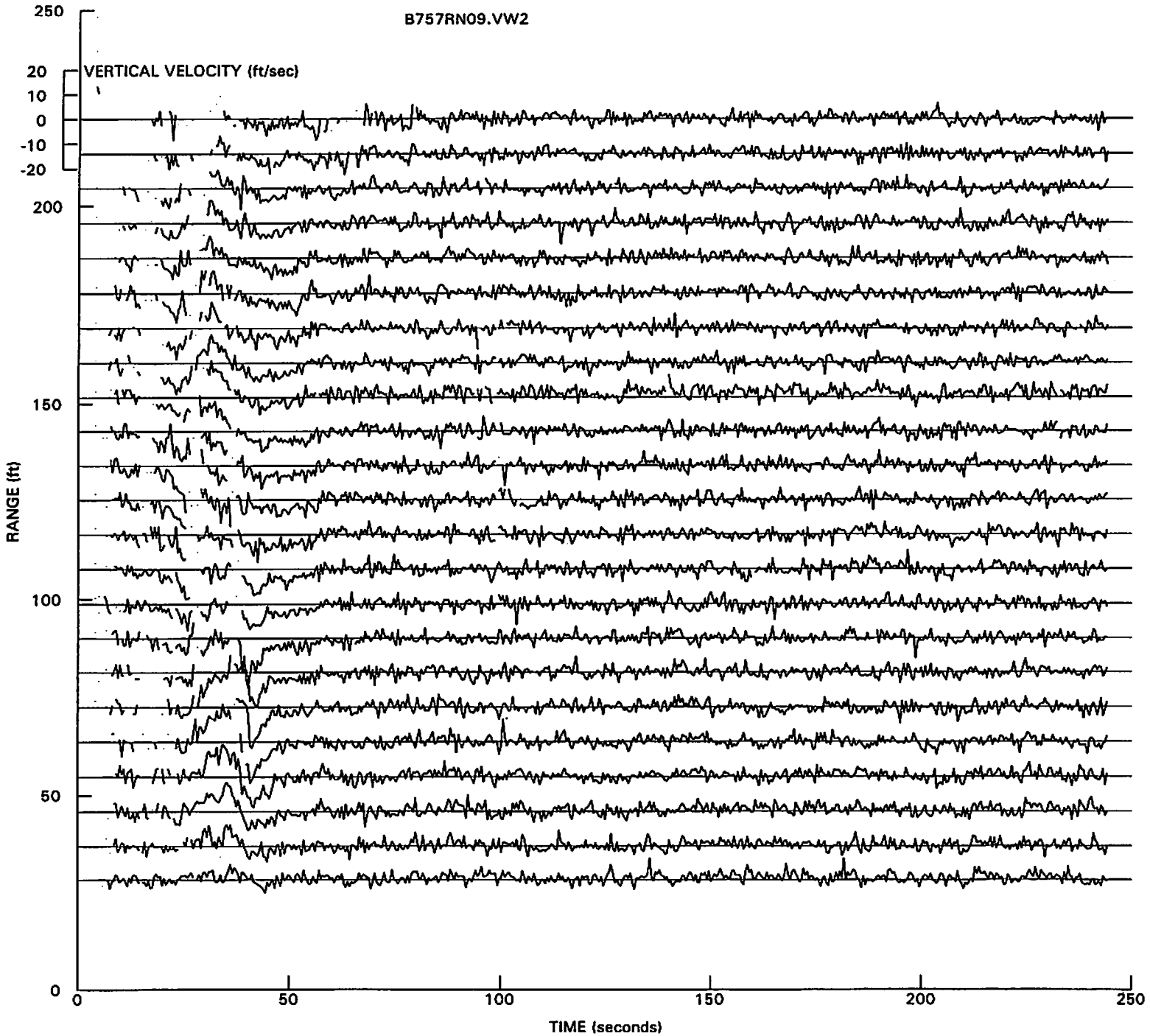
B757RN09.VW2
VERTICAL VELOCITY (ft/sec)
20
10
0
-10
-20
250
200
150
100
50
0
RANGE (ft)
0
50
100
150
200
250
TIME (seconds)

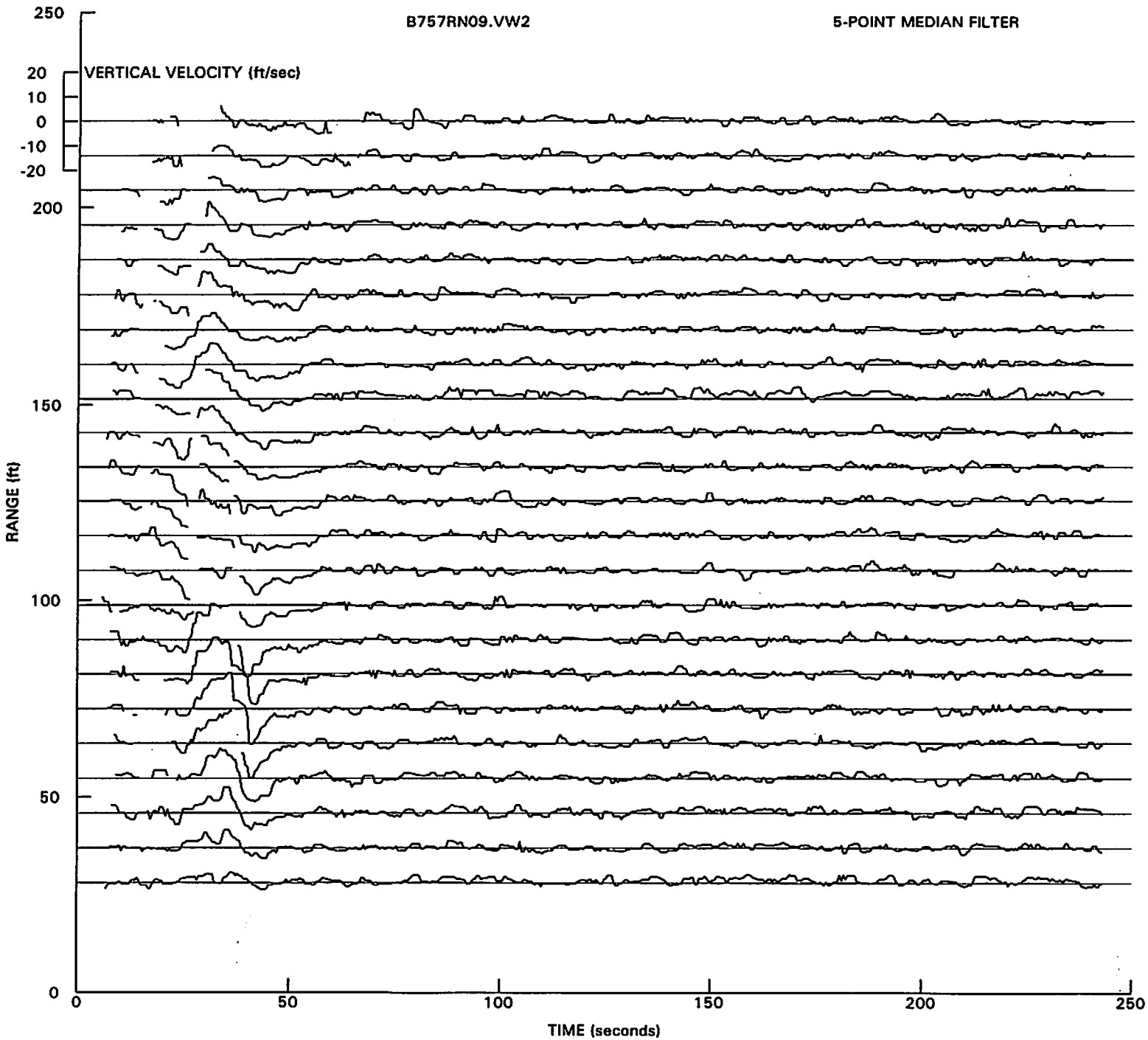
B757RN09.VW2
5-POINT MEDIAN FILTER
VERTICAL VELOCITY (ft/sec)
20
10
0
-10
-20
RANGE (ft)
250
200
150
100
50
0
0
50
100
150
200
250
TIME (seconds)

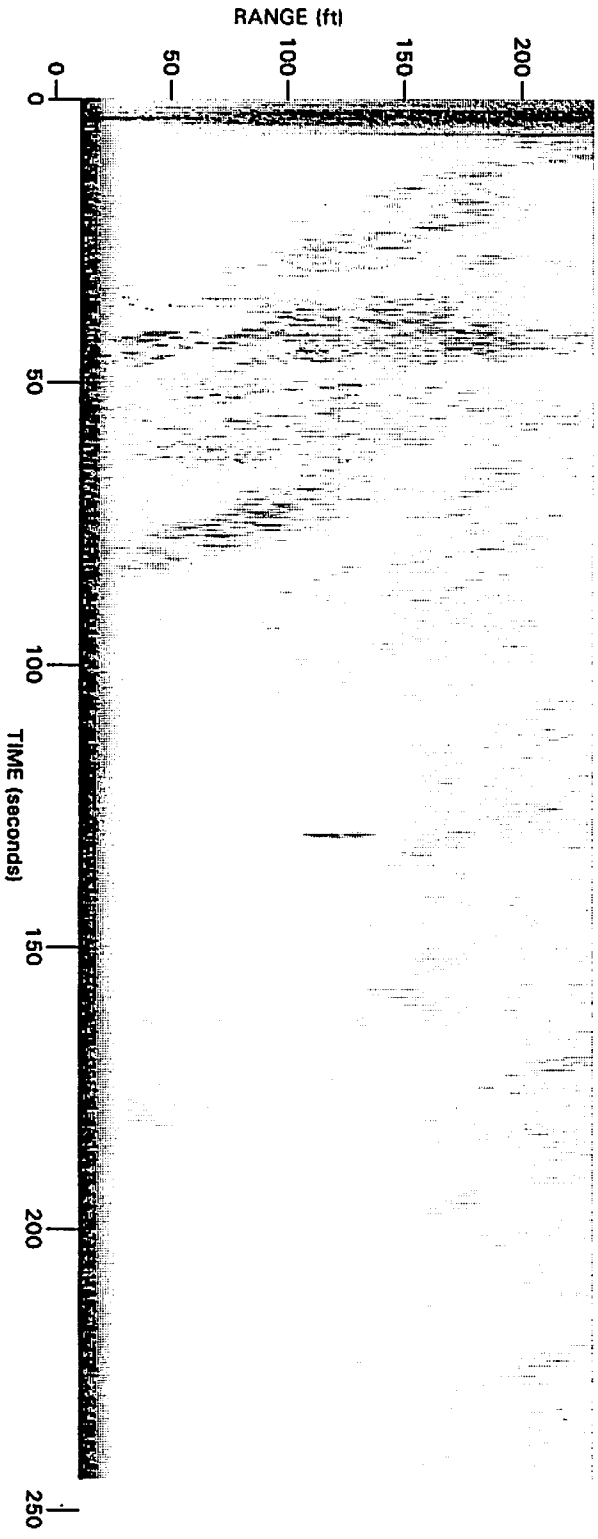

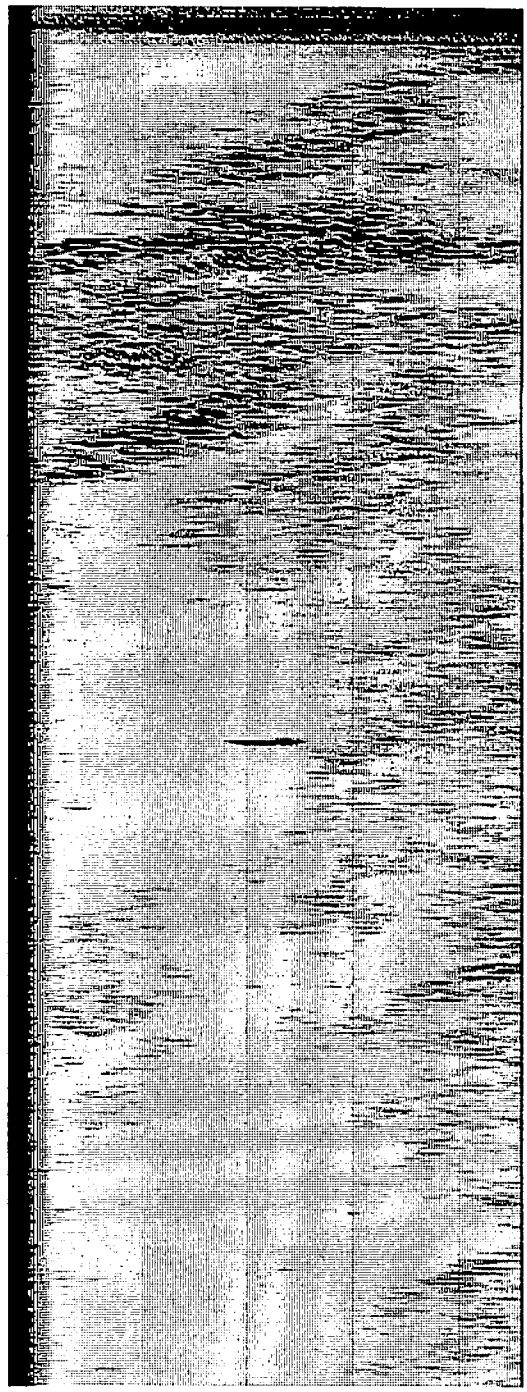

B757RN09.CH3

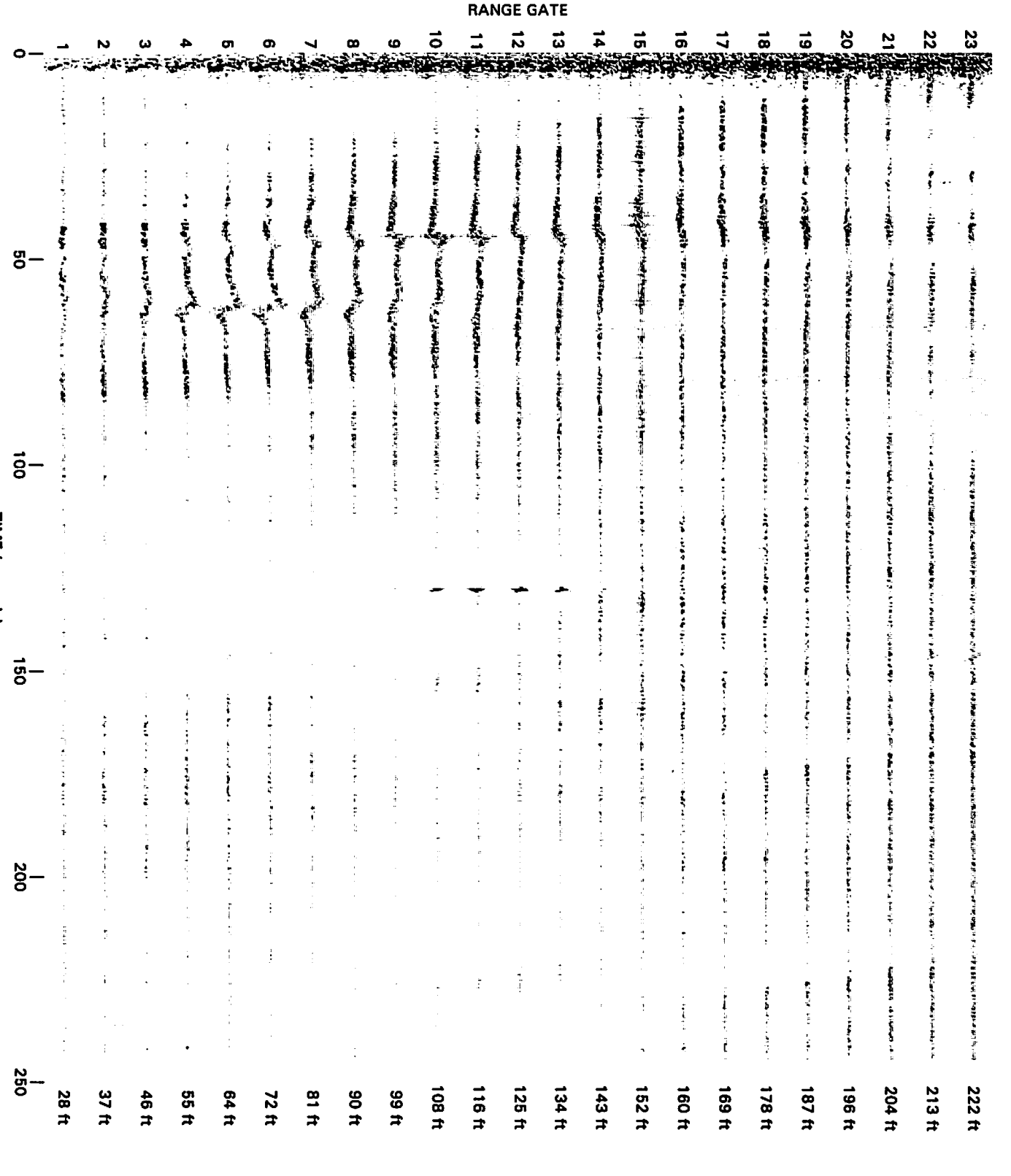

B757RN09.FT3

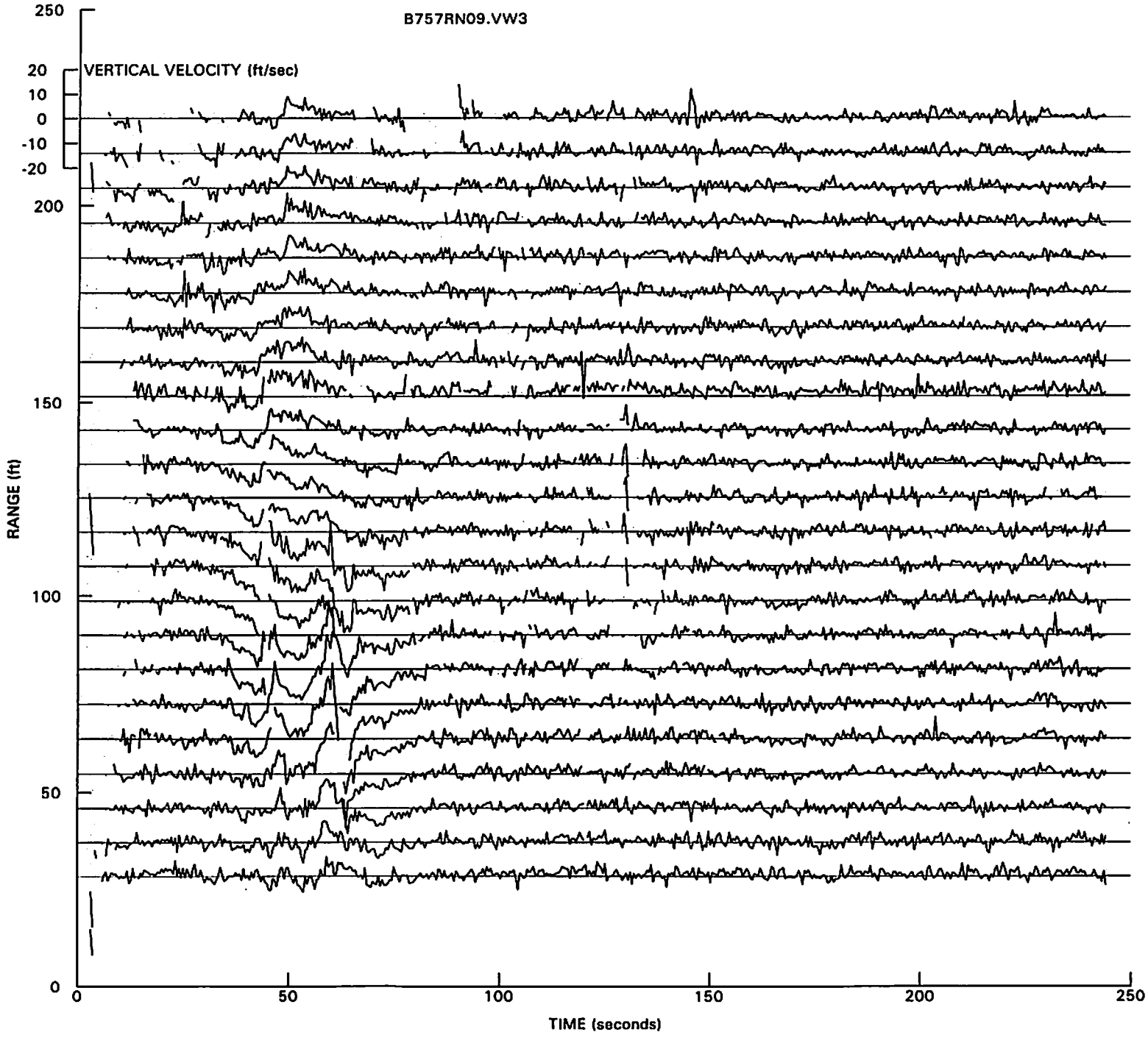
B757RN09.VW3
VERTICAL VELOCITY (ft/sec)
20
10
0
-10
-20
250
200
150
100
50
0
RANGE (ft)
0
50
100
150
200
250
TIME (seconds)

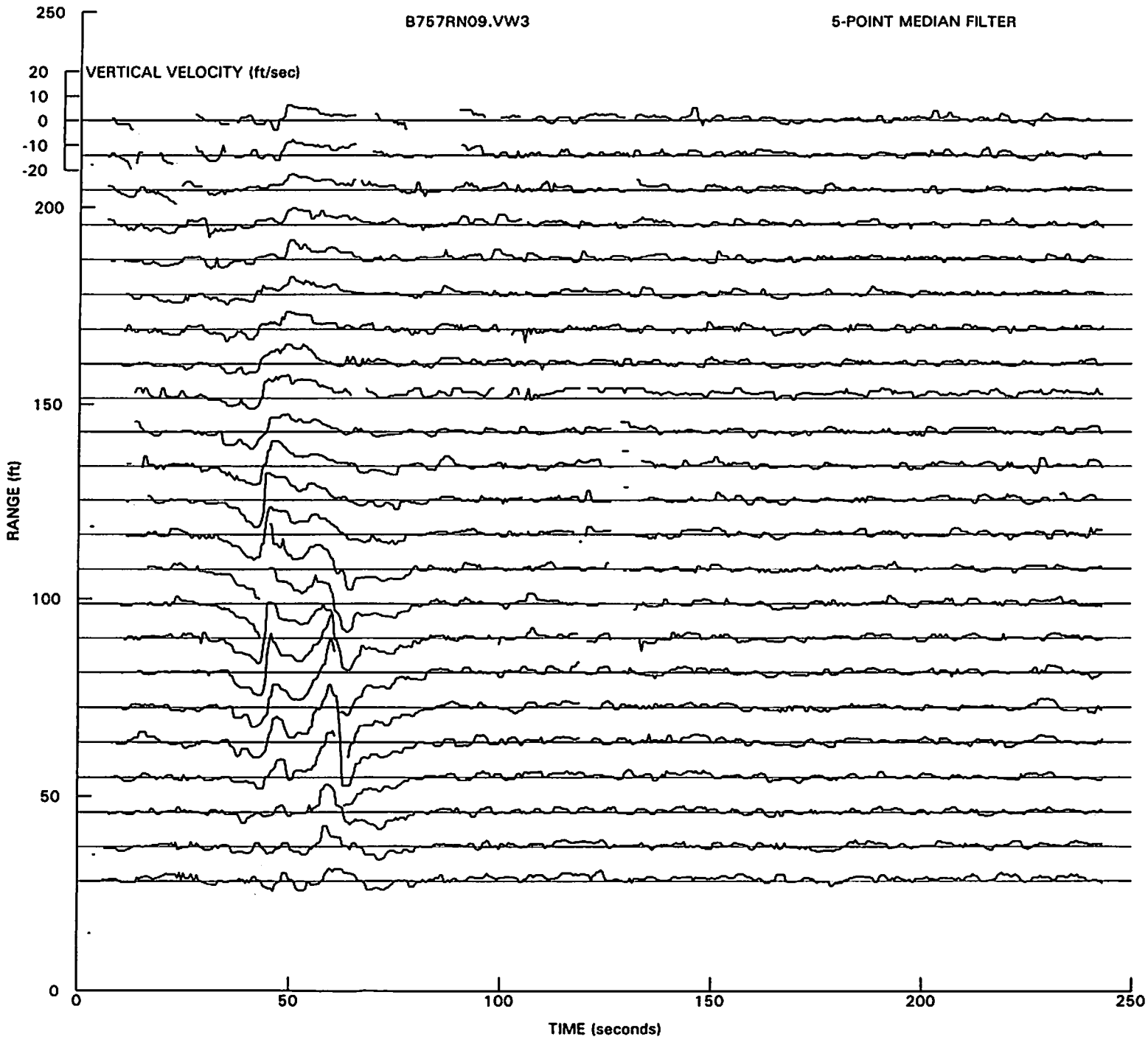
B757RN09.VW3
5-POINT MEDIAN FILTER
VERTICAL VELOCITY (ft/sec)
20
10
0
-10
-20
250
200
150
100
50
0
RANGE (ft)
0
50
100
150
200
250
TIME (seconds)

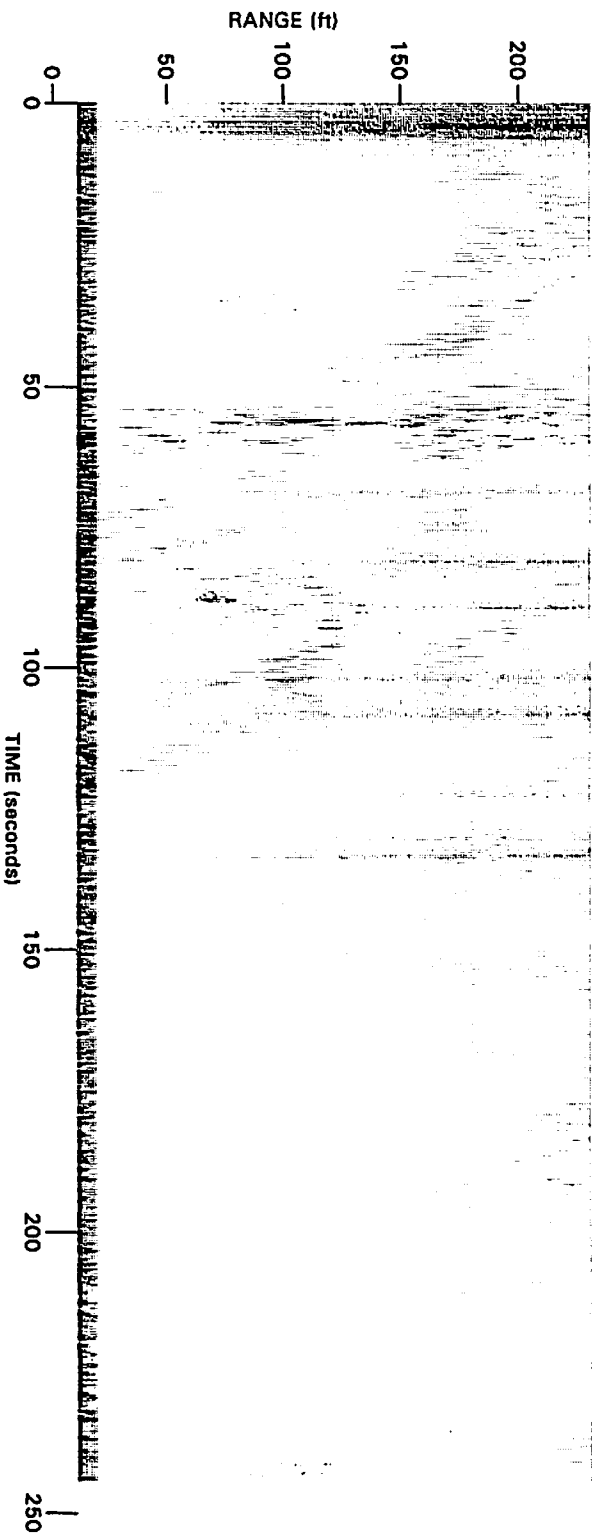

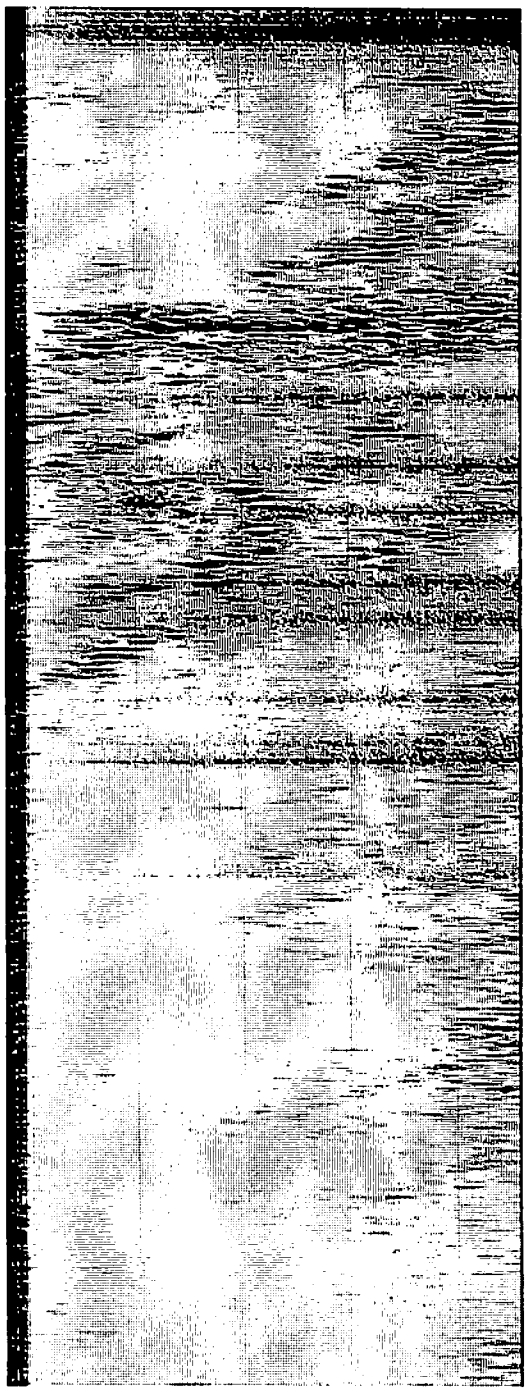

B757RN09.CH4

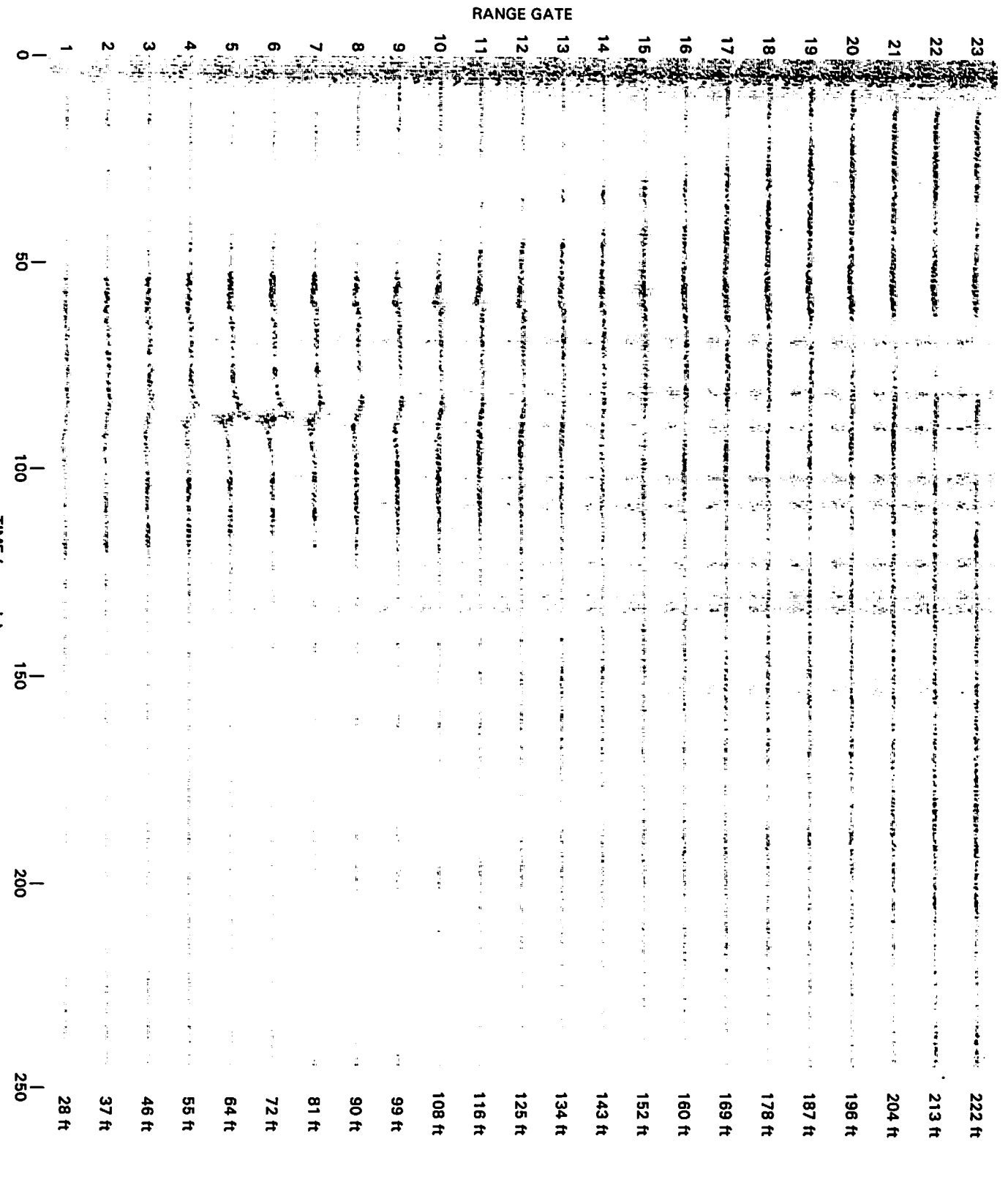

B757RN09.FT4

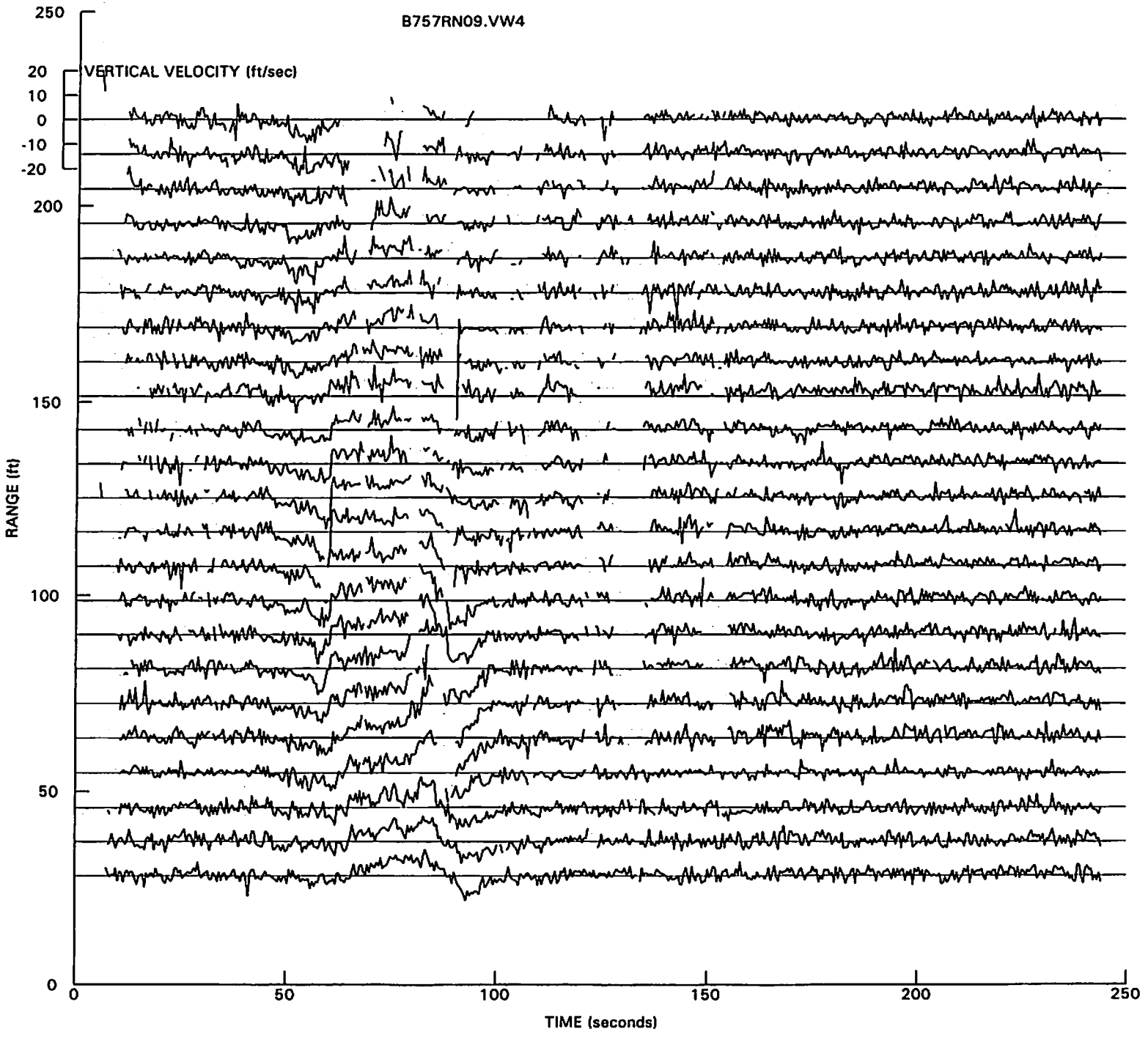
B757RN09.VW4
VERTICAL VELOCITY (ft/sec)
20
10
0
-10
-20
250
200
150
100
50
0
RANGE (ft)
0
50
100
150
200
250
TIME (seconds)

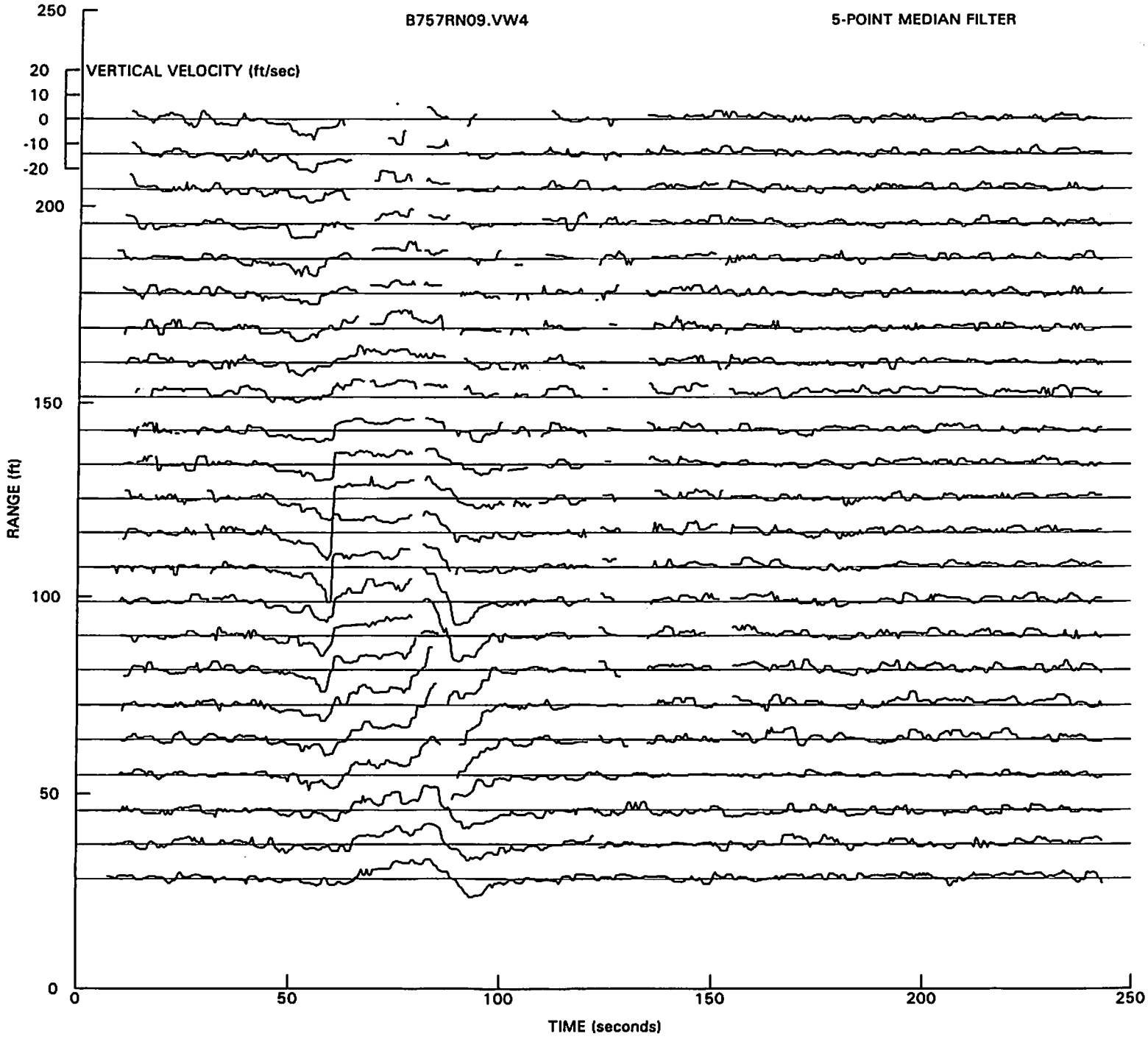
B757RN09.VW4
5-POINT MEDIAN FILTER
VERTICAL VELOCITY (ft/sec)
20
10
0
-10
-20
250
200
150
100
50
0
RANGE (ft)
0
50
100
150
200
250
TIME (seconds)

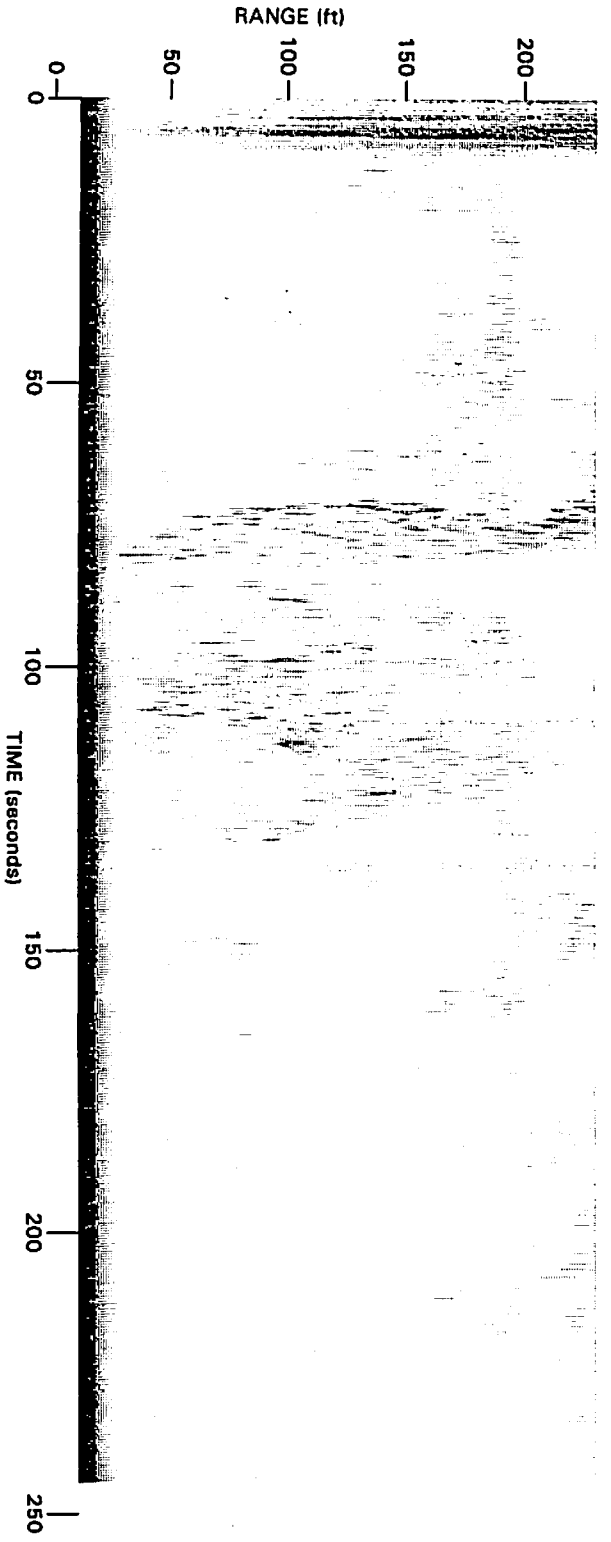

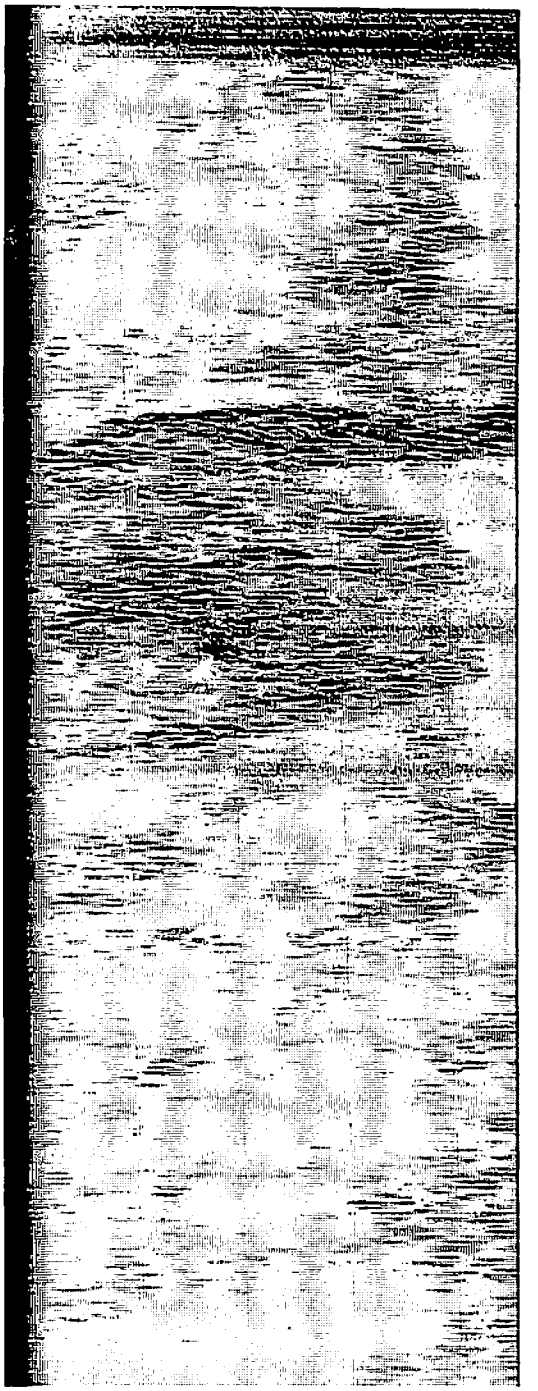

B757RN09.CH5

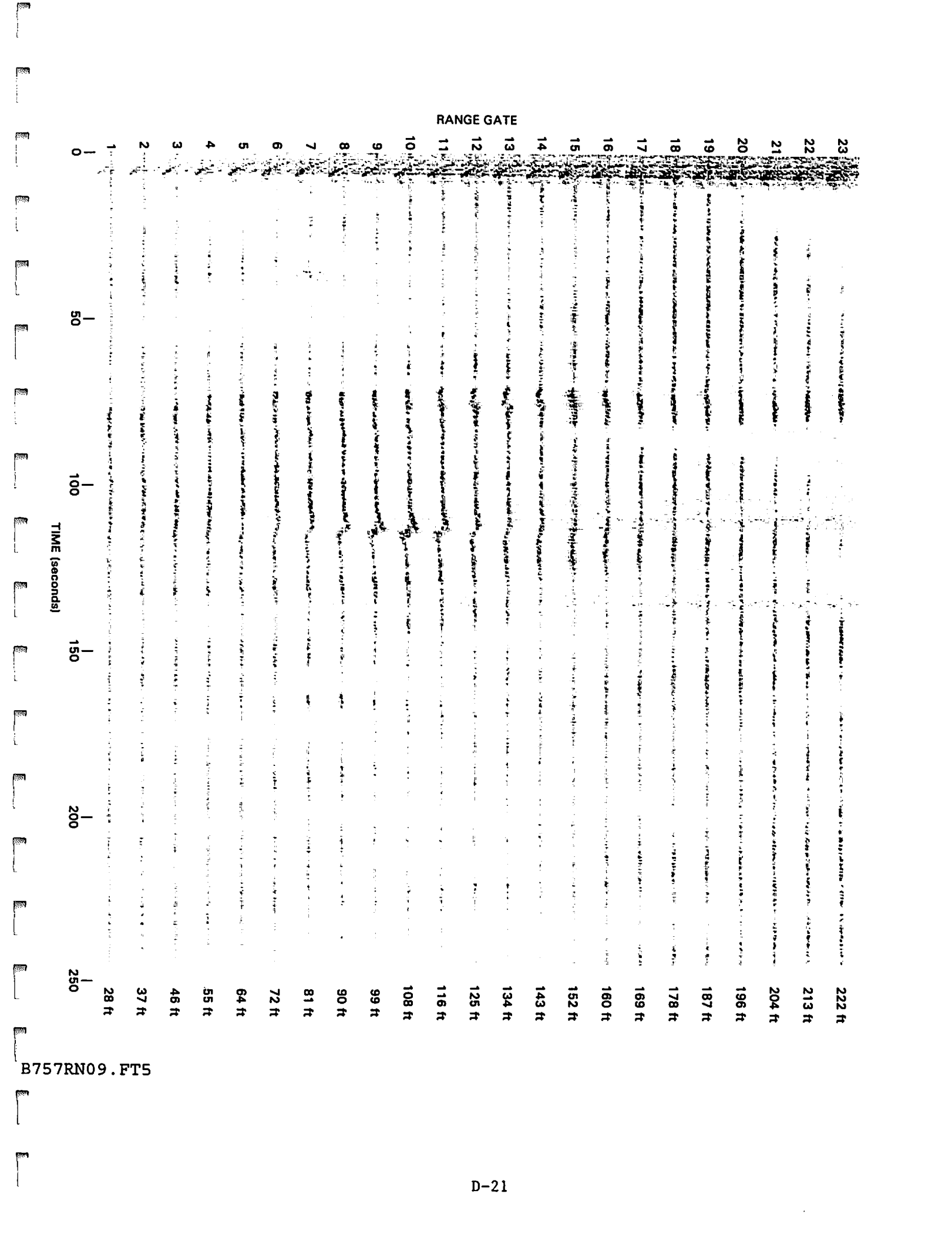

B757RN09.FT5

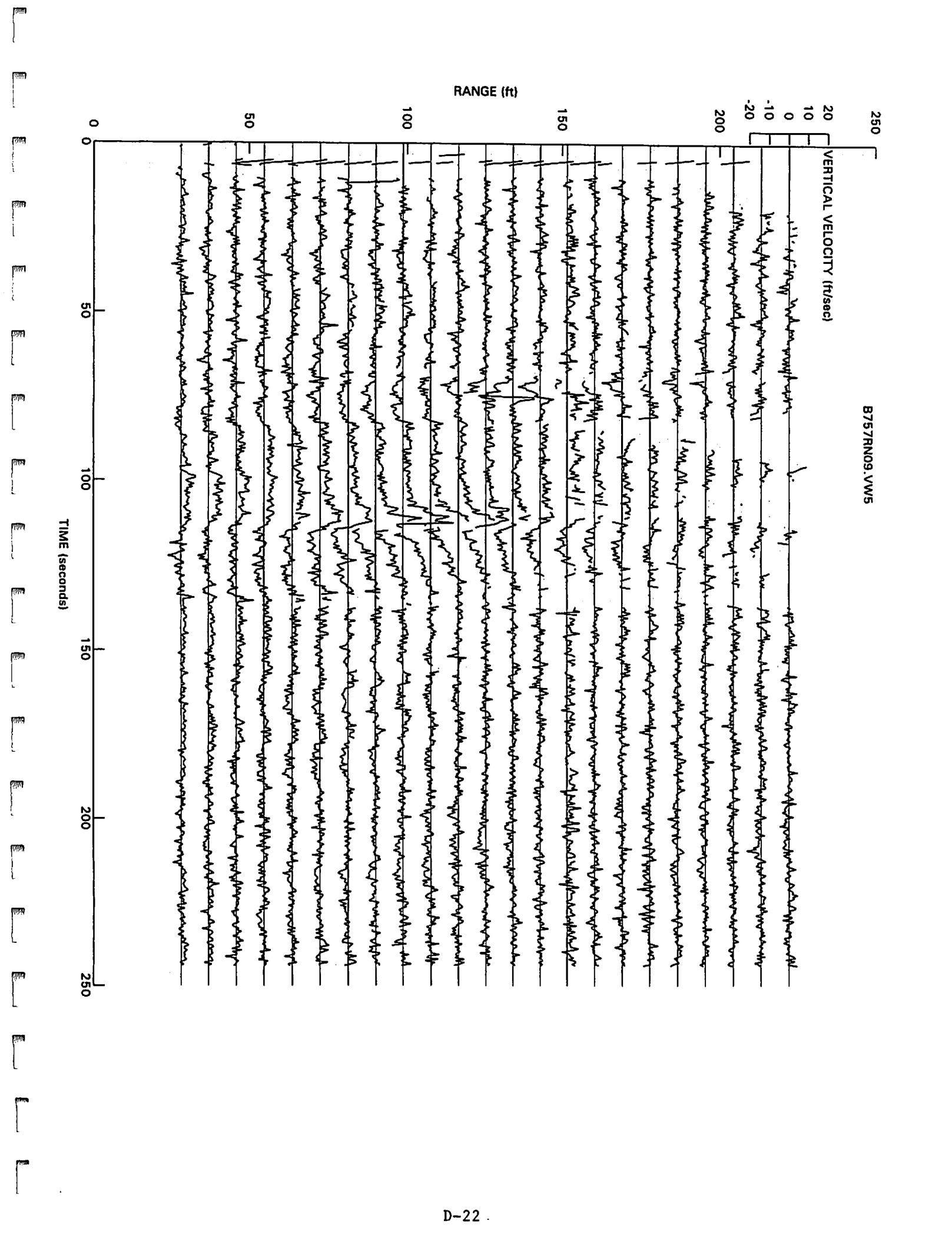
B757RN09.VW5
VERTICAL VELOCITY (ft/sec)
20
10
0
-10
-20
RANGE (ft)
250
200
150
100
50
0
0
50
100
150
200
250
TIME (seconds)

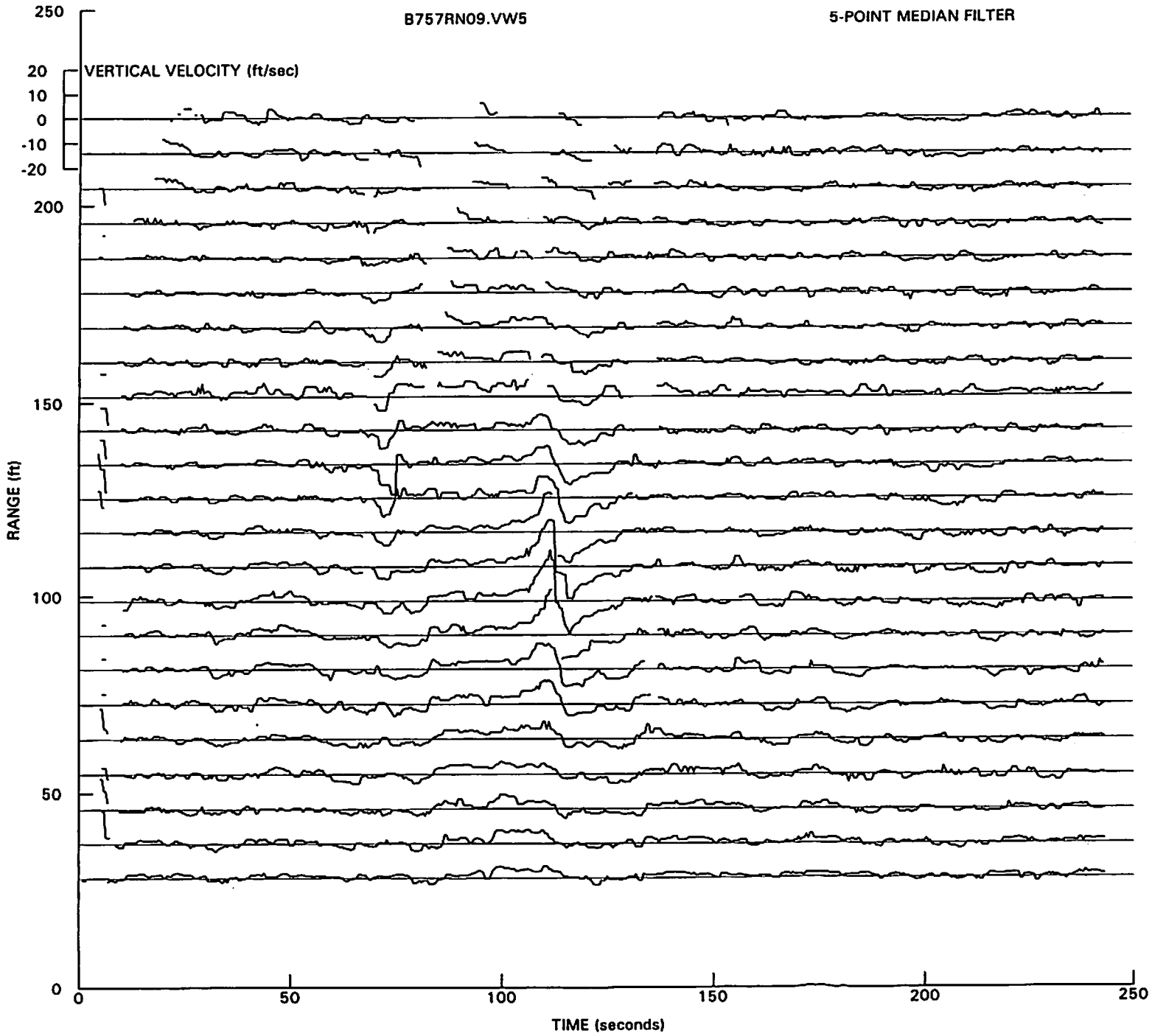
B757RN09.VW5
5-POINT MEDIAN FILTER
VERTICAL VELOCITY (ft/sec)
20
10
0
-10
-20
RANGE (ft)
250
200
150
100
50
0
0
50
100
150
200
250
TIME (seconds)

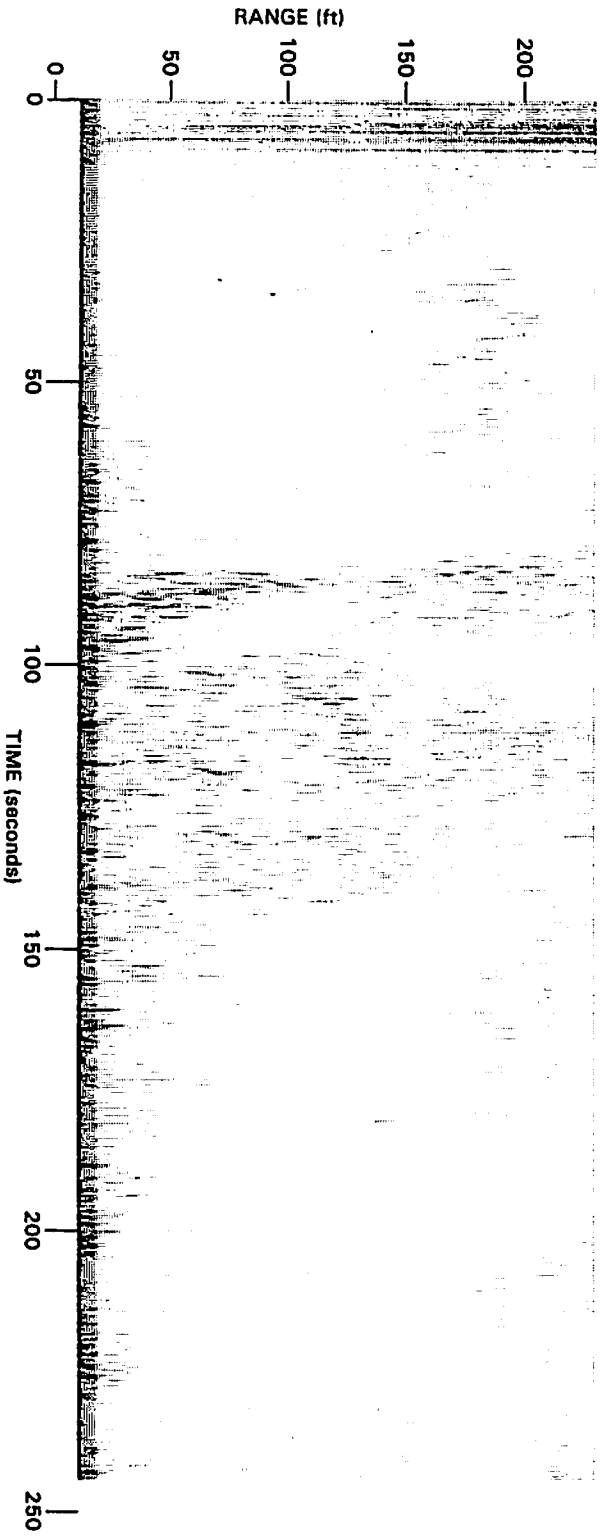

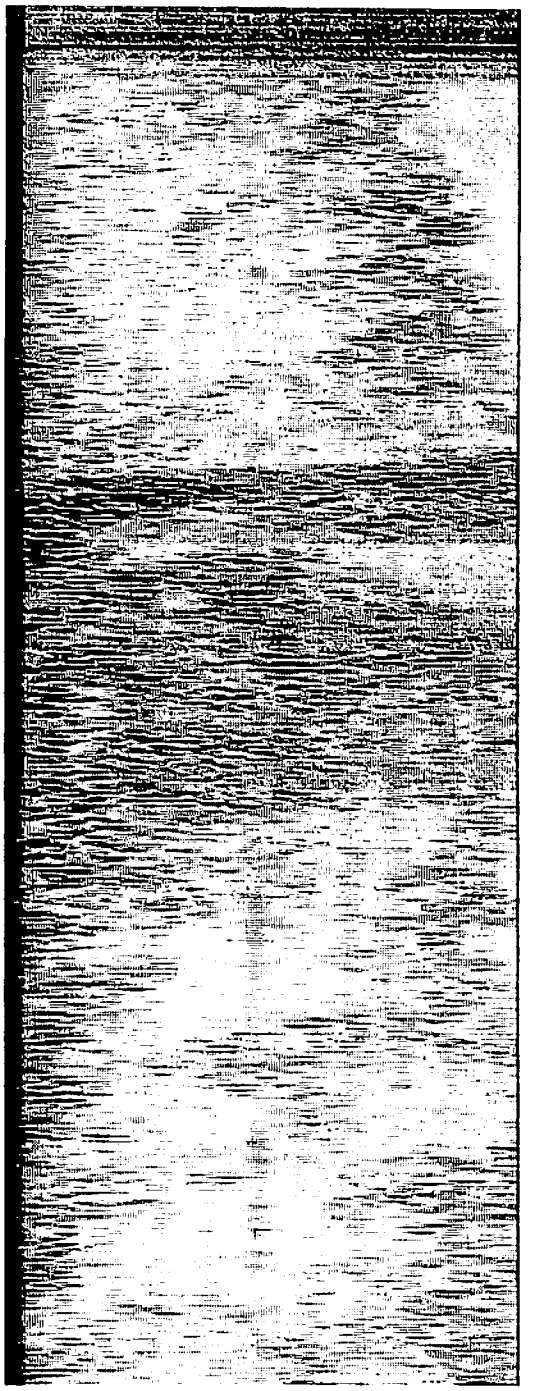

757RN09.CH6

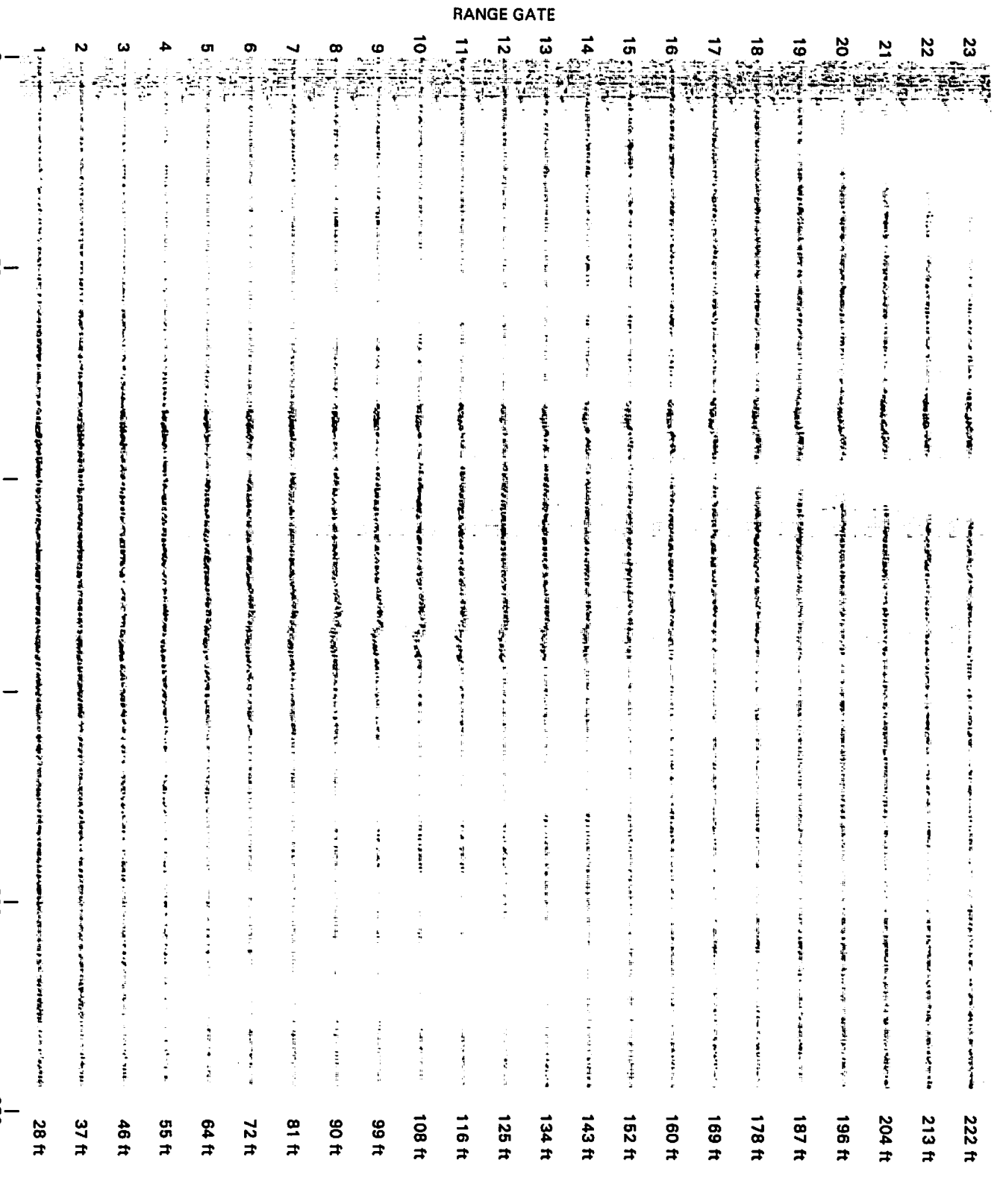

B757RN09.FT6

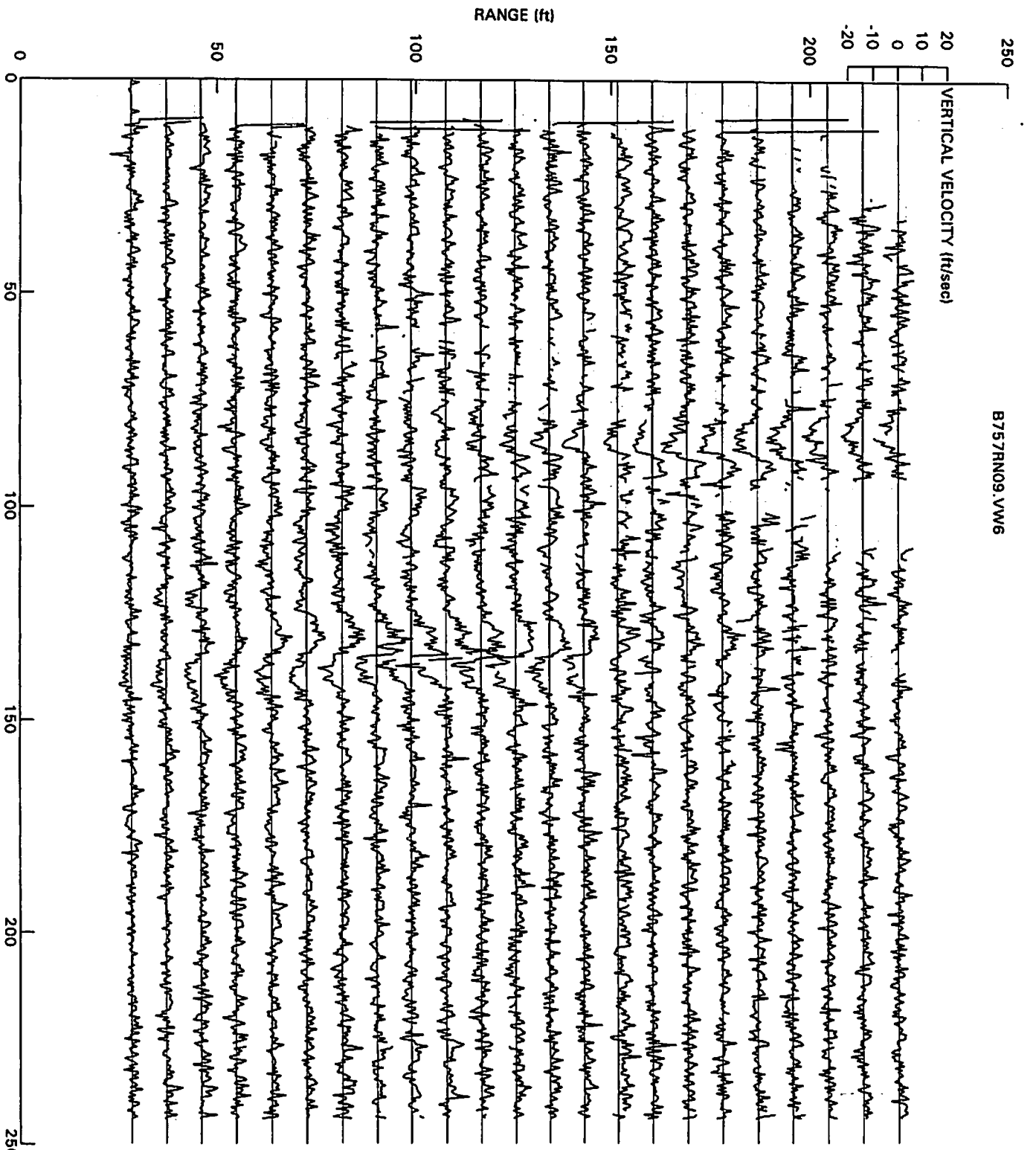
B757RN09.VW6
VERTICAL VELOCITY (ft/sec)
20
10
0
-10
-20
RANGE (ft)
250
200
150
100
50
0
0
50
100
150
200
250
TIME (seconds)

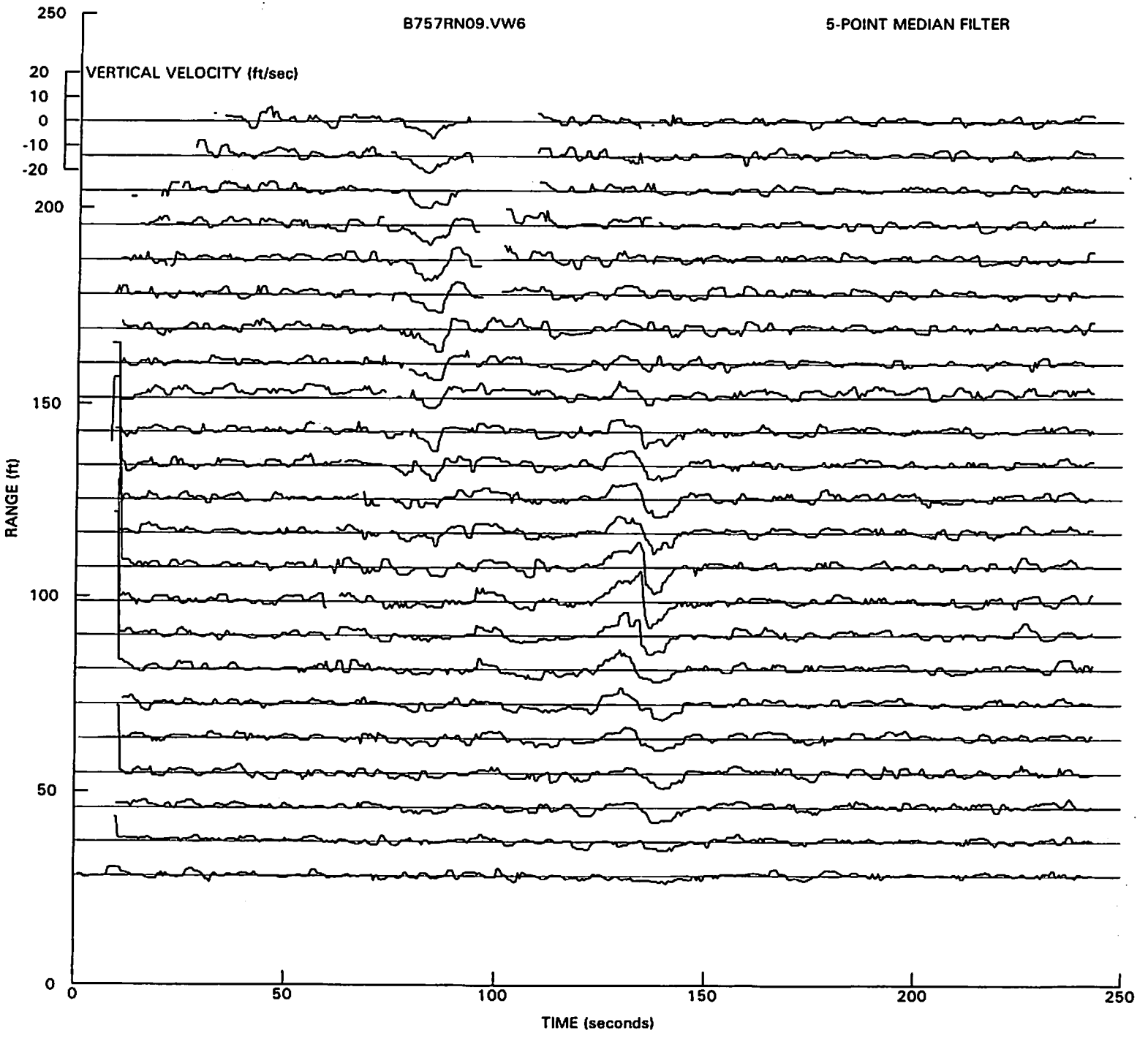
B757RN09.VW6
5-POINT MEDIAN FILTER
VERTICAL VELOCITY (ft/sec)
20
10
0
-10
-20
250
200
150
100
50
0
RANGE (ft)
0
50
100
150
200
250
TIME (seconds)

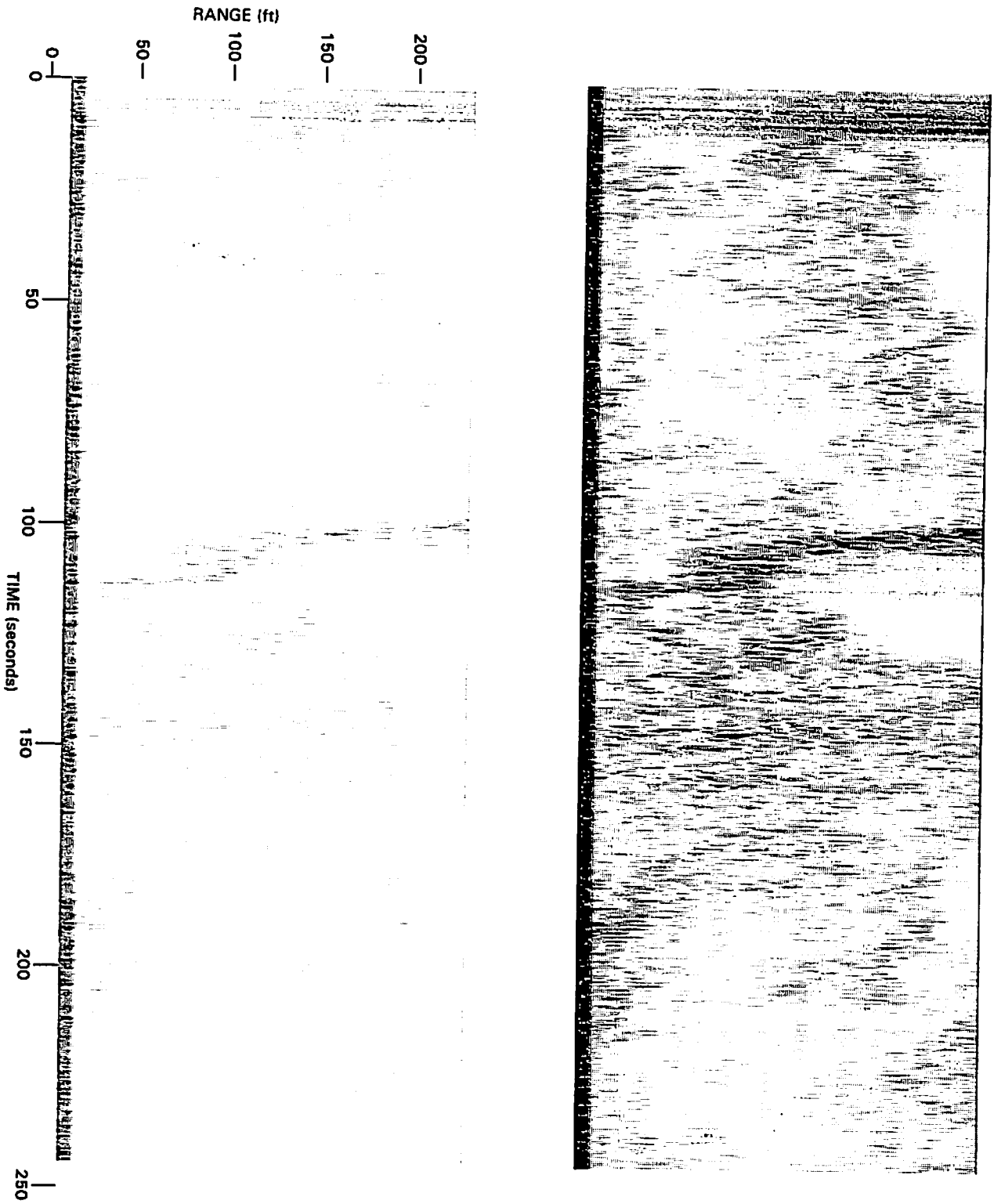

757RN09.CH7

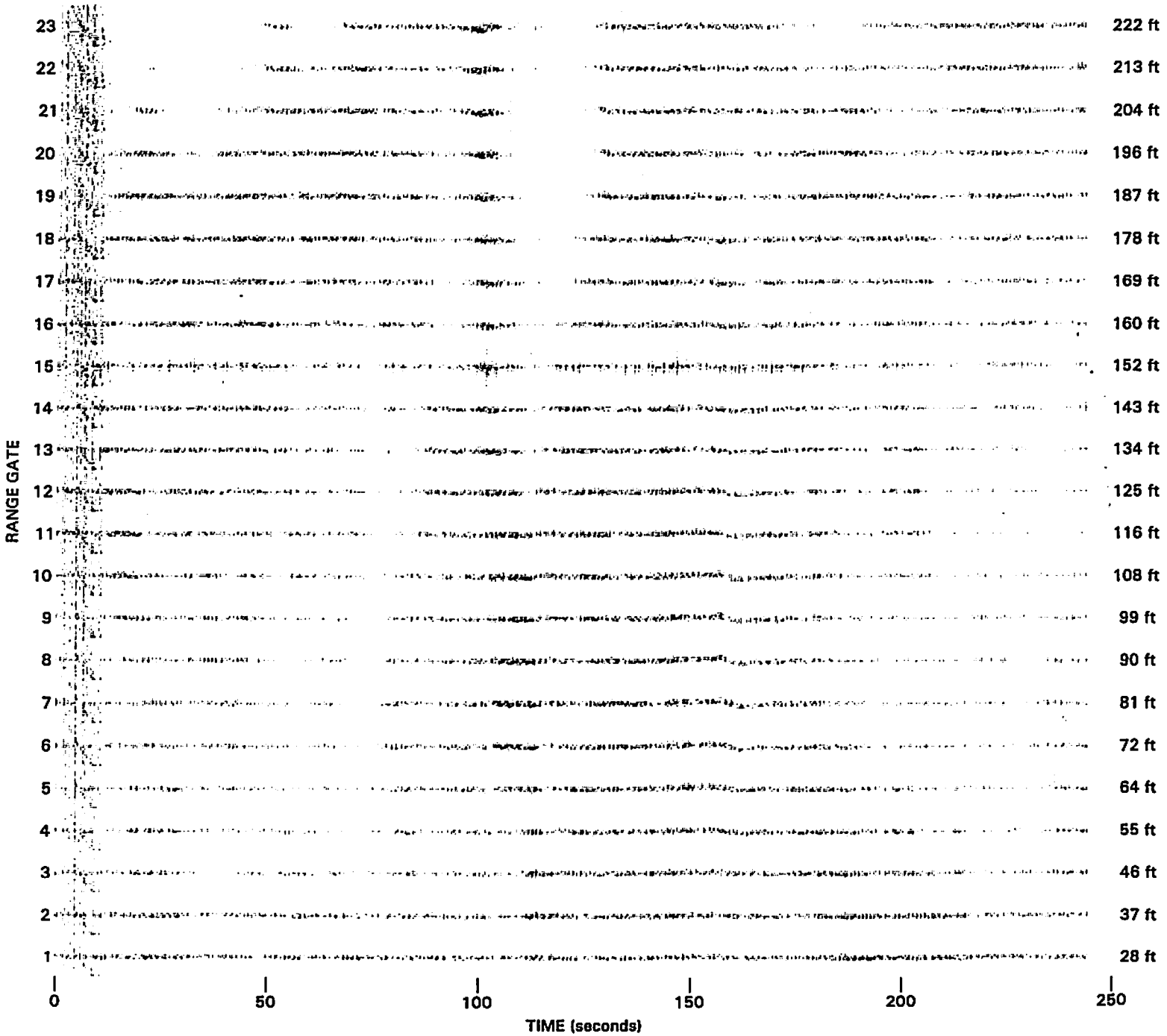

B757RN09.FT7

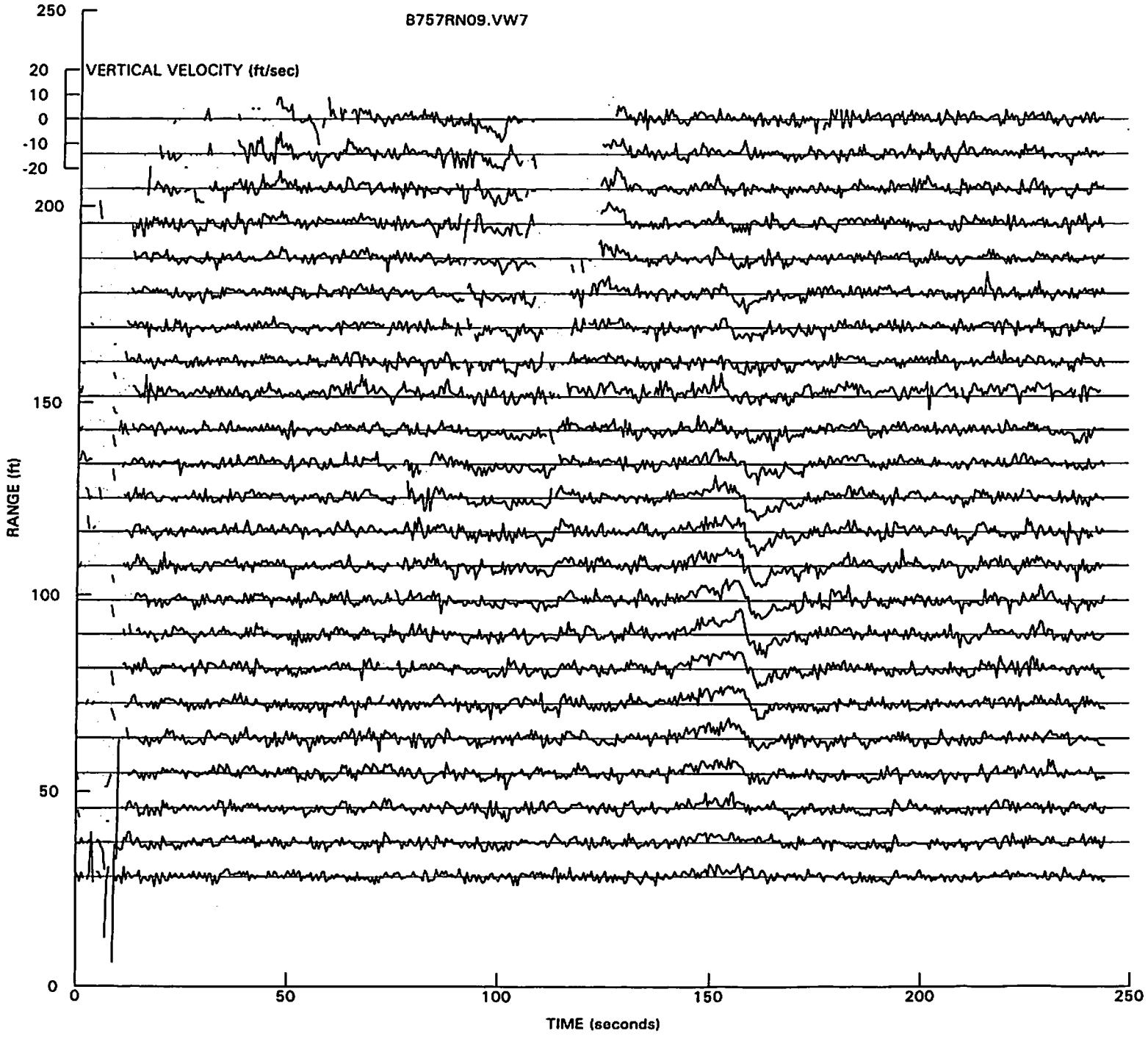
B757RN09.VW7
VERTICAL VELOCITY (ft/sec)
250
20
10
0
-10
-20
200
150
100
50
0
RANGE (ft)
0
50
100
150
200
250
TIME (seconds)

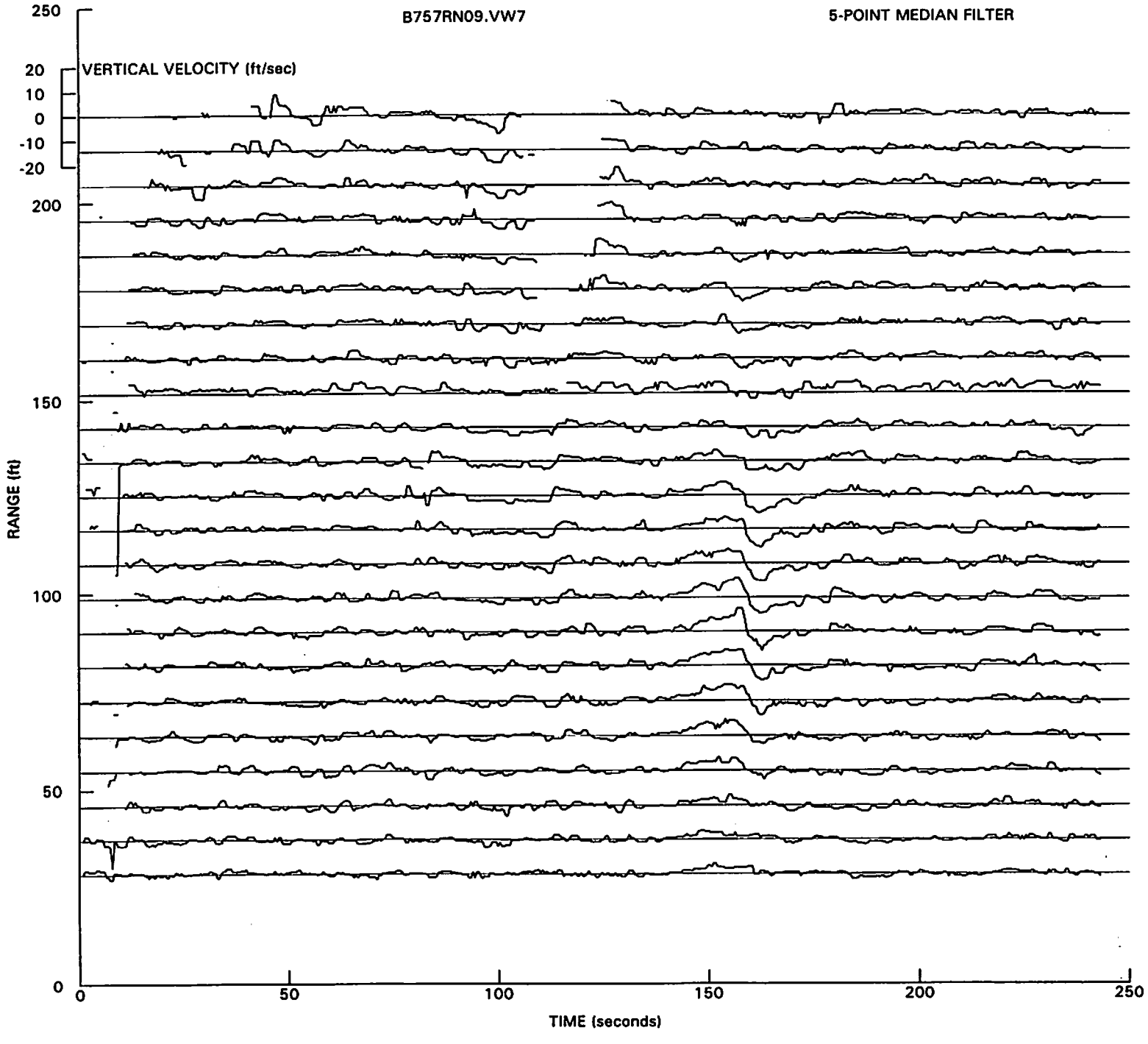
B757RN09.VW7
5-POINT MEDIAN FILTER
VERTICAL VELOCITY (ft/sec)
20
10
0
-10
-20
250
200
150
100
50
0
RANGE (ft)
0
50
100
150
200
250
TIME (seconds)

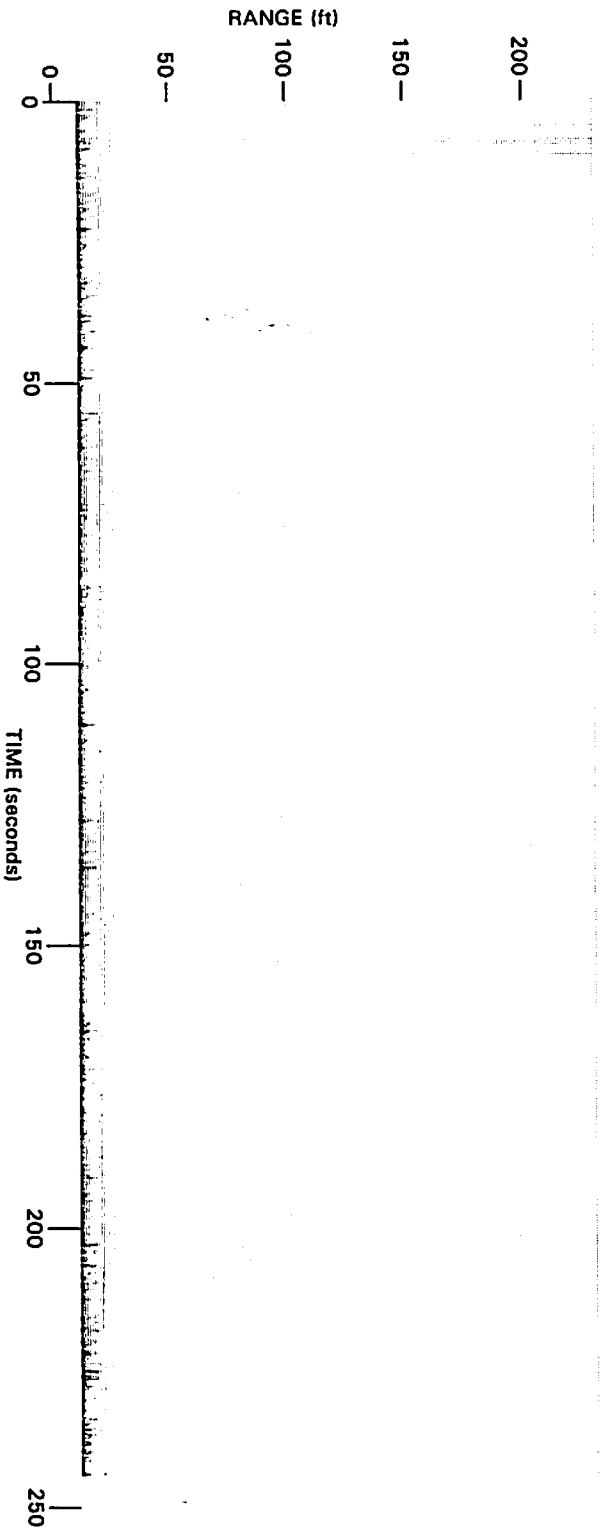

B757RN09.CH8

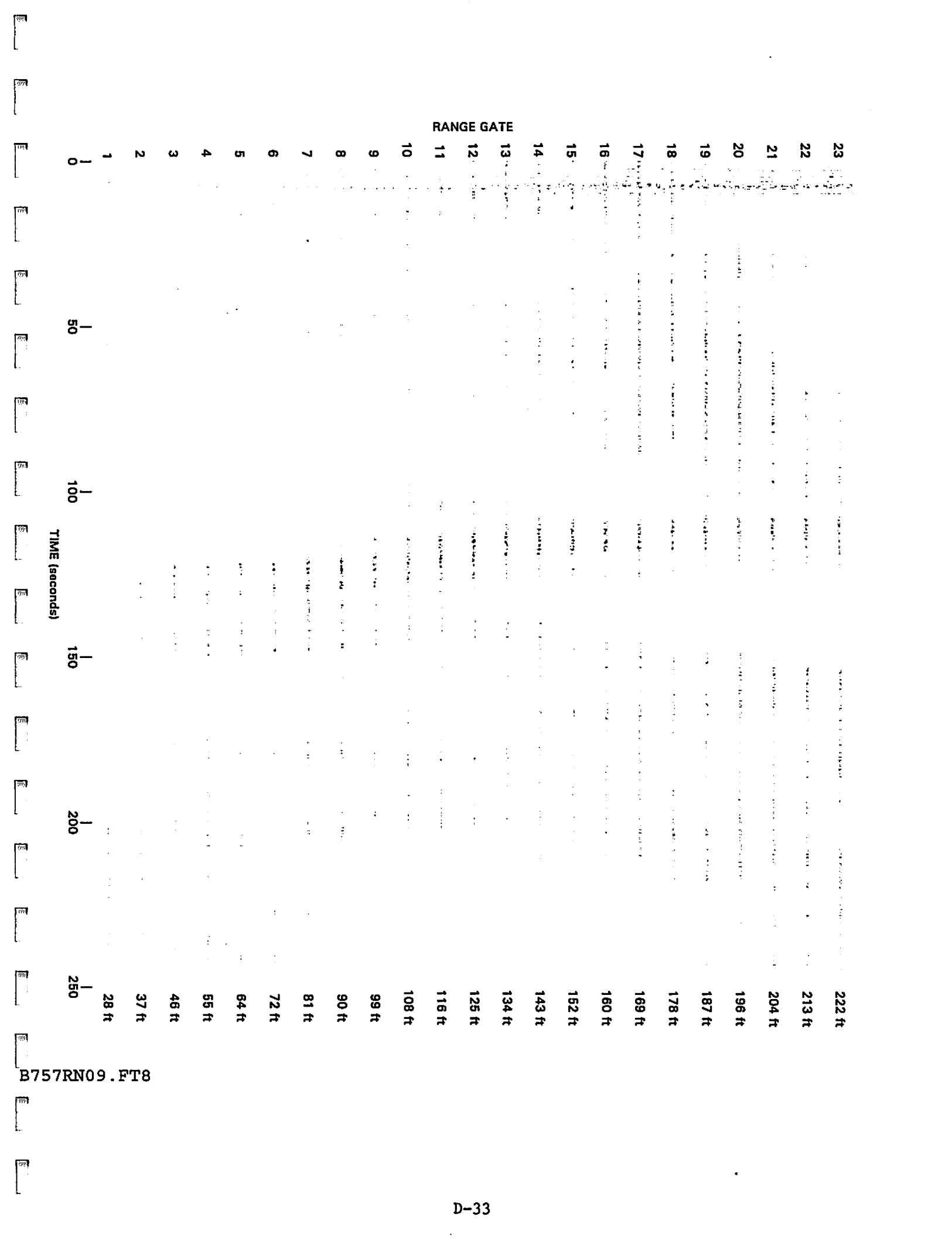

B757RN09.FT8

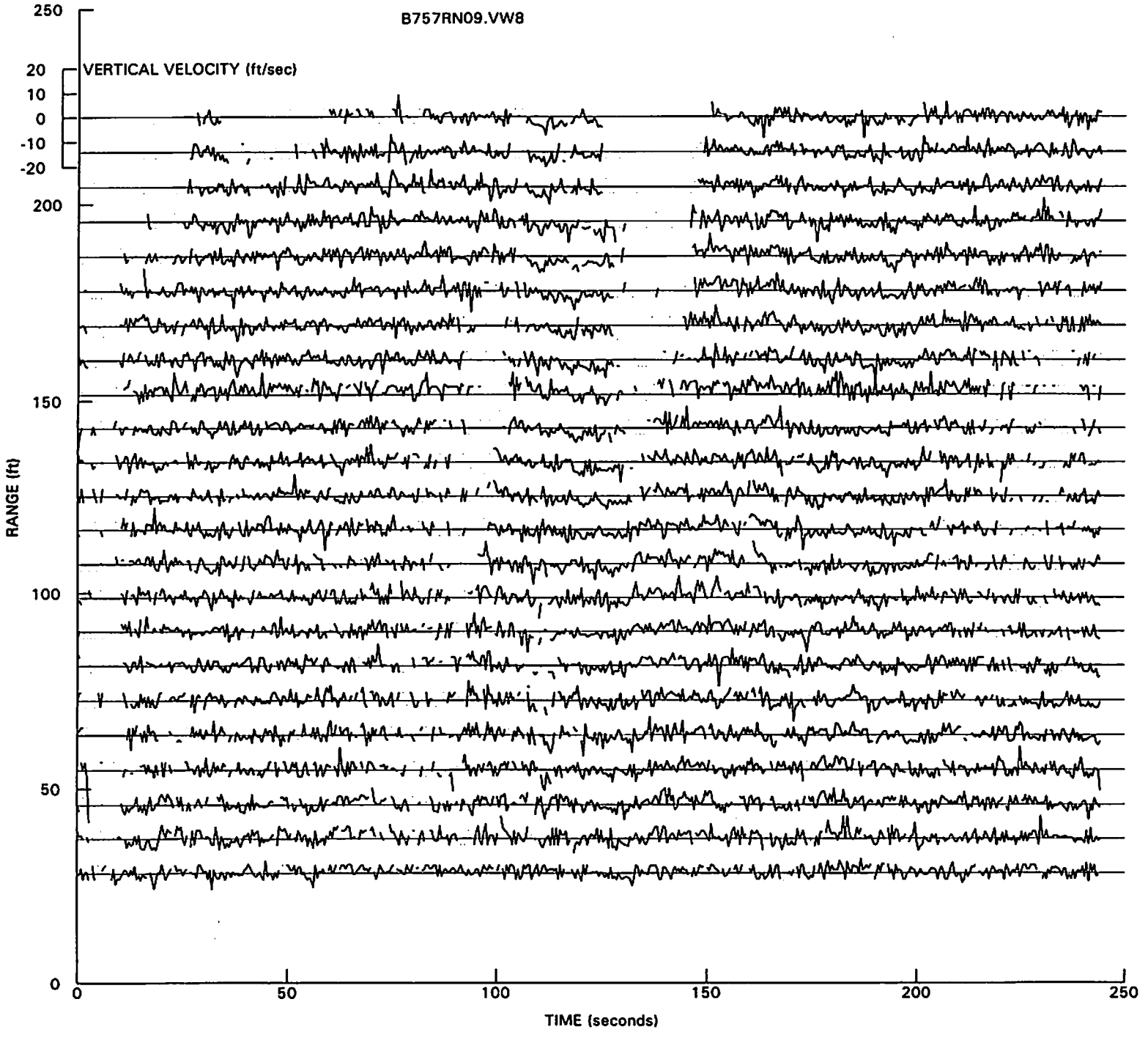
B757RN09.VW8
VERTICAL VELOCITY (ft/sec)
20
10
0
-10
-20
250
200
150
100
50
0
RANGE (ft)
0
50
100
150
200
250
TIME (seconds)

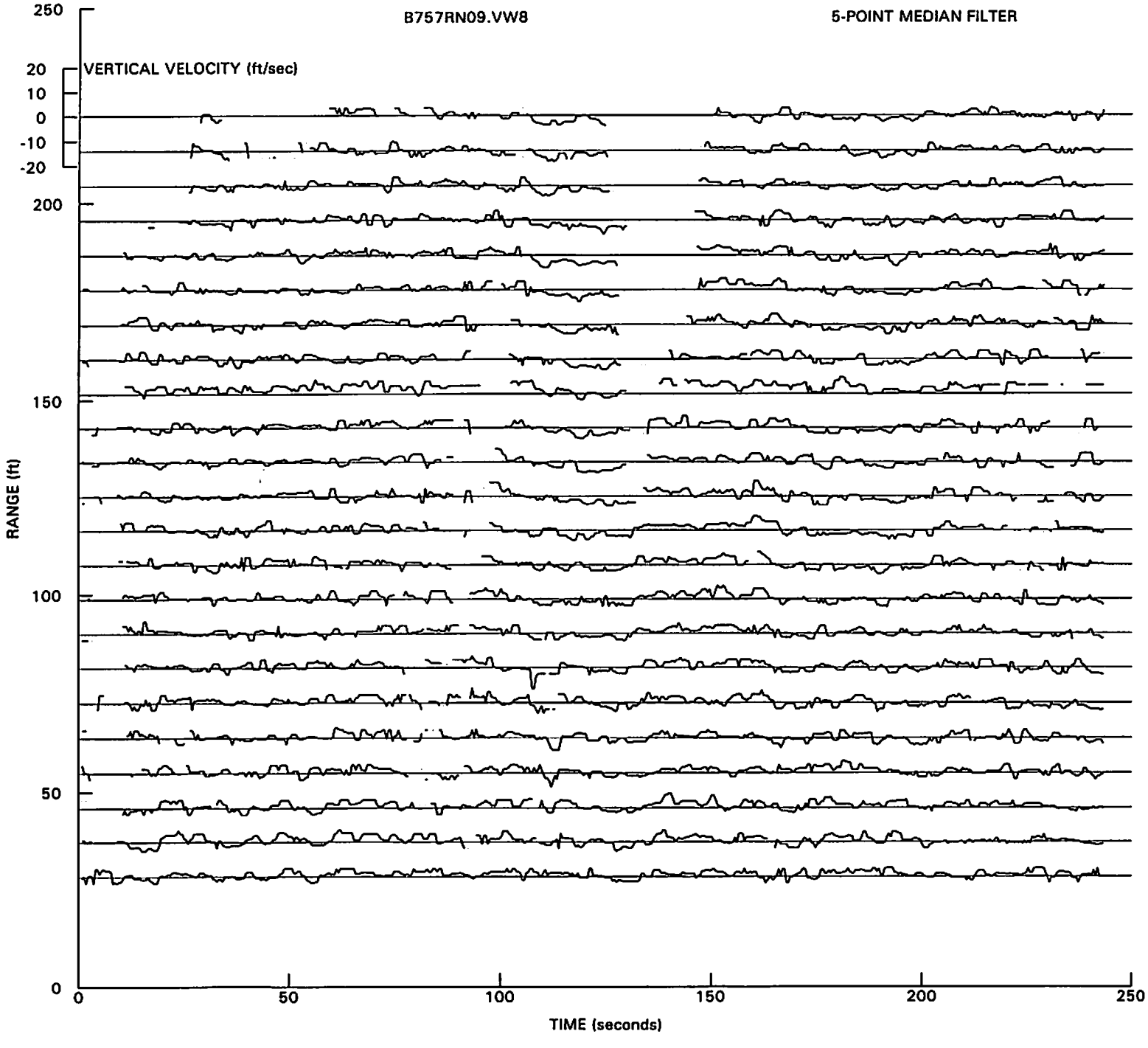
B757RN09.VW8
5-POINT MEDIAN FILTER
VERTICAL VELOCITY (ft/sec)
20
10
0
-10
-20
250
200
150
100
50
0
RANGE (ft)
0
50
100
150
200
250
TIME (seconds)

ATTACHMENT E

WIND AND TURBULENCE FROM TOWER HOT-FILM ANEMOMETERS

ATTACHMENT E

WIND AND TURBULENCE FROM TOWER HOT-FILM ANEMOMETERS

During the first three Idaho Falls test days, the Volpe Center recorded wind speed data at 4000 Hz from the hot-film anemometers located at tower positions 110, 120, 130, 140, 150, 160 and 170 feet. The data were analyzed in three ways:

1) Stripcharts were made of the first 7.5 seconds of data. The plot for B-757 Run 9 is attached.

2) The mean speed and standard deviation were calculated for the first five seconds of the run (well before any vortices had reached the tower). The following results were obtained for Run 9:

Height (ft)	110	120	130	140	150	160	170
Mean Speed (ft/s)	8.4	9.6	8.0	10.1	10.6	12.2	13.1
Std Dev. Speed (ft/s) 0.57	0.70	0.70	0.67	0.62	0.54	0.46	

Note that there seem to be sensor biases of about one ft/s in the mean speeds. The turbulence appears to be somewhat less at the top two locations.

3) The first four seconds of the run were processed with an FFT to obtain the power spectral density (PSD). The power spectral amplitude (square root of PSD) was plotted against frequency or eddy wavelength (using the ambient wind speed to convert from frequency to wavelength). The spectral plots against wavelength for B-757 Run 9 are attached.

The hot-film anemometers measure the wind speed in the plane perpendicular to their axis which was oriented parallel to the aircraft flight path in order to measure the vortex tangential velocity. Since the mean wind away from the vortices is horizontal, the mean wind speed is a measure of the crosswind with respect to the aircraft path and the standard deviation of the wind speed represents the crosswind component of the turbulence.

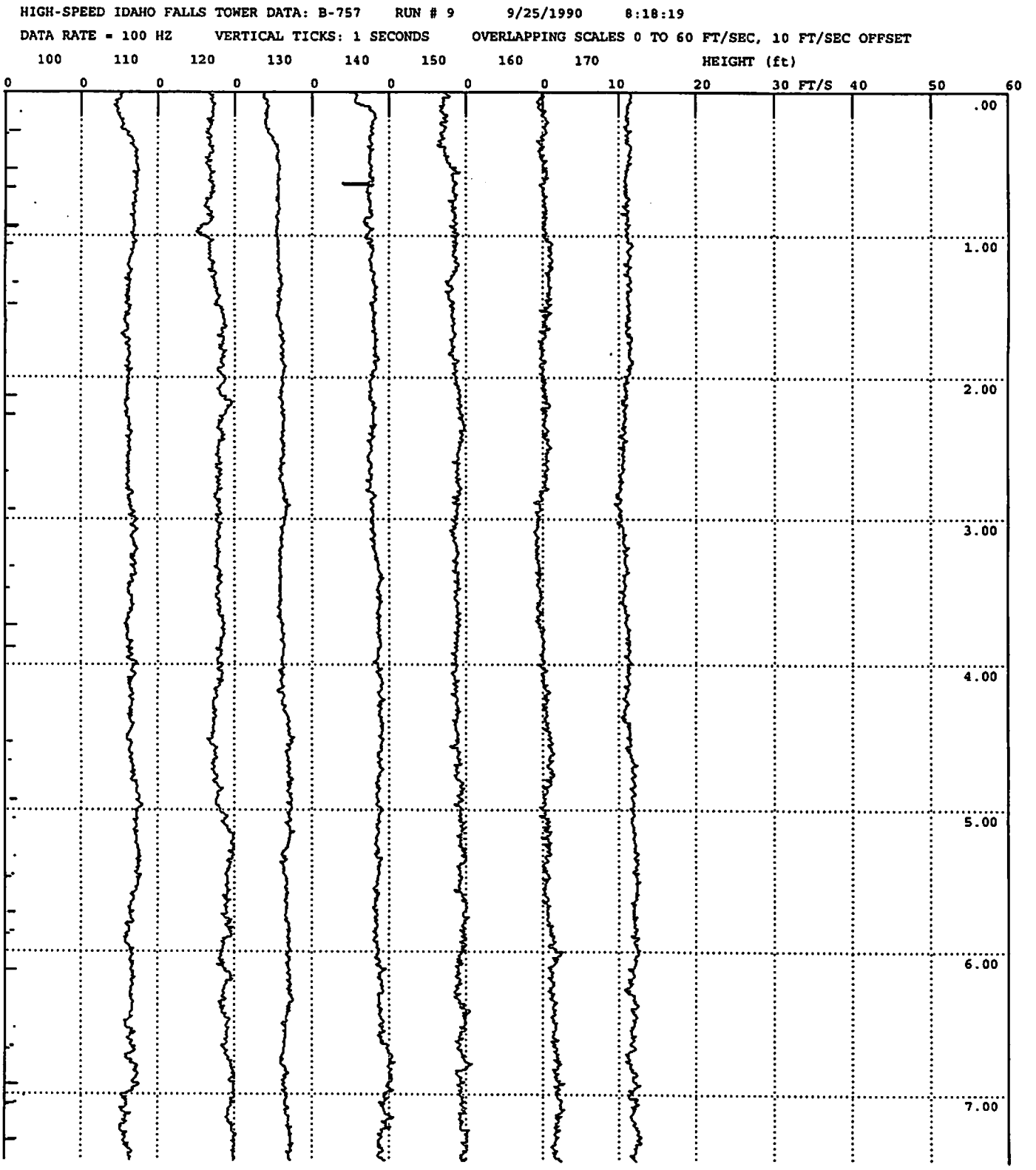

FIGURE 4. 1 HIGH RESOLUTION ANEMOMETER DATA RUN 9 B-757

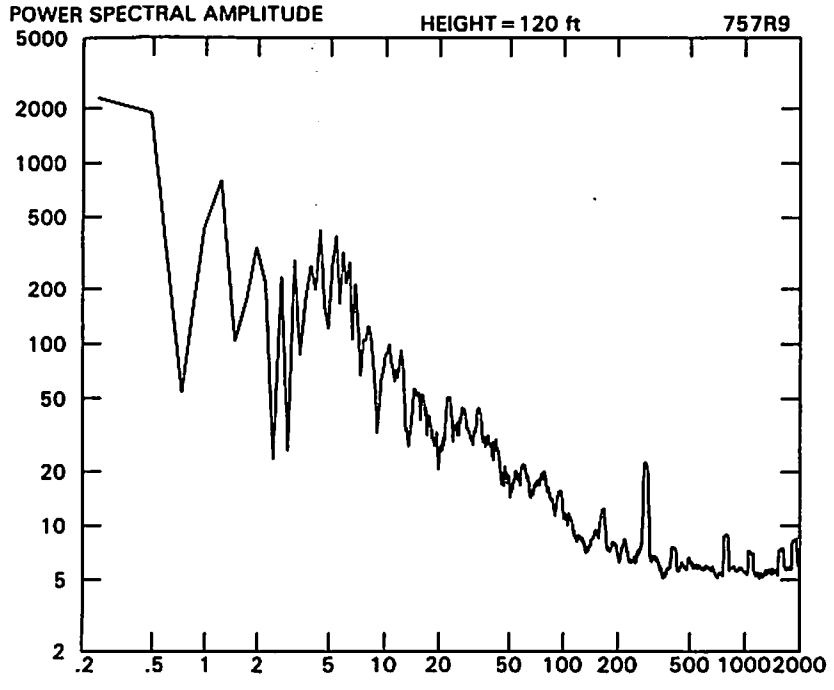
POWER SPECTRAL AMPLITUDE
HEIGHT = 120 ft
757R9
5000
2000
1000
500
200
100
50
20
10
5
2
.2
.5
1
2
5
10
20
50
100
200
500
1000
2000

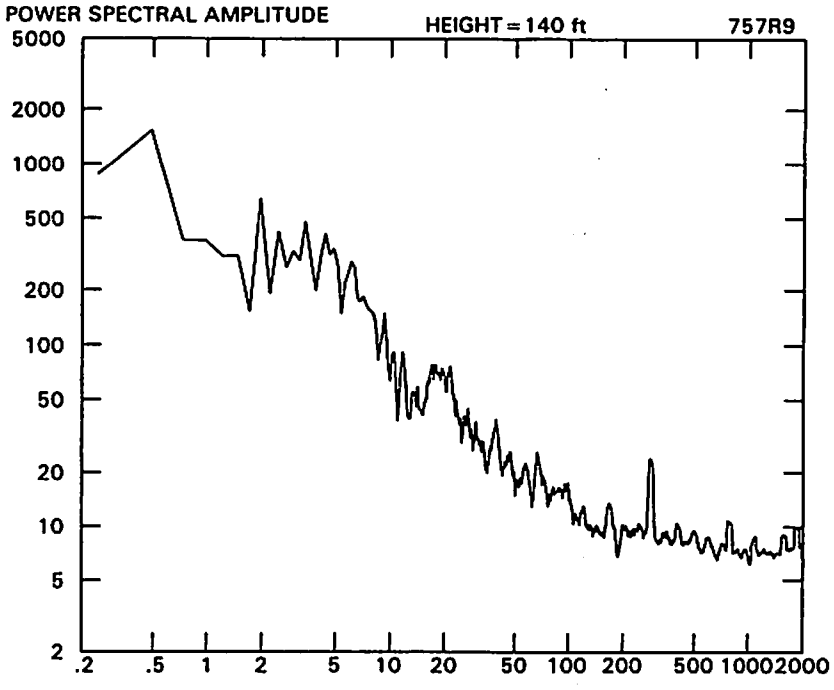
POWER SPECTRAL AMPLITUDE
HEIGHT = 140 ft
757R9
5000
2000
1000
500
200
100
50
20
10
5
2
.2
.5
1
2
5
10
20
50
100
200
500
1000
2000

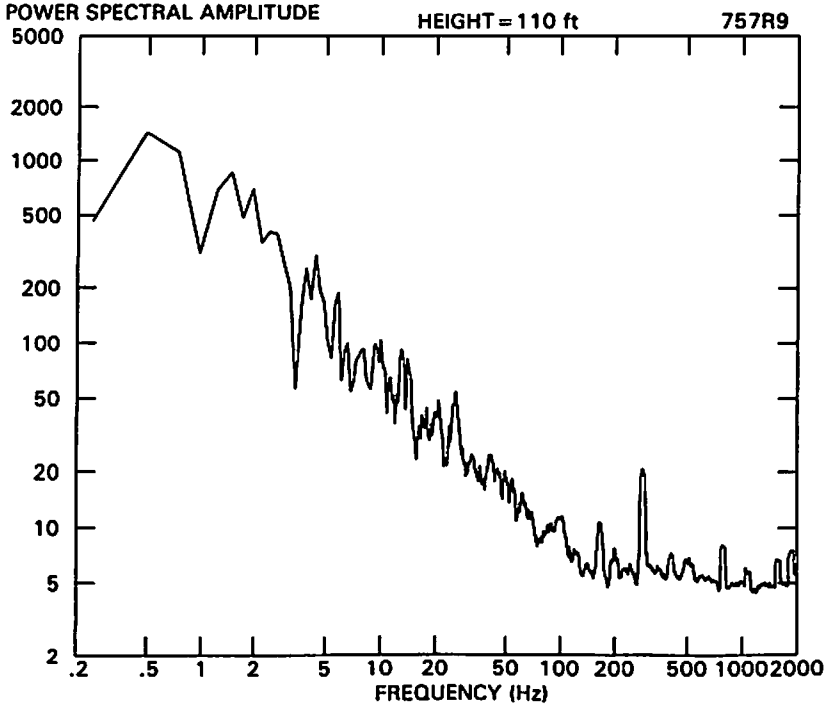
POWER SPECTRAL AMPLITUDE
HEIGHT = 110 ft
757R9
5000
2000
1000
500
200
100
50
20
10
5
2
.2
.5
1
2
5
10
20
50
100
200
500
1000
2000
FREQUENCY (Hz)

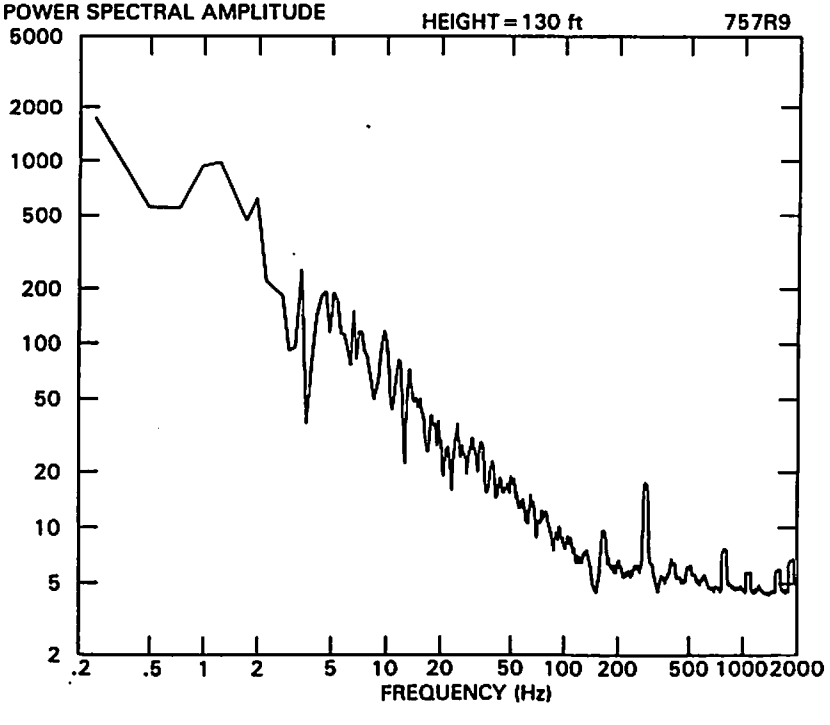
POWER SPECTRAL AMPLITUDE
HEIGHT = 130 ft
757R9
5000
2000
1000
500
200
100
50
20
10
5
2
.2
.5
1
2
5
10
20
50
100
200
500
1000
2000
FREQUENCY (Hz)

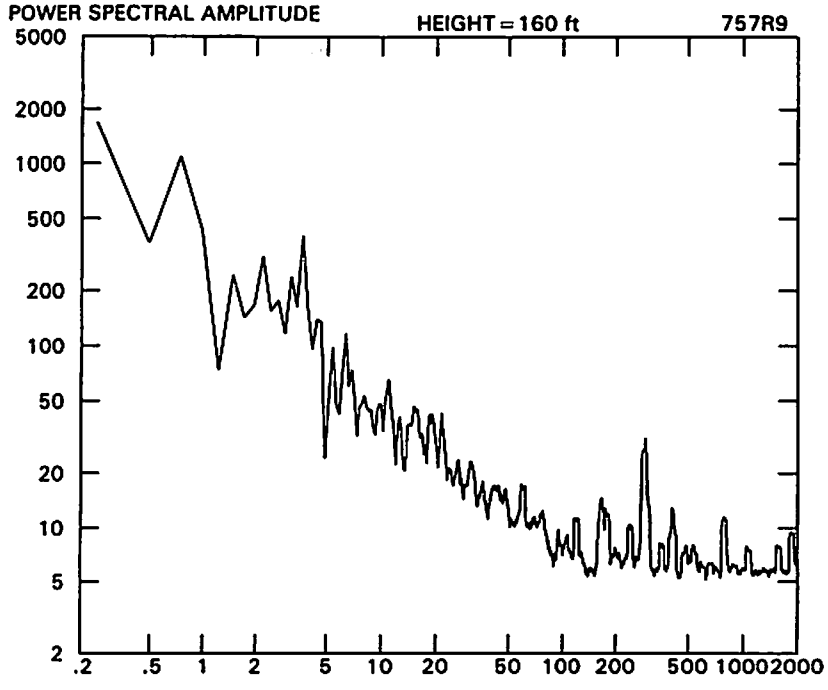
POWER SPECTRAL AMPLITUDE
HEIGHT = 160 ft
757R9
5000
2000
1000
500
200
100
50
20
10
5
2
.2
.5
1
2
5
10
20
50
100
200
500
1000
2000

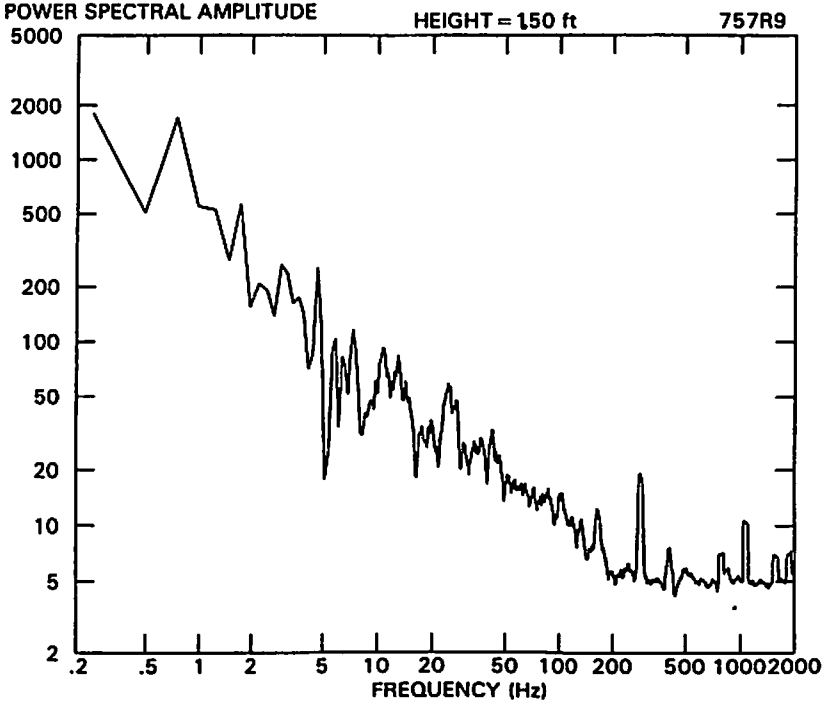
POWER SPECTRAL AMPLITUDE
HEIGHT = 150 ft
757R9
5000
2000
1000
500
200
100
50
20
10
5
2
.2
.5
1
2
5
10
20
50
100
200
500
1000
2000
FREQUENCY (Hz)

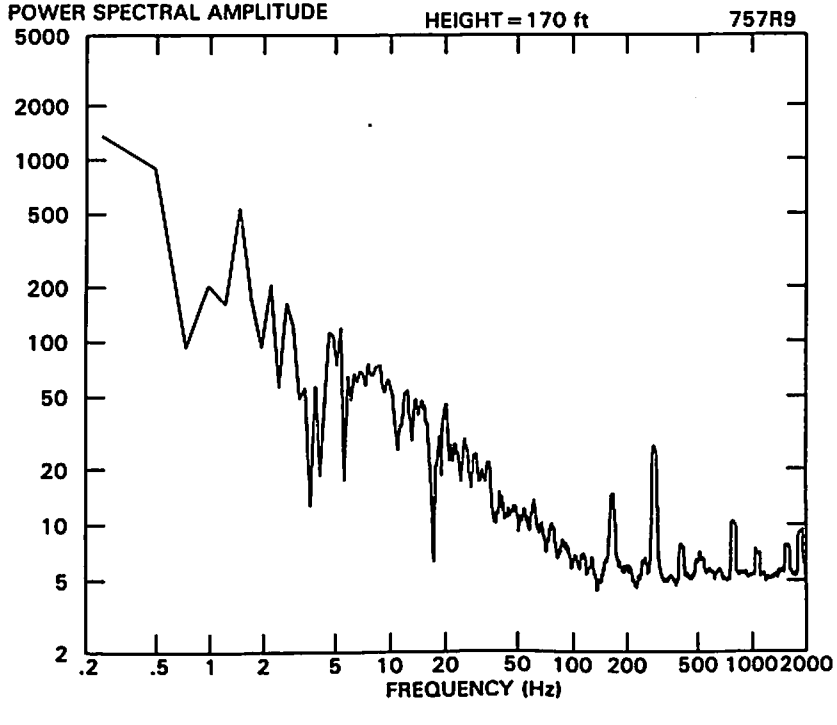
POWER SPECTRAL AMPLITUDE
HEIGHT = 170 ft
757R9
5000
2000
1000
500
200
100
50
20
10
5
2
.2
.5
1
2
5
10
20
50
100
200
500
1000
2000
FREQUENCY (Hz)

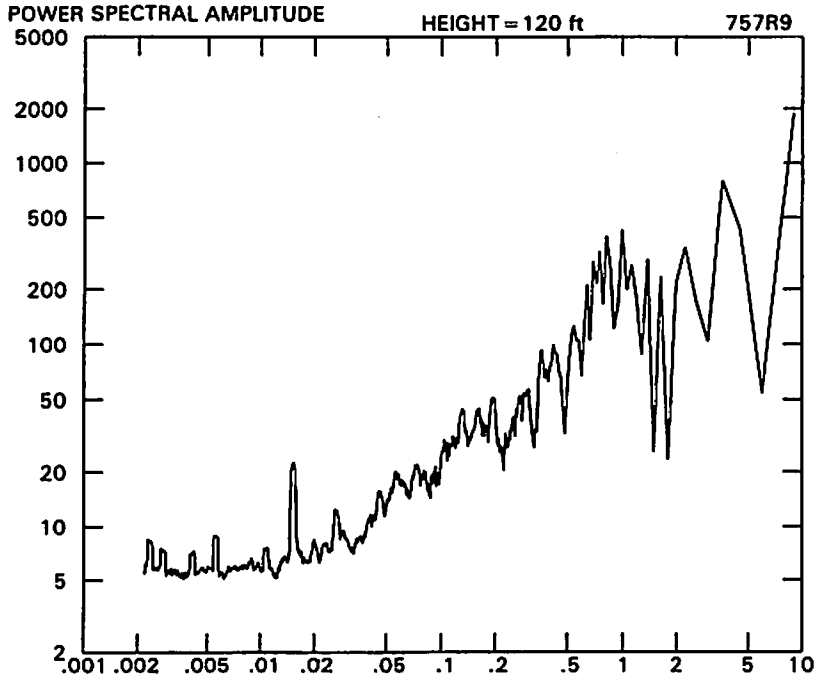
POWER SPECTRAL AMPLITUDE
HEIGHT = 120 ft
757R9
5000
2000
1000
500
200
100
50
20
10
5
2
.001 .002 .005 .01 .02 .05 .1 .2 .5 1 2 5 10

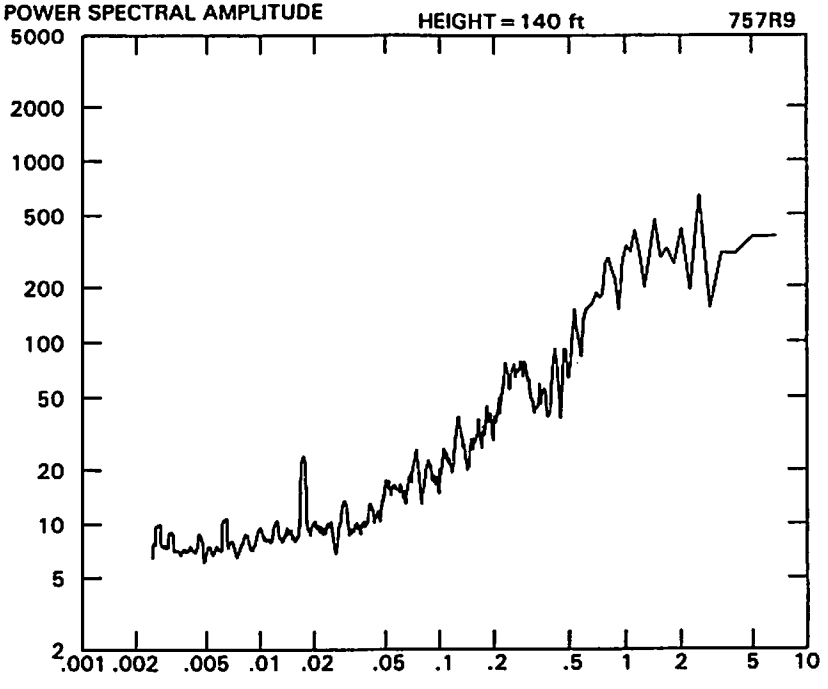
POWER SPECTRAL AMPLITUDE
HEIGHT = 140 ft
757R9
5000
2000
1000
500
200
100
50
20
10
5
2
.001 .002 .005 .01 .02 .05 .1 .2 .5 1 2 5 10

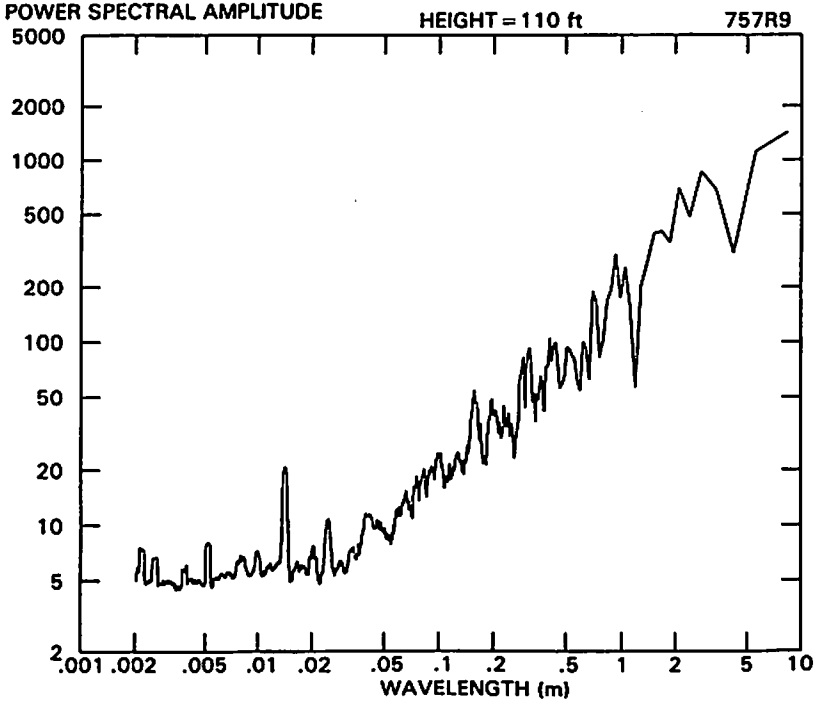
POWER SPECTRAL AMPLITUDE
HEIGHT = 110 ft
757R9
5000
2000
1000
500
200
100
50
20
10
5
2
.001 .002 .005 .01 .02 .05 .1 .2 .5 1 2 5 10
WAVELENGTH (m)

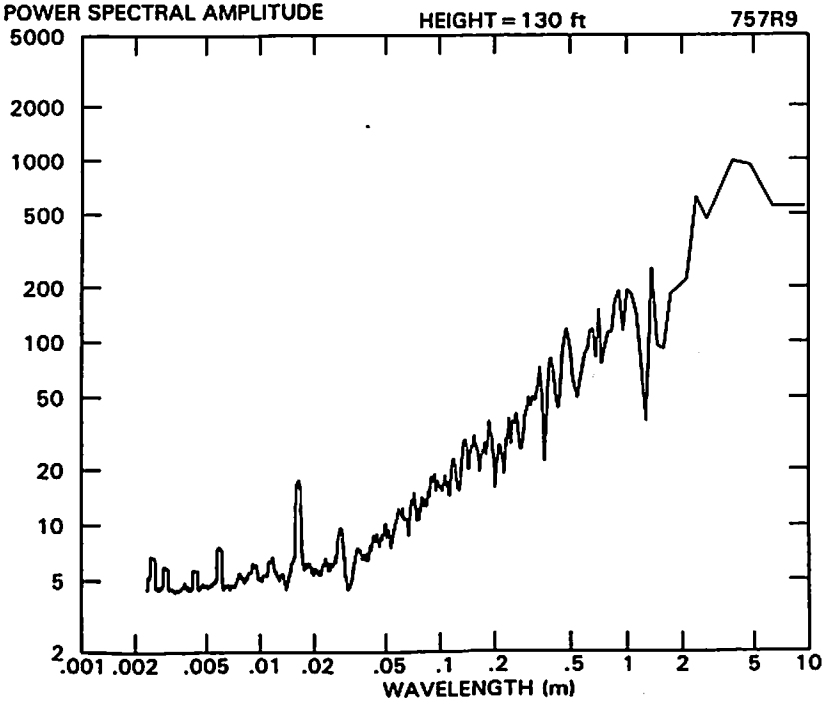
POWER SPECTRAL AMPLITUDE
HEIGHT = 130 ft
757R9
5000
2000
1000
500
200
100
50
20
10
5
2
.001 .002 .005 .01 .02 .05 .1 .2 .5 1 2 5 10
WAVELENGTH (m)

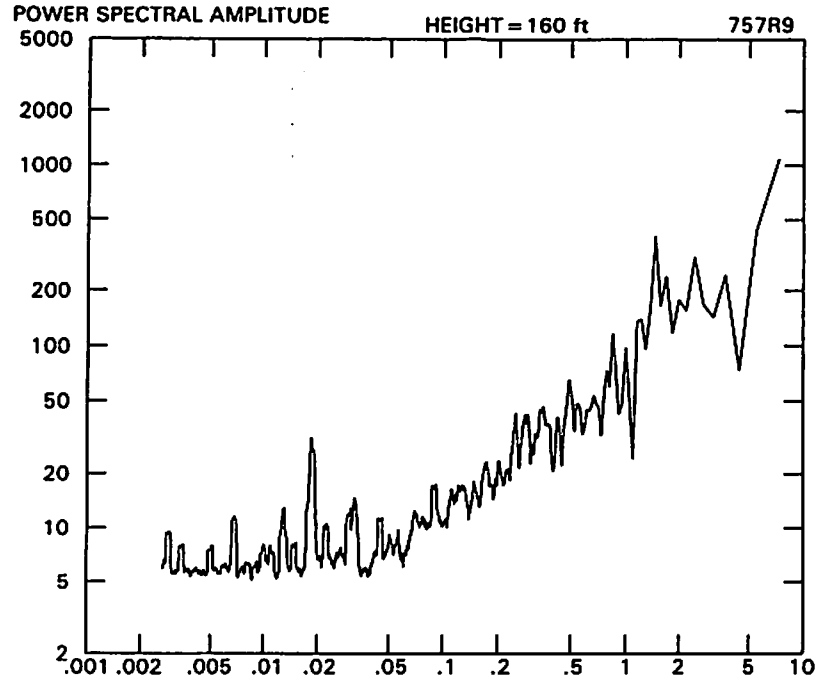
POWER SPECTRAL AMPLITUDE
HEIGHT = 160 ft
757R9
5000
2000
1000
500
200
100
50
20
10
5
2
.001 .002 .005 .01 .02 .05 .1 .2 .5 1 2 5 10

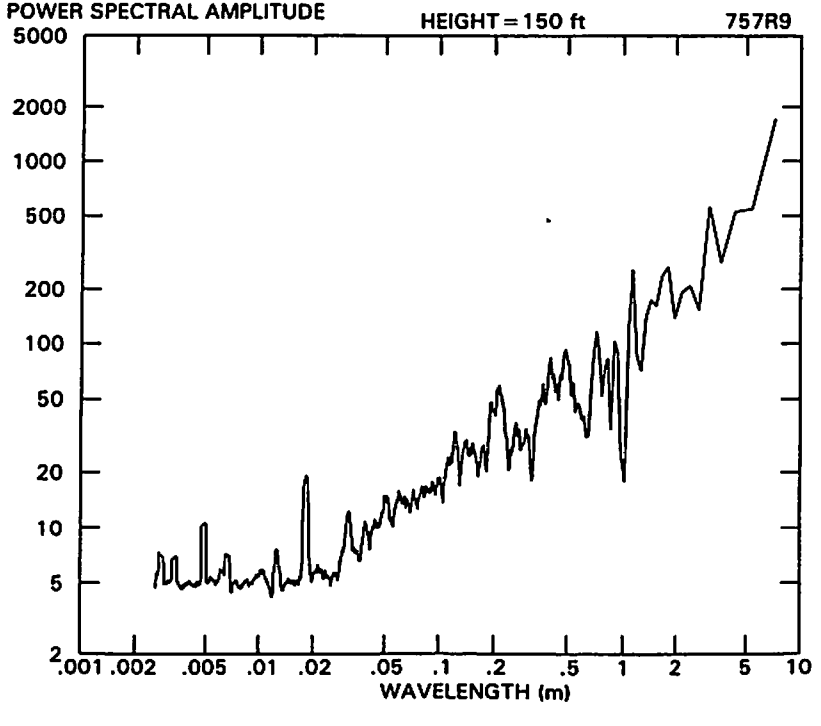
POWER SPECTRAL AMPLITUDE
HEIGHT = 150 ft
757R9
5000
2000
1000
500
200
100
50
20
10
5
2
.001 .002 .005 .01 .02 .05 .1 .2 .5 1 2 5 10
WAVELENGTH (m)

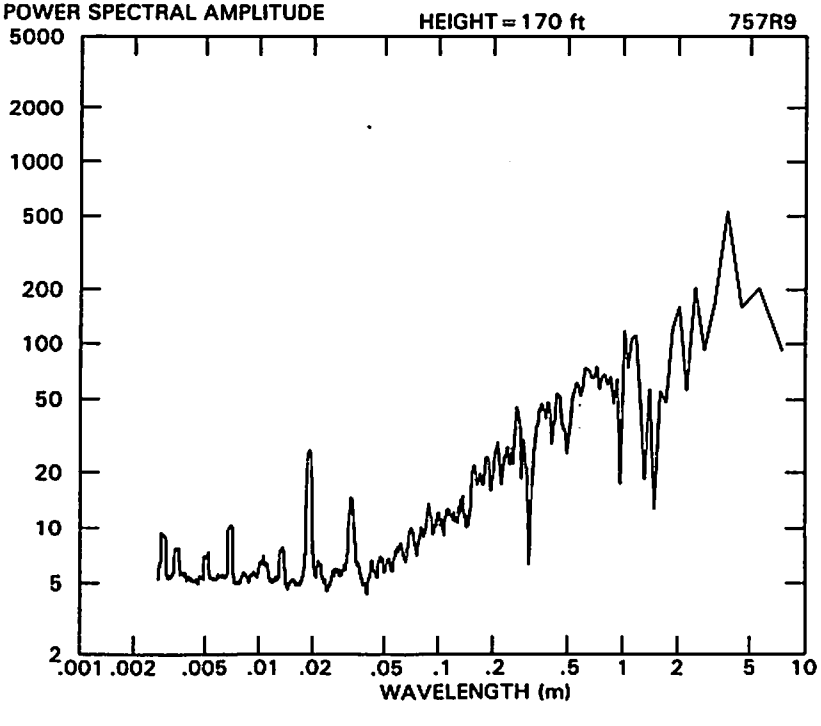
POWER SPECTRAL AMPLITUDE
HEIGHT = 170 ft
757R9
5000
2000
1000
500
200
100
50
20
10
5
2
.001 .002 .005 .01 .02 .05 .1 .2 .5 1 2 5 10
WAVELENGTH (m)

ATTACHMENT F

LDV MEASUREMENTS OF AMBIENT CROSSWIND

ATTACHMENT F

LDV MEASUREMENTS OF AMBIENT CROSSWIND

A first-cut algorithm (highest spectral peak) was developed to obtain the ambient crosswind from LDV data. This algorithm frequently responds to the vortex winds instead of the desired ambient wind. Consequently only those scan frames with no vortices give valid crosswind profiles. Those frames are attached. The assumption is made that the ambient wind is horizontal.

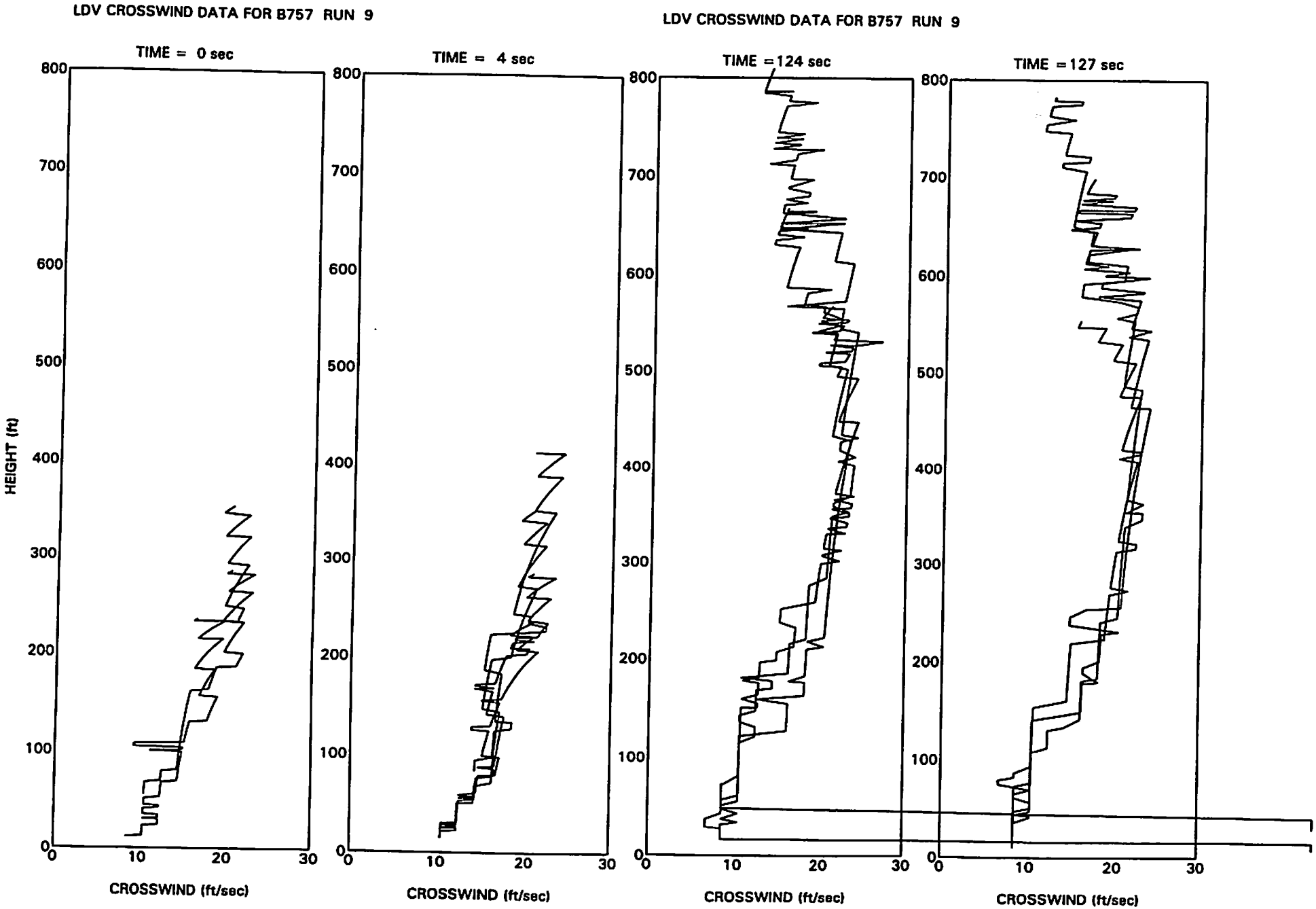
LDV CROSSWIND DATA FOR B757 RUN 9
TIME = 0 sec
TIME = 4 sec
LDV CROSSWIND DATA FOR B757 RUN 9
TIME = 124 sec
TIME = 127 sec
HEIGHT (ft)
0
100
200
300
400
500
600
700
800
0
10
20
30
CROSSWIND (ft/sec)